# Mechanisms of PKC gamma-mediated Inhibition of Dendritic Growth in Cerebellar Purkinje Cells

**Inauguraldissertation**

zur

Erlangung der Würde eines Doktors der Philosophie

vorgelegt der

Philosophisch-Naturwissenschaftlichen Fakultät

der Universität Basel

von

**Etsuko Shimobayashi**

aus Japan

**Basel, 2016**

Genehmigt von der Philosophisch-Naturwissenschaftlichen Fakultät

auf Antrag von


Prof. Josef Kapfhammer
Prof. Markus Rüegg
Prof. Nicole Schaeren-Wiemers


Basel, 21.06. 2016


Prof. Dr. Jörg Schibler
Dekan der Philosophisch-
Naturwissenschaftlichen Fakultät

# *Table of Contents*

# List of Abbreviations

AOA1        Ataxia with Oculomotor Apraxia type1

AMPA        (RS)-a-Amino-3-hydroxy-5-methyl-4-isoxazolepropionic acid

APTX        Aprataxin

AS          Albino Swiss

BDNF        brain-derived neurotrophic factor

bHLH        basic helix-loop-helix

Ca          calcium

Car8, CA8   Carbonic anhydrase 8

CARP        carbonic anhydrase-related protein

CB6         B6CF1, mouse strain

CF          climbing fiber

CGN         cerebellar granule cell

CNS         central nervous system

DAG         diacylglycerol

DCN         deep cerebellar neuron

DFM         Dulbecco's modified Eagle medium:F-12 nutrientbased medium

DHPG        (RS)-3, 5-Dihydroxyphenylglycine

DIV         days in vitro

E           embryonic day

EAAT        excitatory amino acid transporter

EGL         external granule layer

ER          endoplasmic reticulum

EtD         50% EtOH/50% DMSO

GABA        γ-amino butyric acid

| | |
|---|---|
| GN | granule neuron |
| GNP | granule neuron precursor |
| Hsp70 | Heat-shock protein 70 |
| IGL | internal granule layer |
| IP3 | inositol 1, 4, 5-trisphosphate |
| ITPR (IP3R) | inositol 1, 4, 5-trisphosphate receptor |
| LTD | long term depression |
| LTP | long term potentiation |
| MARCKS | Myristoylated alanine-rich C kinase substrate |
| MD cell | multidendritic cell |
| mGluR1 | metabotropic glutamate receptor, type 1 |
| ML | molecular layer |
| MLIs | molecular layer interneurons |
| mPKC | mutant Protein Kinase C |
| MW | molecular weight |
| *mwk* | moonwalker |
| P | postnatal day |
| PB | phosphate buffer |
| PC | Purkinje cell |
| PCL | Purkinje cell layer |
| PCR | polymerase chain reaction |
| PD | pseudosubstrate domain |
| PDK-1 | phosphoinositide-dependent kinase-1 |
| PF | parallel fiber |
| PIP2 | phosphatidylinositol 4, 5-bisphosphate |
| PKA | protein kinase A |

| | |
|---|---|
| PKC | protein kinase C |
| PKN | protein kinase N |
| PLC | phospholipase C |
| PM | preparation medium |
| PMA | phorbol-12-myristate-13-acetate |
| PNS | peripheral nervous system |
| PS | phosphatydylserine |
| qPCR | quantitative PCR |
| RGC | retinal ganglion cell |
| RL | rhombic lip |
| ROR α | retinoid-related orphan receptor α |
| RP | retinitis pigmentosa |
| RT | room temperature |
| SCA | spinocerebellar ataxia |
| sEPSP | slow excitatory postsynaptic potential |
| SGC | soluble guanylate cyclase |
| Shh | sonic hedgehog |
| SS | stock solution |
| TRPC3 | transient receptor potential cation channel, type 3 |
| UBN | unipolar brush neuron |
| VDCC | voltage dependent calcium channel |
| VDR | vitamin D kinase receptor |
| vGluT | vesicular glutamate transporter |
| *wdl* | waddles mice |

# *Summary*

Spinocerebellar ataxias (SCA) are a group of cerebellar diseases characterized by progressive ataxia and cerebellar atrophy accompanied by a loss of Purkinje cells. Within SCA, Spinocerebellar ataxia type 14 (SCA14) is a subtype inherited in an autosomal dominant fashion and caused by missense, deletion or splice site mutations in the PRKCG gene, which is coding for protein kinase C (PKC) gamma (γ) (Yabe et al., 2003). Previous studies in our lab have shown that chronic activation of PKC with the PKC activator phorbol-12-myristate-13-acetate (PMA) in organotypic cerebellar slice cultures drastically inhibits the growth and development of the Purkinje cell dendritic tree (Metzger et al., 2000). This result is intriguing and could mean that the degeneration of the Purkinje cell dendritic tree in SCA14 may be caused by the increased activity of PKC. Another study has shown most SCA14 mutations in PKCγ showed an increased activity of PKCγ in transfected cells (Adachi et al., 2008). These findings raise the possibility that SCA14 might be related to increased PKC activity. The mechanisms by which increased PKC activity may lead to inhibition of Purkinje cell dendritic growth and perhaps even to degeneration are not known and it is not clear which proteins are involved in PKC signalling related to dendritic growth in Purkinje cells.

In this project, we took advantage of a mouse model for SCA14, which was developed in our lab. In S361G mutated PKC gamma (mPKCγ) transgenic mice carrying a PKCγ transgene with a mutation from a human SCA14 allele we have shown that PKC activity is increased and Purkinje cell dendritic growth is strongly inhibited in slice cultures. We then tested whether other SCA14 mutations, in particular located in the C1 domain, would show similar effects on Purkinje cell dendritic development as the S361G mutation. We constructed several PKCγ mutants carrying mutations from human SCA14 patients and transfected them to Purkinje cells. We found that mutations in the catalytic domain caused severe inhibition of Purkinje cell dendritic development. In contrast, mutations in the C1 domain didn't show this effect. Our findings suggest that mutations in the PKCγ gene causing SCA14 can have different effects on PKC biological activity in Purkinje cells and that multiple mechanism may be involved in the pathogenesis of SCA14. In order to search for molecules involved in signal

transduction of mPKCγ, we performed a gene chip microarray analysis using mPKCγ transgenic mice and identified Carbonic anhydrase 8 (Car8) and type 1 inositol 1, 4, 5-trisphosphate receptor (IP3R1) as mRNAs and proteins being upregulated in mPKCγ transgenic mice. Furthermore, Car8 over-expression in Purkinje cells resulted in the formation of small, stunted dendritic trees in Purkinje cell similar to those after PKCγ activation implying that Car8 negatively regulates dendritic development. On the other hand, Car8 knocked down failed to rescue the morphology of the dendritic tree in Purkinje cells from mPKCγ transgenic mice or after pharmacological PKC activation. This indicates that Car8 is not directly downstream of mPKCγ signalling for Purkinje cell dendritic development but is likely to be part of a larger signalling network including PKCγ and IP3R1 which controls dendritic growth of Purkinje cells.

# 1. *Introduction*

## 1.1. Cerebellum and Purkinje cells

### 1.1.1. Cerebellum

The meaning of cerebellum is "little brain" because of its volume and its separation from the main brain. Indeed the cerebellum is much smaller compared to the cerebrum in mammalian species, which located dorsal to brain stem and is partially hidden by the large occipital lobes of the cortex. However, the surface area of the cerebellar cortex is larger as expected because of the complex folding. The area of the cerebellar cortex in humans is 1,128 cm$^2$, whereas that of the neocortex is 1,900 cm$^2$. The large area of cerebellum indicates that the cerebellum has important functions. It is well known that the cerebellum plays important roles in coordinated movement and motor learning. In addition, recent investigations have shown that the cerebellum is also involved in higher cognitive functions and mental health (Tanaka et al., 2009).
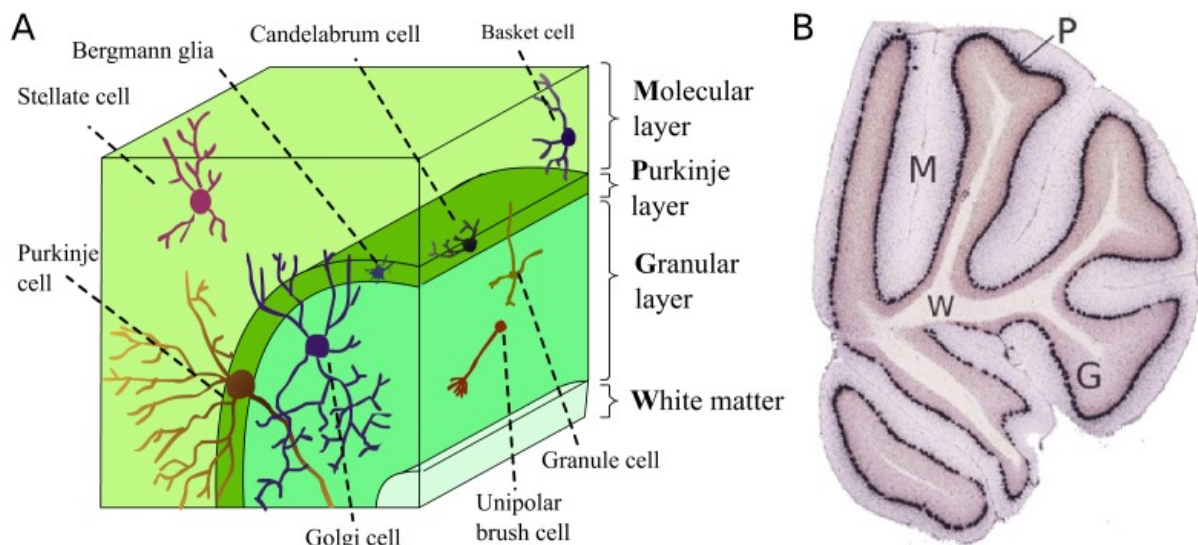
**Fig. 1 Cerebellar layers and cell types.**
(A) Cell types and their location across the cerebellar cortical layers. (B) The different layers can be easily discriminated. P - the Purkinje layer; G - the granular layer; M - the molecular layer; W - the white matter. Figure from (Kirsch et al., 2012).

Furthermore, human neuroimaging and animal behaviour studies have recently implicated that the cerebellum might have important roles in the processing of signals for perception and emotion (Bastian et al., 2011; D'Angelo et al., 2012; Schmahmann et al., 2010), particularly in circumstances involving predictions or timing. From those finding, the cerebellum is now recognized as an important part of brain for both motor and non-motor function.

Histologically, the cerebellar cortex consists of three layers (molecular layer, Purkinje cell layer and internal granular layer) and contains five major types of neurons (Purkinje, granule, basket, stellate and Golgi cells), which form a relatively simple and well characterized neuronal circuitry (Fig. 1). Within cerebellar cells, Purkinje cell integrate the signals from the all other neurons and are the only cell projecting outside the cerebellar cortex (Fig. 2)
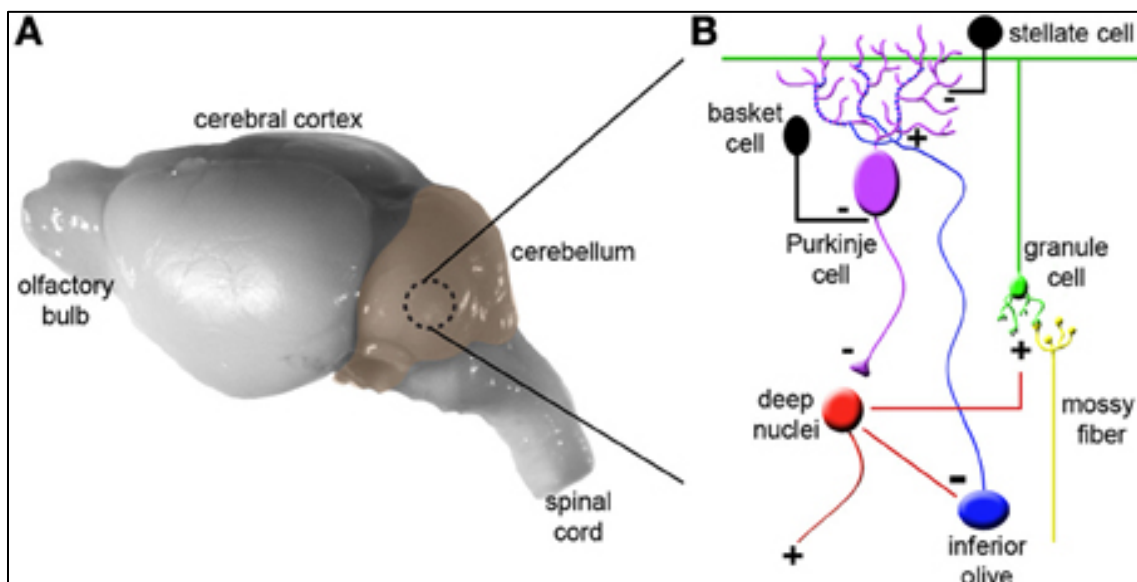


**Fig. 2 Cytoarchitecture and connectivity in the cerebellum**.
(A) Mouse brain shown from a lateral view with the cerebellum highlighted in color. (B) The basic cerebellar circuit is comprised of granule cells, Purkinje cells, stellate and basket cell interneurons, and deep nuclei. Afferent information is delivered to the cerebellum by climbing fibers and mossy fibers. The plus and minus signs indicate whether each synapse is excitatory or inhibitory. Note that inhibitory connections between the cerebellar nuclei and inferior olive complete the olivo-cortico-nuclear loop and excitatory projections from the cerebellar nuclei loop back to the cerebellar cortex. Panel (B) was modified from (Reeber et al., 2013). For simplicity we have not shown Golgi cells, unipolar brush cells, Lugaro cells, and candelabrum cells. Figure from (Reeber et al., 2013)

The Purkinje cell axons actually leave the cerebellar cortex and they synapse on deep cerebellar nucleus neurons where neurons represent virtually all of the output from the cerebellum, and there Purkinje cells inhibit neurons through secretion of γ-amino butyric acid (GABA). Therefore Purkinje cells are key neuron which connect cerebellar cortex and outside. Furthermore Purkinje cells have highly elaborate dendritic arbors and receive two types of excitatory inputs: parallel fibers (PFs) forming around 100,000-200,000 contacts on one Purkinje cell dendritic arbor and a single climbing fiber (CF) which makes around 500 climbing fiber synapses (Kitamura et al., 2012). The parallel fiber input is determined by mossy fibers, which originate from over two-dozen brain and spinal cord nuclei (Reeber et al., 2013). Approximately 25 million mossy fibers enter the cerebellum and synapse on approximately 50 billion granule cells (Andersen et al., 1992). Granule cells then converge massively (100,000 to 1) onto the dendrites of Purkinje cells. This striking expansion from mossy fibers to granule cells and the equally striking convergence from granule cells onto the Purkinje cells is believed to provide a computational benefit, that means the ability of the cerebellum to discriminate a large number of different patterns (Brunel et al., 2004). It is true that the major information flow in the cerebellum is mossy fibers-granule cells-Purkinje cells-cerebellar and vestibular nuclear neurons while it is also important flow that a climbing fiber codes an error signal reflecting the motor performance failure. When a motor performance comes up in failure, the excitatory signal conveyed by a climbing fiber works to depress the synaptic transmission between parallel fibers and a Purkinje cell, the phenomenon is called long term depression (LTD). Not only the excitatory inputs but also various inhibitory interneurons regulate the excitatory inputs onto Purkinje cells and specialized astrocytes called Bergmann glia maintain efficient synaptic signalling. Altogether Purkinje cells send inhibitory signals to the deep cerebellar nuclei, which control the final output of the cerebellum (White et al., 2013). An excitatory feedback projection terminating in mossy fiber-like endings exists between the deep cerebellar nuclei and the granule cell layer, and an inhibitory feedback connection is made from the cerebellar nuclei to the inferior olive. These two connections form parts of the nucleo-cortical and olivo-cortico-nuclear loops respectively (Chaumont et al., 2013). This canonical cerebellar circuit, which was once thought to be simple and synonymous with motor signalling, is now thought to have

13

underlying complexities that also mediate non-motor brain behaviours (Timmann et al., 2010).

### 1.1.2. Dendritic growth of Purkinje cells

Purkinje cells are one of the best known neurons in the cerebellar cortex due to their large somata and elaborated dendritic trees (Tanaka et al., 2009). Jan Evangelista Purkinje described Purkinje cells in 1837 and they were the first cerebellar neurons to be discovered. After his discovery, introduction of novel staining procedures such as Golgi techniques revealed the elaborated dendritic trees of Purkinje cells. Due to their unique features, Purkinje cells are an important model for searching mechanisms underlying neuronal development and degeneration. There are two important points. First, Purkinje cells develop their elaborate dendritic trees postnatally in the human and rodent brain (Kapfhammer et al., 2004). Second, Purkinje cells are critically affected in various neurological diseases ranging from genetic defects to acquired injury or poisoning (Sarna et al., 2003). These two points are shown below in detail.

*Purkinje cells development can be divided into four stages (Fig. 3, next page).*

a)  First, in midgestation, Purkinje cells are produced in the mouse from E11-E13 in the ventricular zone (Wang et al., 2001) and then migrate and position beneath the external granular layer.

b)  Second, in the neonatal period, the primitive processes of the Purkinje cell change to Purkinje cell with numerous thin perisomatic extensions develop.

c)  Third, in the second and third postnatal weeks, Purkinje cells form a primary dendrite and undergo rapid dendritic elongation and branching in the sagittal plane to elaborate their typical dendritic tree (Sotelo et al., 2009).

d)  Finally, as Purkinje cell dendrites branch, climbing fibers and parallel fibers contact specific sets of dendritic spines (Rossi et al., 1995).
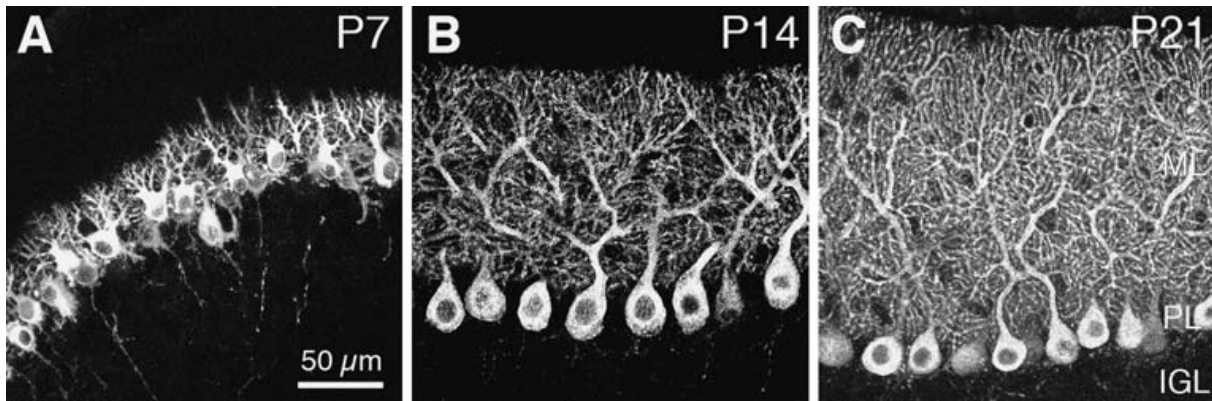
**Fig. 3 Dendrite formation of cerebellar Purkinje cells, postnatal development of the cerebellar cortex.**

Slices of mice on postnatal day (P) 7 (A), 14 (B) and 21 (C). (A) In the first postnatal week, there is little total dendritic expansion. (B and C) In the second and third postnatal weeks, Purkinje cells form a primary dendrite and undergo rapid dendritic elongation and branching. Pictures are from (Tanaka et al., 2009).

As for Purkinje cells dendritic development, most Purkinje cells have a single primary dendrite, whereas a few have two or more primary dendrites. During dendritic development, Primary dendrites extend toward the molecular layer (ML) and branch extensively to form secondary and tertiary dendrites. A large number of synapses are made between spines on tertiary dendrites and parallel fibers, which are the axons from granule cells and are the most numerous neurons in the central nervous system (CNS). In addition, as mentioned above Purkinje cells are innervated by climbing fibers which are axons from inferior olive neurons and also innervated by inhibitory interneurons (basket and stellate cells). Purkinje cell dendrites develop in a planar form and the plane is oriented perpendicular to the long axis of the cerebellum (Tanaka et al., 2009).

*Purkinje cells related diseases*

As mentioned, Purkinje cells dysfunction results in multiple cerebellar diseases. Ataxia is a classical sign of cerebellar dysfunction. A unifying cellular phenotype observed in the nervous system of ataxic mice and humans, regardless of the type of ataxia, is extensive Purkinje cell degeneration. More details of cerebellar disease are given in the spinocerebellar ataxia chapter.

**1.2. Spinocerebellar ataxia**

1.2.1. Overview

The word "ataxia" is from Greek meaning "loss of order," it is used clinically to describe an aberrant regulation of limb movements with poor coordination between limbs. Cerebellar ataxia is the most common form of ataxia and is caused by dysfunction either within the cerebellum or in its afferent and efferent pathways. Spinocerebellar ataxia (SCA) is caused by anomalous function of the spinocerebellum, the part of the cerebellar cortex that receives somatosensory input from the spinal cord (Carlson et al., 2009). Although there are sporadic forms of SCA, the term is most often used to refer to the hereditary forms, and in particular the autosomal dominant forms. The autosomal dominant SCAs are typically late-onset, progressive, and often fatal neurodegenerative disorders. They are characterized by cerebellar ataxia and frequently other symptoms related to dysfunction of additional neural pathways (Duenas et al., 2006).

Currently 42 SCA types are known (the number is continuously increasing), which are numbered from SCA1 to SCA42 (SCA9 is unassigned, SCA15 and SCA16 were linked to the same chromosomal locus, SCA24 proved to be recessively inherited, SCA33 has not been published). Their prevalence in Europe is estimated at approximately 3:100,000, whereby SCA1, SCA2, SCA3 and SCA6 represent the most frequent SCAs worldwide (Kay et al., 2012). It is also known that prevalence of different SCAs shows a regional difference, for example SCA1 is the dominant SCA in Italy, SCA3 in Germany, and SCA6 in Japan.

The clinical picture of SCAs is heterogeneous with various symptoms. The common symptoms of the SCAs result from damage to the cerebellum and/or its neuronal connections: ataxia of the limbs, head and trunk, dysarthria and cerebellar oculomotor disorders (Paulson, 2009: Soong et al., 2007). These are often accompanied by extracerebellar symptoms, which sometimes may be characteristic for a given SCA and thus may help in differential diagnosis. They can also include Parkinsonism, retinal degeneration, aspiration, psychiatric symptoms, as well as dysfunction of touch, sight, hearing and proprioception and are accompanied by diverse extracerebellar neurodegeneration patterns (Scho¨ls et al., 2004)**.**

### 1.2.2. Spinocerebellar ataxia 14

SCA14 is a rare spinocerebellar ataxia which is inherited in an autosomal dominant fashion. It is caused by missense point mutations, deletions or splice site mutations in the PRKCG gene (Yamashita et al., 2000), coding for protein kinase C gamma (PKCγ). Now more than 30 types of missense mutations or deletions in PRKCG gene are found as SCA14 related mutations (Fig. 4, next page). PKCγ is primarily expressed in CNS and dominantly expressed in cerebellar Purkinje cells, which is an important factor in cerebellar development (Yabe et al., 2003). General clinical manifestations of SCA14 usually include ataxia, dysarthria, oculomotor disturbance, vertigo, facial myokymia and myoclonus. Less frequent symptoms are a decreased vibration sense, depression, psychosis as well as cognitive decline and, in younger patients, tremor and chorea (Vlak et al., 2006). SCA14 begins in childhood to late adulthood and the lifespan is normally not shortened. In clinics, no features of SCA14 are pathognomonic; therefore, diagnosis depends on molecular genetic testing (Chen et al., 2005). In vivo brain MRI scans showed primarily vermal cerebellar degeneration and post-mortem neuro-histological-pathological studies have demonstrated a pronounced loss of cerebellar Purkinje cells in SCA14 patients (Brkanac et al., 2002).
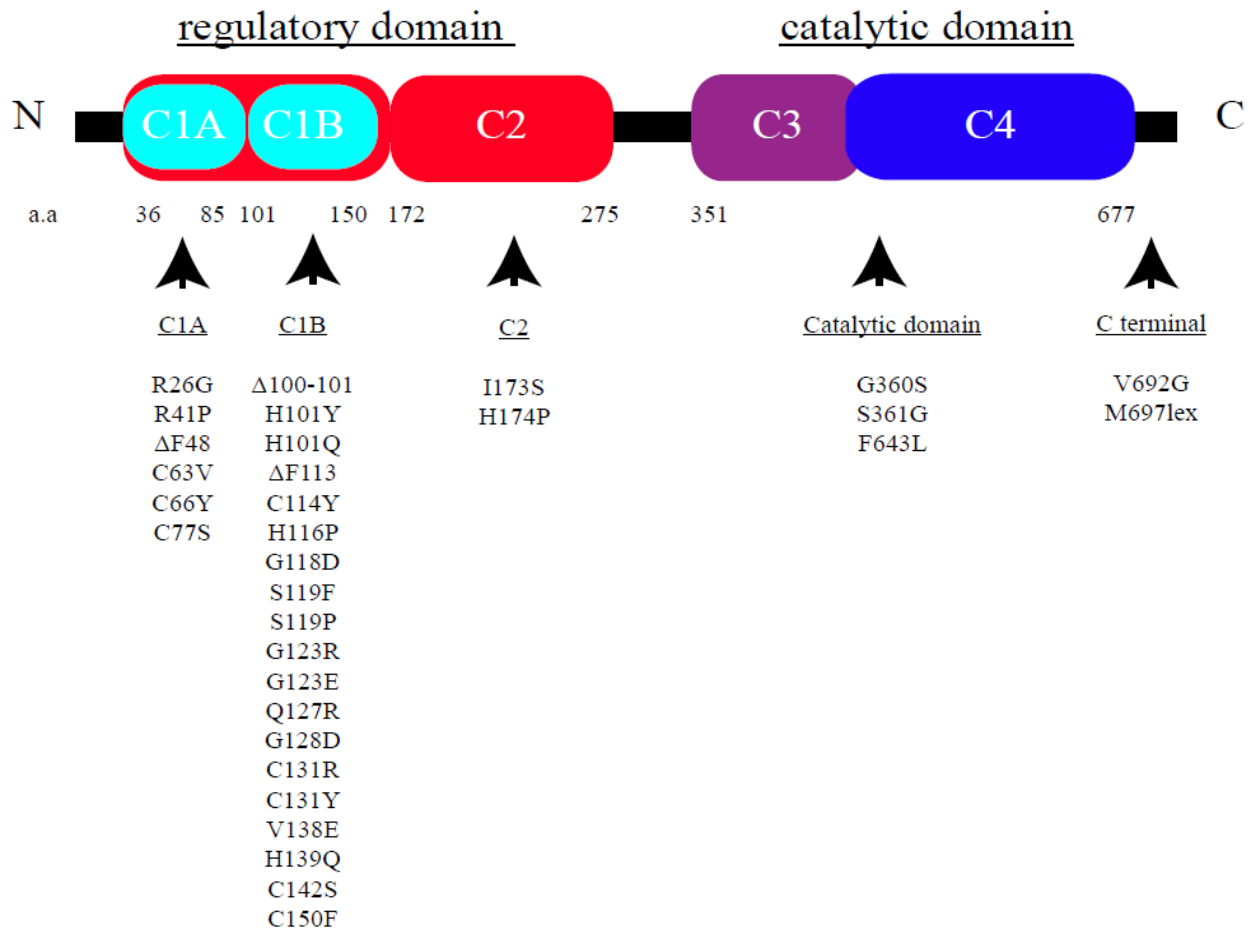
**Fig. 4 SCA14 mutations found in human patients.**
Illustrations of each domain mutations in PKCγ protein. PKCγ consists of an N-terminal regulatory and a C-terminal catalytic kinase domain. The regulatory domain of PKCγ contains two conserved domains, the diacylglycerol (DAG) binding C1 domain and the $Ca^{2+}$ binding C2 domain. The C1 domain is subdivided into the C1A and C1B domains having six conserved cysteines and two histidines in the typical core structure that coordinates two zinc ions. So far thirty two point mutations and deletions were found in SCA14 families.

*Mutant PKCγ Pathogenesis*

As mentioned, more than 30 types of mutations or deletions in PRKCG gene cause SCA14 (Fig. 4). It is not known in which way the different mutations of PKCγ cause SCA14. Remarkably, PKCγ-deficient mice show only mild ataxia and no gross morphological abnormalities in the cerebellum (Chen et al., 1995; Kano et al., 1995),

indicating that a toxic gain of function, dominant negative function or gain of function, rather than loss of function of PKCγ causes SCA14. One possibility is toxic function of PKCγ due to PKCγ protein aggregation. It was reported that mutant PKCγ protein aggregates in the cytoplasm of cultured cells transfected with mutant PKCγ expression vectors (Doran et al., 2008; Lin et al., 2007; Seki et al., 2007) but the role of these aggregates in the pathogenesis of SCA14 is still not clear. When mutant PKCγ transfected cells are treated with an inducer of autophagy, cultured cells demonstrated an accelerated clearance of aggregates, indicating that autophagy contributes to the degradation of mutant PKCγ (Yamamoto et al., 2010). However, in primary cultures of Purkinje cells transfected with mutant PKCγ, abnormal dendritic development of Purkinje cells also occurred independent of aggregation (Seki et al., 2009). There is another report that amyloid-like oligomers and fibril formation of mutant PKCγ may contribute to SCA14 pathogenesis (Takahashi et al., 2015). But they mentioned endogenous PKCγ itself may form amyloid-like aggregates to amplify their local signals in some physiological PKC-dependent pathways, so PKCγ protein aggregation thus might partially contribute to SCA14 but the mechanism is unclear and it's not only the reason of SCA14 pathogenesis.

Another possibility is a dominant negative activity of PKCγ or gain of function of PKCγ. PKCγ is a serine-threonine kinase and it is well known that some mutant kinases have dominant negative activities. Studies of the effect of SCA14 related mutations on kinase activity have been in several groups, but a dominant negative effect has not been shown (Lin and Takemoto, 2007; Seki et al., 2005; Verbeek et al., 2005).

On the other hand, two PKCγ mutations were characterized functionally in vitro and were shown to increase PKCγ catalytic activity, linking Purkinje cell degeneration to a potential gain of function phenotype of PKCγ (Verbeek et al., 2005). Subsequently, Adachi et al. found that 19 out of the 20 tested mutations showed an increased constitutive activity of PKC and increased $Ca^{2+}$ levels in the cytoplasm, which suggests that a gain of function, rather than toxic or dominant negative of function, of PKCγ could underlay the pathology of SCA14 (2008).

*Molecular Genetic Pathogenesis*

Several groups are searching for proteins interacting with mutant PKCγ because PKCγ is a well-known signaling kinase and key protein for several kinase signaling cascades. However it has been found that many PKCγ substrates proteins are not directly associated with ataxia or Purkinje cell loss, such as metabotropic glutamate receptor 5, non-muscle myosin heavy chain II-B, Myristoylated alanine-rich C kinase substrate (MARCKS), GSP43/B-50, HMG-I, RC3/neurogranin and glycogen synthetase (Xiao et al., 2000). Later, Aprataxin (APTX) which is a DNA repair protein and associated with autosomal recessive ataxia with oculomotor apraxia type 1 (AOA1) (Moreira et al., 2001), was found to be a preferential substrate of mutant PKCγ which inhibited nuclear import of APTX, and thus sensitized cells to oxidative stress-induced DNA damage, leading to cell death (Asai et al., 2009). This observation suggests that the pathogenesis of SCA14 may involve altered phosphorylation of proteins in PKCγ dependent pathways and show one path mechanisms that phosphorylated PKCγ increased oxidative stress-induced DNA damage which cause cell death (Asai et al., 2009; Doran et al., 2008). The ubiquitin-proteasome pathway has been implicated in this process (Seki et al., 2007). Furthermore, the observation that mutant PKCγ fails to phosphorylate TRPC channels resulting in sustained $Ca^{2+}$ entry into the cells indicates that altered phosphorylation of substrates proteins of PKCγ links to a role for abnormal $Ca^{2+}$-mediated signaling in neurodegeneration (Adachi et al., 2008). Most of these studies were done in cultured cells with transient overexpression of mutant PKCγ and the detailed molecular mechanisms leading to SCA14 in Purkinje cells expressing mutant PKCγ are still unclear. There is one report of a transgenic mouse model of SCA14 which ubiquitously express human mutant cDNA with the p.His101Tyr-PKCγ mutation, showing loss of Purkinje cells at the age of four weeks and stereotypic clasping responses in the hind limbs (Zhang et al., 2009). Previous work showed that His101Tyr-PKCγ mutation has dominant negative effects on endogenous wild type PKCγ enzyme activity which leads to uncontrolled, open gap junctions in cells overexpressing His101Tyr-PKCγ mutation (Lin et al., 2007). They suggested that loss of control of gap junctions may further propagate ER stress-linked cell death signals in Purkinje cells (Zhang et al., 2009). But this study is not completed and further investigations are needed.

### 1.3. PKC gamma and Purkinje cell dendritic tree development

#### 1.3.1. Overview

The Protein Kinase C (PKC) family was discovered by Yasutomi Nishizuka in 1977 (Inoue et al.,1977). After this finding, numerous signalling cascades were discovered and PKC was recognized as one of the important kinase for regulation of other signaling pathways, gene expression, secretion, and modulation of ion channels as well as cell growth, stress, autophagy, which related to many diseases.

PKC occupies the tip of a branch of the AGC kinases from which the related kinases protein kinase N (PKN), Akt/PKB, p70 S6 kinase, and the phosphoinositide-dependent kinase-1 (PDK1) diverge (Newton,1995) (Fig. 5A, next page).

PKCs are actually a family of serine/threonine kinases with at least ten different isoforms being identified by now. The isoforms can be split into three families according to their requirement for different co-factors (Fig. 5B, next page):

1. The conventional, or classical (c) PKCs: α , βI, βII and γ ,
2. The novel (n) PKCs: δ, ε, η and, θ
3. The atypical (a) PKCs: ζ and ι (referred to as PKCι in murine systems).

Differential splicing gives rise to the two forms of β: βI and βII, which differ only in their extreme C-terminal end, while a constitutively active form of PKCζ is expressed from an internal promoter within the PKCζ gene and is known as PKMζ. A further isoform, PKCμ , was originally thought to belong to the PKC family but is now referred to as protein kinase D (PKD) (Rozengurt, 2011). PKD is serine/threonine protein kinases and the initial description of PKD as an atypical isoform of PKC contributed to a perception that PKD belongs to a subfamily of PKC. However, it was found that the catalytic domain of PKD has highest sequence homology with myosin light chain kinase and CAMKs and now PKD1, 2 and 3 are classified as a new protein kinase family within the CAMK group, separate from the AGC group (Rozengurt, 2011).

Within the PKC family, PKCγ is a member of the classical PKCs (cPKC) which was first isolated as one of more than 10 PKC cDNAs from a brain cDNA library. The cPKCs (PKCα, PKCβ, and PKCγ) are activated by diacylglycerol (DAG) and $Ca^{2+}$ in the presence of phosphatydylserine (Nishizuka et al.,1995). The function of the different domains is explained in the next chapter.
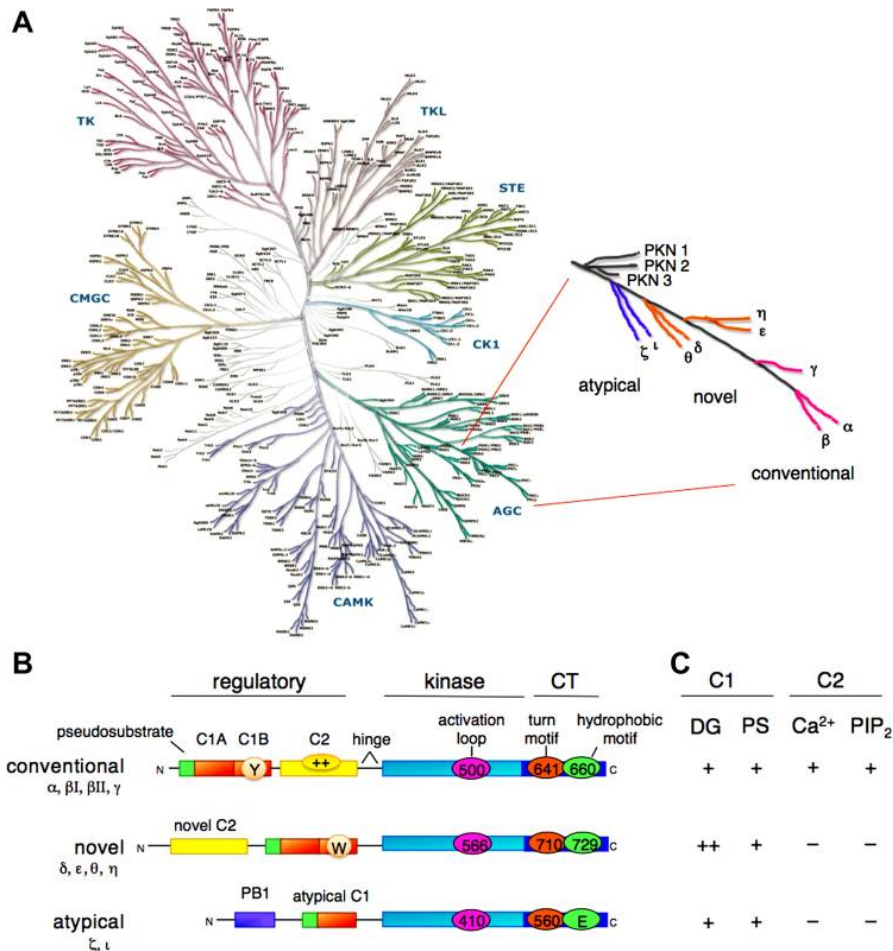
**Fig. 5 Protein kinase C (PKC) family members, showing position on branch of AGC kinome, domain composition, and cofactor dependence.**

(A)  Human kinome, showing the position of the AGC kinases (bottom right). PKC isozymes (enlarged on right) are poised on a branch that includes Akt, p70 S6 kinase, and PDK1 (phosphoinositide-dependent kinase 1). The PKN family diverges, then the atypical PKC isozymes, the novel PKC isozymes, and finally, most divergent, the conventional PKC isozymes. (B) Domain composition of PKC family members, showing pseudosubstrate (green rectangle), C1 domain [orange rectangle; Y/W switch that dictates affinity for diacylglycerol (DAG)-containing membranes indicated by circle in C1B domain], C2 domain [yellow rectangle; basic patch that drives binding to PIP2 (phosphatidylinositol-4,5-bisphosphate), indicated by oval with ++], connecting hinge segment, kinase domain (cyan), and carboxyl-terminal tail (CT; dark blue rectangle). Also shown are the 3 priming phosphorylations in the kinase domain and CT, with numbering indicated for PKCβII, PKCε, and PKCζ (note atypical PKC isozymes have Glu at phospho-acceptor position of hydrophobic motif).
(C) Table showing dependence of each family cofactors, diacylglycerol (DAG), and phosphatidylserine (PS) in C1 domain and $Ca^{2+}$ and PIP2 in C2 domain. Picture from (Newton, 2010)

### 1.3.2. PKC Domain Function

In the following I will present the most important aspects of the different PKC domains (Zeng et al., 2012). The major domain structure was already shown in Fig. 4 and Fig. 5.

*PS: Pseudosubstrate Domain*

The pseudosubstrate region interacts with its kinase domain, forming a hairpin structure which maintains the enzyme in a closed/inactive conformation, therefore this domain functions is a suppressor of its kinase activity. The pseudosubstrate site is resembles a PKC substrate with an alanine substitution at the phosphoacceptor site therefore it cannot be phosphorylated. The blocking property of the pseudosubstrate domain for kinase activity has been exploited in the development of specific PKC inhibitors (Kirwan et al., 2003). The PKMζ form of PKCζ lacks this pseudosubstrate domain, which is thought to be in a constitutively active formation (Hernandez et al., 2003).

*C1: DAG/Phorbol Ester Binding Domain*

For cPKCs and nPKCs this domain confer upon the ability to bind DAG/phorbol esters, within the C1 domain the C1b region is thought to be critical for this function. These domains were originally discovered in PKCs itself but are now known to be found in multiple other DAG-binding proteins (Colon-Gonzalez et al., 2006). In typical PKC (cPKCs and in nPKCs), the C1 domain is present as a tandem repeat (C1a and C1b) which is a cysteine-rich zinc finger structure. The DAG-binding site is a hydrophilic cleft formed from two pulled apart β-sheets, whereas the C1 domain surface surrounding the binding cleft is hydrophobic. Once DAG binds to DAG-binding site, the hydrophobic surface is completed which drives conformational change in the overall protein structure. In the atypical PKC isozymes (aPKCζ and aPKCι), the ligand-binding pocket of the C1 domain does not allow the entry of DAG nor phorbol esters (Kazanietz et al.,1994; Pu et al., 2006). C1b is also found to be the key region involved in the stereospecific interaction of PKC with phosphatydylserine (PS) (Johnson et al., 2000), although the C2 domain interacts with anionic phospholipids in a $Ca^{2+}$ dependent manner. In PKCε, there is a 22 amino acid actin-binding sequence located between

the C1a and C1b domains that is unique to this PKC isoform, while the C2 domain appears to play an important role in the interaction of cPKC-α, -βI and -βII with F-actin (Slater et al., 2000).

*C2: Binds $Ca^{2+}$ and phospholipids*

The presence of aspartate residues in the C2 domain of cPKCs confers upon them the ability to bind $Ca^{2+}$, which is then crucial for activation of the kinase. nPKC isozymes do not have a $Ca^{2+}$-regulated C2 domain therefore their activation only by DAG is possible because of a single residue change in their C1B domain that allows them to bind DAG-containing membranes with two-fold greater affinity for DAG than cPKCs (Giorgione et al., 2006). In cPKCs both the C2 and C1 domains are involved in the interaction of activated PKC with the plasma membrane: C1 in a DAG/PMA and phospholipid dependent manner and C2 in a $Ca^{2+}$ dependent manner. aPKCs do not have a C2 domain but have a PB1 domain.

*Phox/Bem1 (PB1): a Distinctive Characteristic of the aPKCs*

This scaffolding domain of approximately 80 amino acids is found in many different proteins and are grouped into three types: type I (or type A), type II (or type B), and type I/II (or type AB). The type I domain group contains a conserved OPCA motif that interacts with a conserved lysine residue from a type II domain. The type I/II PB1 domain, containing both the OPCA motif and the invariant lysine, is present in the aPKCs (Moscat et al., 2009). This domain is important for interaction with other proteins.

*V3: Hinge Region*

The third variable region (V3) region forms the "hinge" of the molecule, allowing the pseudosubstrate to interact with the kinase domain (see above). The V3 region is susceptible to proteolytic cleavage (Liu et al.,1998), which allow the catalytic domain to be free and generates a constitutively active form of the kinase in some PKC isoforms (Steinberg, 2008). The V3 region might also be important region for the translocation of some PKC isoforms but so far very little is still known about the function of this region. (Quittau-Prevostel et al., 2004).

*Catalytic Domain*

This domain is highly conserved between the PKCs, and it is also highly conserved between many families of kinases and well conserved over the species, meaning this region is of course crucial and also implying poor specificity over isoforms and the species. There are two or three major conserved kinase domains and it is optimal when the kinase domain is appropriately phosphorylated on at least two (ζ and ι) or three (α, β, γ, δ, ε, η and θ) sites. These phosphorylations play important role for stabilising the active catalytic conformation (Newton, 2010).

*Control of PKC activation by membrane-targeting following binding of second messengers*

Activation of cPKC requires the binding of second messengers to the C2 and C1 regulatory domains. External stimuli acting upon membrane receptors (i.e. G-protein-coupled receptors or receptor tyrosine kinases) initiate a cascade of events that includes the hydrolysis of phosphatidylinositol 4, 5-bisphosphate (PIP2) into the $C^{2+}$-mobilizing messenger inositol 1, 4, 5-trisphosphate (IP3) and DAG. An increase in the intracellular $Ca^{2+}$ concentration after IP3 production which bind to IP3 receptor and increase cytoplasm $Ca^{2+}$ induces $Ca^{2+}$ binding to the C2 domain of the cytosolic PKC. The C2 domain serves as a membrane-targeting molecule that binds anionic phospholipids in a $Ca^{2+}$ dependent fashion (Mellor and Parker,1998). Therefore, cPKC with bound $Ca^{2+}$ moving by diffusion in the cytoplasm will associate to the plasma membrane (Schaefer et al., 2001). It will then diffuse in the plane of the membrane until it encounters a DAG molecule. Its C1 domain will bind DAG, establishing a high-affinity interaction between cPKC and the plasma membrane. This interaction induces release of the auto-inhibitory pseudosubstrate domain from catalytic domain, switching cPKC to the open conformation. cPKC is then a mature active enzyme that is able to interact with its substrate and initiate the signal transduction processes.

*Control of PKC activation by phosphorylation*

In addition to allosteric activation, phosphorylations of Serine/Threonine or Tyrosine residues in distinct PKC isoforms control kinase activity, cellular localisation and function. First evidence that PKC is phosphorylated in vivo appeared in 1985 (Fry et

al., 1985). PKC is first synthesized as an inactive state, dephosphorylated precursor with an apparent molecular weight of 74 kDa; this was chased to a transient 77 kDa phosphorylated form and then to the final 80 kDa mature form (Dutil et al., 1994). In the cPKCs, three priming phosphorylation sites were identified and phosphorylation of the activation loop site was shown to be essential for cPKCs catalytic activity (Cazaubon et al., 1994). Phosphorylation of the two carboxyl-terminal sites plays a more complex role in the control of cPKC phosphorylation rate and important for keeping the kinase in a phosphatase resistant state (Bornancin and Parker, 1996).

*Control of PKC activation by desensitization mechanisms*

Down-regulation of cPKC activity and the consequent termination of signalling are achieved by several mechanisms. Activation of cPKCs and nPKCs with their agonists, such as phorbol esters, eventually leads to their dephosphorylation and subsequently rapid degradation, which is mainly thought via the ubiquitin-proteasome pathway. PKC is ubiquitinated after the treatment of cells with their agonists, phorbol esters or bryostatin, although the precise compartment where PKC is dephosphorylated remains to be determined (Hansra et al., 1999).

Dephosphorylated cPKCs can be also rescued from degradation. Heat-shock protein 70 (Hsp70) binds dephosphorylated PKCβII at its turn motif preventing its degradation. PKCβII can be then re-phosphorylated and cycled back into the pool of functional enzymes (Gao et al., 2002) (Fig. 6, next page).
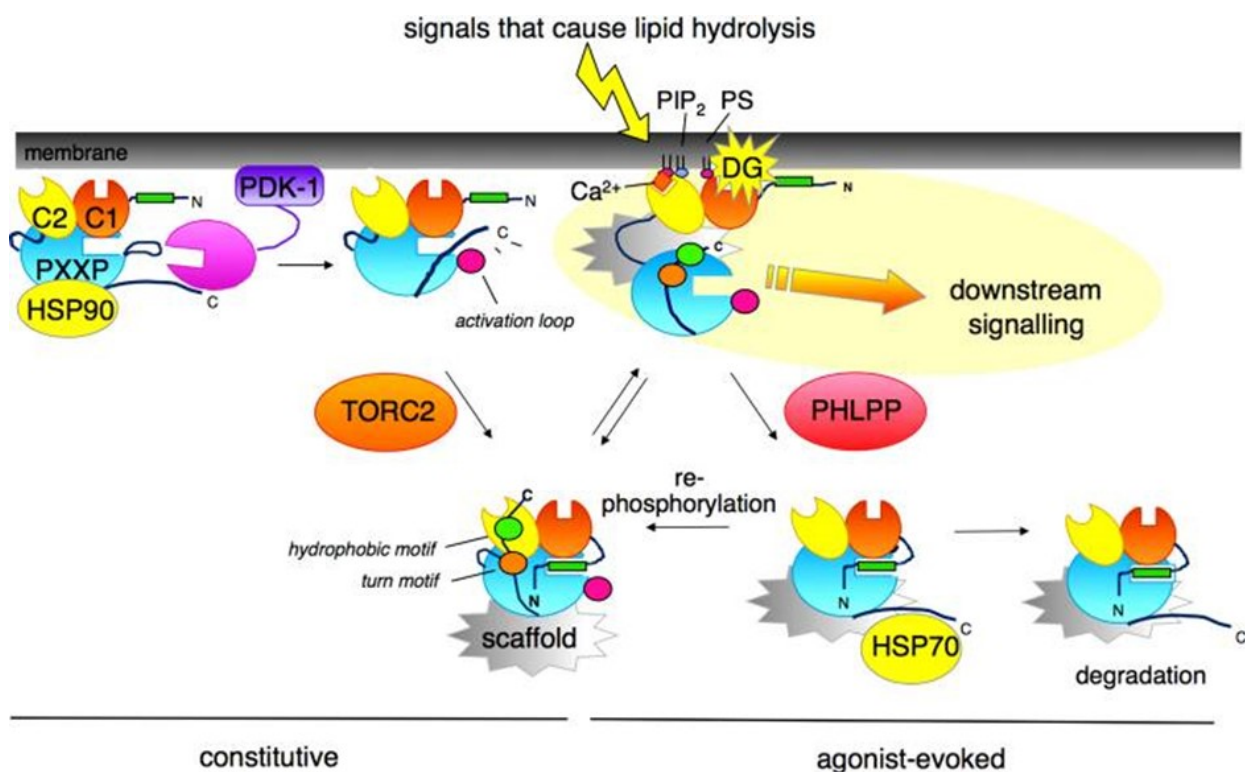
**Fig. 6 Model for the life cycle of PKC, from biosynthesis to degradation.**
Newly synthesized PKC associates with a membrane fraction, where it is processed by a series of ordered and tightly coupled phosphorylations. Heat shock protein-90 (HSP90) binds to the PXXP clamp in the kinase domain, an event required for priming phosphorylations. Two upstream kinases control priming phosphorylations: PDK-1, bound to the exposed carboxyl terminus of newly synthesized PKC, phosphorylates the activation loop (pink circle); this step appears to be first, and necessary for the processing PKC. The mTORC2 complex promotes the phosphorylation of the turn motif (orange circle), second phosphorylation event, and hydrophobic motif (green circle), the final phosphorylation event. The fully phosphorylated mature PKC localizes to the cytosol with the pseudosubstrate (green rectangle) occupying the substrate-binding cavity. Signals that cause lipid hydrolysis recruit PKC to membranes. For conventional PKC isozymes, binding of $Ca^{2+}$ to the C2 domain recruits them to the plasma membrane via interaction with PIP2, an event that allows efficient binding of the membrane-embedded ligand DAG. For novel PKC isozymes, the intrinsic affinity of the C1 domain is sufficiently high to allow direct recruitment to membranes by agonist-evoked levels of DAG. Membrane-bound PKC adopts an open conformation, in which the pseudosubstrate is released from the kinase domain, allowing downstream signals. This open conformation is sensitive to dephosphorylation: the phosphatase (PH domain leucine-rich repeat protein phosphatase) dephosphorylates the hydrophobic motif, an event that shunts PKC to the detergent-insoluble fraction where it is further dephosphorylated and degraded (bottom right species). Figure from (Newton, 2010)

27

In a rat intestinal cell line, two distinct mechanisms of PKCα down-regulation have been shown to co-exist (Leontieva and Black, 2004). One mechanism is ubiquitin–proteasome-dependent mechanism. Exposure to the PKC agonist PMA induced desensitization by ubiquitination of the fully phosphorylated enzyme at the plasma membrane and subsequent degradation at the proteasome. Interestingly, in the same intestinal cell line, exposure to a different PKC agonist, bryostatin 1, induced PKCα desensitization not only by the ubiquitin–proteasome-dependent mechanism just mentioned, but also through a caveolae-dependent internalization of the active enzyme followed by dephosphorylation and degradation. Corinne et al. showed that the PKCα associated endosomes co-localize with caveolin and that cholesterol binding drugs could inhibit PKCα downregulation, leads to the conclusion that PKCα has been degradated through a caveolae-mediated process (2000). It was also shown in other cell types, such as MCF7, to be trafficked from the plasma membrane to an endosomal compartment through caveolae in its active phosphorylated form (Prevostel et al., 2000). Active PKCα is found to be sorted to a Rab-11-positive perinuclear compartment (Becker et al., 2003), where finally PKCα is thought to be dephosphorylated and degradation. Ubiquitination of fully phosphorylated active PKCα followed by degradation, as described above, is unusual in this case. Indeed, dephosphorylation appears to precede degradation, which can then proceed through the ubiquitin–proteasome degradation mechanism (Lee et al., 1996).

*General PKC signal transduction*

cPKC is expressed universally in every tissue but expression levels of the isoforms of cPKC are different throughout tissues and cells. PKC typically phosphorylates serine or threonine residues in basic sequences but displays significantly less specificity compare to protein kinase A (Kennelly et al., 1991). There are several well-known substrates such as Myristoylated alanine-rich C kinase substrate (MARCKS) protein, MAP kinase, translation inhibitor protein IκB, Vitamin D kinase receptor (VDR), Raf kinase and the EGFR. In addition, activated PKC was shown to regulate transcription, and to be involved in learning and memory in neural cells as well as many other functions. It is evident from these findings that PKC has a central role in intracellular signal transduction (Newton, 1995).

### 1.3.3. Protein kinase C gamma

*Overview*

Among PKC subtypes, the γ isoform of PKC (PKCγ) is specifically expressed in the CNS and is especially abundant in cerebellar Purkinje cells (Saito et al., 1988; Saito and Shirai, 2002). In the spinal cord, PKCγ is an important intracellular signalling kinase found in a specific subset of excitatory interneurons in the inner region of lamina II and in axons of the corticospinal tract (Malmberg et al., 1997; Mori et al., 1990; Polgár et al., 1999). In the Purkinje cells of the cerebellum, PKCγ is involved in modulation of synaptic plasticity for long term potentiation and depression (Saito and Shirai, 2002). PKCγ-deficient mice showed that the developmental elimination of multiple CF innervation of Purkinje cells is impaired, which suggests that PKCγ is involved in the process of pruning CF synapses from developing Purkinje cells (Kano et al.,1995). Moreover, the PKCγ signalling in Purkinje cells negatively regulate the nonselective transient receptor potential cation channel type 3 (TRPC3), the opening of which elicits slow excitatory postsynaptic potentials at CF-Purkinje cells synapses (Shuvaev et al., 2011).

*PKC gamma genomic and protein structure*

The cDNA for PKCγ was sequenced in 1986 together with those of PKCα and PKCβ, then the genomic structure of PKCγ and its chromosomal mapping were analysed. The human and mouse PKCγ genes are localized on chromosomes 17ql3.4 and 7, respectively. The PKCγ gene is approximately 24.4 kb long and composed of 18 small exons varying between 32 and 406 bp in size (Kofler et al., 2002). The AUG translation initiation site for open reading frames of PKCγ is localized in exon 1 as for other cPKCs. The 5'- flanking region of the mouse PKCγ gene lacks TATA and CAAT boxes but contains binding sites for several transcription factors (Takanaga et al., 1995) which indicates expression level of PKCγ is regulated by these transcription factors.

PKCγ has C1 and C2 domains which bind DAG and $Ca^{2+}$, respectively as mentioned above (Bittova et al., 2001). Both second messengers are necessary for the activation of cPKCs (Nishizuka et al., 1995). The C1 domain of PKCγ consists of C1A and C1B, both of which bind DAG or its agonist with high affinity (Irie et al., 2002). The structures of the PKCα, PKCβ. and PKCγ C1 domains are very similar and show high homology,

on the other hand, C2 domains which bind to $Ca^{2+}$ show quite low homology. The functional differences resulting from this low homology are unclear, but it is shown that PKCγ have higher affinity to $Ca^{2+}$ than the other isoforms in the presence of phosphatydylserine (Saito and Shirai, 2002).

*PKC gamma specific functions in nervous system*

The generation of PKCγ knockout mice was reported in 1993 by Abeliovich et al. (1993). The PKCγ deficient mice are viable and their brain anatomy is rather normal when they are observed by light microscopy. Behaviours such as grooming, feeding and mating seem normal, although the mutant mice moved with a mild ataxic gait. It was also examined whether lack of PKCγ effected for long term potentiation (LTP) in the CA1 region of the hippocampus (Abeliovich et al., 1993). Although synaptic transmission evoked by stimulating hippocampal axons in PKC gamma deficient mice is indistinguishable from the wildtype mice, LTP is rarely induced by the commonly used high frequency stimulation in PKCγ deficient mice. While, the knockout mice can learn to carry out hippocampus-dependent tasks, although they exhibit mild deficits in spatial and contextual learning (Abeliovich et al., 1993). On the other hand, the involvement of PKCγ in long term depression (LTD) induction is strongly suggested by reports which show that 1) LTD is blocked by PKC inhibitors, 2) PKC activators such as phorbol ester induced depression of synaptic transmission, and 3) PKCγ is the major PKC isotype in Purkinje cells (Saito and Shirai, 2002). Thus, the deletion of PKCγ would be predicted to abolish LTD. It was also reported that in the L7-PKCI transgenic model in which the pseudosubstrate PKC inhibitor was selectively expressed in Purkinje cells under the control of the pcp-2 (L7) gene promoter therefore the PKC activity is specifically inhibited in the Purkinje cells, result that establishment of LTD at the parallel fiber-Purkinje cell synapses was impaired (Lefort et al., 2015). However, LTD is fully inducible in cerebellar slices of the PKCγ deficient mice (Chen et al.,1995). It is noteworthy that a PKC inhibitor peptide (PKC 19-36) completely blocks LTD in wild-type mice but does not abolish LTD in PKCγ deficient mice (Hémart et al., 1995). This suggests that PKCγ plays a crucial role in LTD in normal condition or wild type of mice but once PKCγ is not available in cells, other isotypes of PKC or other kinases can compensate for the PKCγ deficiency. This compensation for the lack of PKCγ by

other isotypes of PKC or other kinases makes it difficult to elucidate the specific function of PKCγ in PKCγ deficient mice. PKCγ deficient mice exhibit impaired motor coordination but are fully capable of discrete motor learning (Kano et al., 1995). In mature PKCγ deficient mice, 40% of Purkinje cells remain innervated by multiple CFs, while normally these multiple innervations are eliminated during the 3rd week after birth in wild-type mice, which result in one-to-one innervation between the Purkinje cells and CFs. This result suggest that PKCγ is also crucial for one-to-one innervation between the Purkinje cells and CFs. There are several reports of other knockout mice which exhibit this persistent multiple innervation of Purkinje cells by CFs. Mice deficient in metabotropic receptor 1 (mGluRI) (Kano et al., 1997) or phospholipase C (PLC) (Kano et al., 1998) show a similar phenotype of multiple CFs innervation and motor discoordination. Taken together, the results from PKCγ deficient mice as well as mGluRI or PLC deficient mice suggest that an mGluR1-PLC-PKCγ signaling pathway in cerebellar Purkinje cells is involved in the elimination of CFs and play important role for motor coordination with persistent multiple innervation of Purkinje cells by CFs.

*Modulation of receptor function*

As mentioned above, PKCγ is specifically expressed in CNS and abundantly expressed in Purkinje cells. It is also reported that PKCγ is abundant in the dorsal horn of the spinal cord and has been suggested to be important in sensory signal processing including pain. Several studies have shown that activation of μ-opioid receptors in the spinal cord induce prolonged PKC translocation (Narita et al., 1994) and that inhibition of PKC prevents the development of anti-nociceptive tolerance to μ-opioid agonists (Narita et al., 2001). Within PKC isotypes, the evidence that selective μ-opioid receptor agonists increase the amount of membrane-associated PKCγ but no other PKC isotypes, and desensitize μ-opioid receptor mediated G-protein activation has been reported (Narita et al., 2001). This showed the involvement of PKCγ signaling for pain. Using PKCγ deficient mice, it has been demonstrated that activation of PKCγ is critical for the development of morphine induced reinforcing and enhancement of nociceptive responses (Martin et al., 1999). Also the result from PKC inhibitor, Gö6976 treatment, showed that PKC is involved in morphine mediated c-Jun N-Terminal Kinase activation, which lead G protein-coupled receptor desensitization (Kuhar et al., 2015).

Furthermore, PKCγ deficient mice failed to develop a neuropathic pain syndrome after partial nerve section (Malmberg et al., 1997). These findings suggest that PKCγ has crucial role for induction of the psychological dependence on morphine and the development of a PKCγ-specific inhibitor may enable us to alleviate pain by protecting the tolerance. It is also interesting that epinephrine-induced hyperalgesia is also attenuated in mice lacking PKCε, a presynaptic localized isotype of nPKC (Khasar et al., 1999). Later study showed that epinephrine induces short-term hyperalgesia, which depends on protein kinase A (PKA) and PKCε activity (Wei-Yu et al., 2015). Although both PKCγ and PKCε act at different levels, both isotypes play an important role in pain responses.

The modulation of GABAA receptors by PKC was also reported (Krishek et al., 1994 and Lin et al., 1994). It is shown that PKCβ, PKCγ, and PKCε are associated with GABAA receptors (Brandon et al., 1999; Kumar et al., 2002). There are controversial reports upon the role of PKC for GABAA receptors. The response of GABAA receptors expressed in Xenopus oocytes is inhibited by PKC activator, phorbol esters and the mutation of the GABAA receptor in a possible PKC phosphorylation site, Ser343, reduced the effect of PKC activation (Krishek et al., 1994). In contrast, the activity of GABAA receptors expressed in fibroblasts is enhanced by active PKC (Lin et al., 1994). Taken together PKC has crucial role for GABAA receptors modulation negatively or positively depending on cells.

Ethanol and benzodiazepines are known to enhance the function of GABAA receptors and the effect of ethanol on GABAA receptor α1 subunit surface expression is PKC-dependent (Kumer et al., 2010). The mutation of Ser343 in the gamma 2L subunit which is a possible PKC phosphorylation site prevented ethanol potentiation but not benzodiazepine potentiation. GABAA receptors isolated from brain membranes of PKCγ deficient mice do not respond to ethanol (Harris et al., 1995). Behaviourally, PKCγ deficient mice show reduced sensitivity to the acute effects of ethanol on righting reflex and body temperature, but show normal responses to pentobarbital. PKCγ deficient mice display decreased tolerance development to the sedative hypotonic and hypothermic effects of ethanol (Bowers et al., 2001), suggesting that these PKCγ deficient mice may be a good model for the study of alcoholism. In contrast to PKCγ deficient mice, PKCε deficient mice show hypersensitivity to allosteric activation by

ethanol and fluinitrazepam and exhibit reduced ethanol self-administration (Hodge et al., 1999). These findings suggest that two PKC isotypes, PKCγ and PKCε, modulate the sensitivity of GABAA receptors to ethanol but have opposite actions on GABAA receptor activity.

### 1.3.4. Mutations of the PKC gamma gene related to disease

Genomic mapping was performed in order to search for functional PKC mutations associated with familial genetic abnormalities and revealed that a major locus of retinitis pigmentosa (RP) exists at chromosome position 19q, which includes the PKCγ gene. Additionally, a point mutation in PKCγ that segregates with RP was found in two RP families. The mutation is in the catalytic domain of PKCγ (Osborne et al., 1992), in which the effect on the kinase activity of PKCγ is unclear, but it is possible that this mutation affects PKCγ kinase activity because this point mutation is present between the turn motif (Thr655) and the hydrophobic motif (Thr674) (Newton, 1997) which are important conserved kinase domains.

Another report suggests that PKCγ is a candidate gene for Parkinson syndrome. The AS/AGU rat, which has a nonsense mutation in PKCγ, exhibits altered behaviour and brain pathology like progressive dopaminergic neuronal degeneration in the substantia nigra, and lower extracellular levels of dopamine in the striatum, which resembling Parkinson syndrome (Shirafuji et al., 2014). It has been shown that this mutation in PKCγ leads to the early termination at the C2 domain without possessing the catalytic domain (Craig et al., 2001). This new stop codon would truncate the PKCγ protein at 280 amino acids, resulting in expression of truncated PKCγ. At an early age in the AS/AGU rat, the extracellular dopamine levels are markedly decreased and later loss of dopaminergic cells in the substantia nigra and dysfunction of movement are reported (Campbell et al., 2000). It is also noteworthy that LTP in the CA1 region of the hippocampus from AS/AGU rats is normal (Shahraki et al., 2002), while LTP in PKCγ deficient mice is impaired under the conventional condition described above. These results indicated C1 domain of PKCγ has crucial role for LTP and truncated PKCγ in AS/AGU rats still has function for LTP.

Overall, functional PKCγ is crucial for memory and motor coordination as well as neuronal development.

# 2. *Aims of the project*

## 2.1. Estimation of the amount of mutant PKC gamma protein expression in mPKCγ transgenic mice

Previously it was shown that chronic activation of PKC in organotypic slice cultures strongly inhibits Purkinje cell dendritic growth (Schrenk et al., 2002). The question arises weather mPKCγ has an increased PKC activity and therefore may cause inhibition of Purkinje cell dendritic growth.

In order to search for mechanisms of Purkinje cell dysfunction, our laboratory has established mutant PKCγ transgenic mice as a model for SCA14. These transgenic mice are carrying a mutation from a human SCA14 allele in the catalytic domain of PKC gamma in Purkinje cells. They show a mild ataxic phenotype and abnormal Purkinje cell morphology in organotypic slice culture while Purkinje cell morphology in vivo is mostly normal. One reason for the rather mild phenotype could be that the transgenic expression of the mutated PKCγ may be rather weak and could be balanced by the presence of the normal PKCγ protein expressed from the endogenous alleles. In order to be able to evaluate the proportion of mutated mRNA and protein present in Purkinje cells of S361G transgenic mice I have analysed transgene expression level in these mice with real time quantitative PCR and Western blot analysis.

## 2.2. Will mutations from SCA14 patients located in different domains PKCγ have similar effects on Purkinje cell dendritic development?

We have previously shown that mutant PKCγ transgenic mice carrying a mutation from a human SCA14 allele located in the kinase activity had abnormal Purkinje cell dendritic growth and development (Ji et al., 2014). These results indicate that S361G mutant PKCγ has an increased biological activity, which results in inhibition of Purkinje cell development. This finding raises the question whether or not other SCA14 mutations will also negatively regulate Purkinje cell dendritic growth. In this project I constructed vectors carrying mutations located in different protein domains of PKCγ and transfected them to Purkinje cells in dissociated cerebellar cultures.

Then I analysed whether SCA14 mutations from different domains of PKCγ will show the same effect on Purkinje cell development and morphology.

## 2.3. Search for molecules involved in signalling of mutant PKC gamma in Purkinje cells

The major project of my thesis was to search for potential signalling molecules downstream of mutant PKCγ which might be related to dendritic growth inhibition of Purkinje cells. As mentioned, in the S361G mutant PKCγ transgenic mice which served as a SCA14 model it was found that mutant PKCγ has an increased PKC biological activity evident by Purkinje cell dendritic growth inhibition in organotypic slice cultures. This finding suggests that in the SCA 14 mutation there is constitutive activation of PKC which causes inhibition of Purkinje cell dendritic growth. But the intermediate steps of the PKCγ signalling cascade eventually leading to the inhibition of dendritic growth are still unknown. The aim of this project was to search for signalling targets of activated PKCγ related to Purkinje cell morphology.
In order to search for such molecules I performed a gene chip assay searching for mRNAs with an increased expression in cerebellar slice cultures from mutant PKCγ mice compared to slice cultures from control mice. In a second step I identified and further studied potential candidate molecules with an increased expression in Purkinje cells from S361G mutant mice with the aim of confirming or excluding a role of these molecules for the PKCγ-mediated inhibition of dendritic growth.

# 3. *Materials and Methods*

## 3.1. Plasmids construction

### 3.1.1. Plasmids pCMV6-XL4- PKCγ-S361G

*Materials*

- Primers were generated by Microsynth
- Pfu DNA polymerase (Invitrogen)
- QIAquick Gel Extraction Kit (Qiagen, Ca No. 28704)
- QIAprep Spin Miniprep Kit (Qiagen, Ca No. 27104)
- EndoFree Plasmid Maxi prep kit (QIAGEN, Ca No.12362)
- Human PKCγ gene in pCMV6-XL4 (Origene).

*Insert point mutation*

- Mutated PKCγ genes were produced by site-directed mutagenesis PCR with the pCMV6-XL4-PKCγ. PCR was performed with the Pfu DNA polymerase (Invitrogen, Carlsbad, CA, USA) for 30 cycles (30 sec at 95°C, 45 sec at 57°C, and 8 min at 68°C), using the following primers:

S361G forward primer: 5'- gttctaggaaaaggcggttttgggaaggtgatgctg -3',

S361G reverse primer: 5'- catgaggaagctgaagtcggagatg -3'.

- The PCR products were then incubated with DpnI which only digests the parental methylated cDNA and the constructed mutated expression vectors were confirmed by DNA sequencing (Microsynth, Balgach, Switzerland).
- After transformation, Plasmids were obtained with EndoFree Plasmid Maxi prep kit (QIAGEN).

### 3.1.2. Plasmids pL7-Car8-GFP and pL7-PKCγ-GFP

*Materials*

- Primers were generated by Microsynth
- PrimeSTAR® Max Premix Polymerase (Clontech, Ca No. R045A)
- In-Fusion® HD Cloning Kit (Clontech, Ca No. 638912)
- QIAquick Gel Extraction Kit (Qiagen, Ca No. 28704)
- QIAprep Spin Miniprep Kit (Qiagen, Ca No. 27104)

- EndoFree Plasmid Maxi prep kit (QIAGEN, Ca No.12362)
- Car8 and PKCγ plasmids (Origene)
- pL7 GFP vector (Dr. Wolfgang Wagner University Medical Center Hamburg-Eppendorf Center for Molecular Neurobiology Hamburg (ZMNH) Department of Molecular Neurogenetics). The structure of this vector is shown in Fig. 7.
- Ampicillin (100 mg/ml stock)
- LB (Luria-Bertani) medium (pH 7.0)
- LB / Ampicillin plates
- Agarose (SIGMA, Ca No. A9539)
- TBE buffer (89 mM Tris-borate / 2 mM EDTA)
- Ethidium bromid (MERCK)

Restriction sites were added to the Car8 and PKCγ genes by polymerase chain reaction (PCR) using the following primers.

CA8 F primer: 5'- cag gat cca gcg gcc gca tgg ctg acc tga gct tc -3',

CA8 R primer: 5'- ccc ttg ctc acc atg gcc tga aag gcc gct cgg a -3',

PKCγ F primer: 5'- cag gat cca gcg gcc gca tgg ctg gtc tgg gcc cc -3',

PKCγ R primer: 5'- ccc ttg ctc acc atg gcc atg acg ggc aca ggc a -3'.


*Methods*

Amplification of the DNA inserts was done according to the following protocol.

The insert DNA PCR reaction was set up as followed.

- PrimeSTAR® Max Premix (2×)          12.5 µl
- Forward Primer, 5 µM                1 µl
- Reverse Primer, 5 µM                1 µl
- Template 200 ng                     1 µl
- Sterile deionized $H_2O$ up to 25 µl    9.5 µl

PCR reaction was performed as following protocol.

- 98°C          10 sec
- 55°C          5 sec
- 72°C          30 sec/kb

The reaction was done for 35 cycles and PCR products were stored at 4°C.

**Fig. 7 Structure of plasmid pL7**

(A) Schematic of plasmid pL7. The L7 DNA fragment (shown in blue) contains a promoter sequence, as well as all of the exons (dark blue) and introns that comprise the small L7 structural gene. All of the AUG codons present in exons 1A, 1B, 2, 3, and 4 were mutated (Serinagaoglu et al., 2007) to ensure that translation starts within the cDNA inserted into the multiple cloning site (MCS; red). The indicated restriction sites are present only once in the vector (except for BamHI). (B) Schematic maps of plasmids pL7-mGFP. (C) DNA sequences immediately upstream and downstream of the fluorescent protein cDNAs. Restriction sites that occur only once in these plasmids are shown in red. (Wagner et al., 2011)

In order to add the expressing genes at the N terminal of mGFP, *Not1* and *Nco1* restriction sites in MCS were used for cloning.

Gel purification of the PCR products: To get the purified DNA fragment from the PCR product mixture, an Agarose gel was prepared as followed.

- Agarose            1.3 g
- 1 × TBE            130 ml
- Ethidium bromid    6.5 µl

PCR products were mixed with 5 × Sample buffer.

- 5 × Sample buffer    5 µl
- Marker or Sample    20 µl

Agarose Gel electrophoresis was done with 150 V for 1 hour.

After Agarose Gel electrophoresis, purification of DNA fragments from gels were done with QIAquick Gel Extraction Kit (Qiagen).

These purified PCR products and L7-GFP vector were then incubated together in the presence of the restriction enzymes, *NotI* and *NcoI* (New England BioLabs, Massachusetts, USA) in New England CutSmart buffer. After 30-60 min incubation at 37°C, DNA fragment and linearized vector were fused using in-Fusion HD Cloning Kits (Clontech) as following reaction.

- 5 × In-Fusion® HD Enzyme Premix      2 µl
- Vector                               1 µl
- PCR fragment                  2 µl
- $H_2O$ up to                    10 µl

The aluminum seals were peeled back from the tubes.

The 10 µl volume of the mixture was adeded to HD EcoDry pellet and then mixed well by pipetting up and down.

The reactions were incubated for 15 min at 37°C, followed by 15 min at 50°C, then tubes were placed on ice.

Reactions were continued to the transformation procedure.

Transformation:

- DH5$\alpha$ competent cells (In-Fusion® HD Cloning Kits) were taken from -70°C and put on ice.
- DH5$\alpha$ competent cells were put on benchtop to thaw and then put on ice.
- After mixing gently, 1.25 µl ligated DNA was added to each tube.
- Then tubes were incubated on ice for 30 min.

- Tubes were placed for heat shock in 42°C water bath for 45 sec without shaking.

- Tubes were put on ice for 2 min.

- 900 µl S.O.C. medium (2% Tryptone, 0.5% Yeast Extract, 0.4% glucose, 10 mM NaCl, 2.5 mM KCl, 10 mM $MgCl_2$, & $MgSO_4$) was added to each tube.

- Tubes were gently shaken and incubated at 200 rpm for 30-60 min at 37°C.

- Cells were spread on LB agar plates containing 100 µg/mL ampicillin as antibiotic.

- Plates were placed in the 37°C incubator with the agar side up and the lid side down.

- Next day, Plates were collected and several colonies were picked up.

- Using QIAprep Spin Miniprep Kit (Qiagen), Plasmids were extracted.

The constructed expression vectors were confirmed by DNA sequencing (Microsynth).

- After conformation of sequence, plasmid were were obtained with EndoFree Plasmid Maxi prep kit (QIAGEN).

### 3.1.3. Mutated or deleted PKCγ-GFP

*Materials*

- Primers were generated by Microsynth

- GENEART® Site-Directed Mutagenesis System (Invitrogen, Ca No. A13282)

- AccuPrime™ Pfx DNA Polymerase (Invitrogen, Ca No. 12344-024)

- QIAprep Spin Miniprep Kit (Qiagen, Ca No. 27104)

- EndoFree Plasmid Maxi prep kit (QIAGEN, Ca No.12362)

- pL7 GFP vector (Dr. Wolfgang Wagner University Medical Center Hamburg-Eppendorf Center for Molecular Neurobiology Hamburg (ZMNH) Department of Molecular Neurogenetics)

- Ampicillin (100 mg/ml stock)

- LB (Luria-Bertani) medium (pH 7.0)

- LB/ Ampicillin plates

Primers

G118D F primer: 5' -ctgcgaccactgtgactccctcctctacgggctt -3',

G118D R primer: 5'-aaggtg gggctgctgtagctatgc a -3';

Deletion260-280 F primer: 5' -gaggagggcgagtattacaatgtgc -3',

Deletion260-280 R primer: 5'-catggcccccatgaagtcgttgcg -3';

S361G F primer: 5' – gttctaggaaaaggcggtttgggaaggtgatgct g -3',

S361G R primer: 5'-catgaggaagctgaagtcggagatg -3',

S119P F primer: 5'- ttctgcgaccactgtggcttcctcctctacgggcttgt -3',

S119P R primer: 5'- acaagcccgtagaggaggaagccacagtggtcgcagaa -3',

V138E F primer: 5'- cctgctgcgagatgaacgagcaccggcgctgtgtgcgt -3',

V138E R primer: 5'- acgcacacagcgccggtgctcgttcatctcgcagcagg -3',

F643L F primer: 5'- gcagcggcgagaacttagacaagttcttcacgc -3',

F643L R primer: 5'- gcgtgaagaacttgtctaagttctcgccgctgc-3'.


*Methods*

Mutated or deleted PKCγ were produced by site-directed mutagenesis PCR with the pCMV6-XL4-PRKCG. Using the following reaction mixture PCR was performed with AccuPrime™ Pfx DNA Polymerase (Invitrogen).

- 10 × AccuPrime™ Pfx Reaction mix     5 µl
- 10 × Enhancer     5 µl
- Primer mix (10 µM each)     1.5 µl (0.3 µM each)
- Plasmid DNA (20 ng/µl)     1 µl (20 ng)
- DNA Methylase (4 U/µl)     1 µl (4 units)
- 25 × SAM     2 µl
- AccuPrime™ Pfx (2.5 U/µl)     0.4 µl (1 unit)
- $H_2O$     32.6 µl

PCR reaction was performed with following protocol.

- (1) 37ºC   20 min
- (2) 94ºC   2 min
- (3) 94ºC   20 sec
- (4) 57ºC   30 sec
- (5) 68ºC   2 min and 18 cycles (3)-(5)

41

(6) 68ºC   5 min

The PCR products were stored at 4°C.

The reactions were continued to the transformation procedure as mentioned.

The constructed expression vectors were confirmed by DNA sequencing (Microsynth).


### 3.1.4. pcDNA™6.2-GW/miR and pL7-Car8 miRNA-GFP

*Materials*

- Primers were generated by Microsynth
- the BLOCK-iT™ Pol II miR RNAi expression vector (Invitrogen, Ca No.K4935-00)
- QIAprep Spin Miniprep Kit (Qiagen, Ca No. 27104)
- EndoFree Plasmid Maxi prep kit (QIAGEN, Ca No.12362)
- pL7 GFP vector (Dr. Wolfgang Wagner University Medical Center Hamburg-Eppendorf Center for Molecular Neurobiology Hamburg (ZMNH) Department of Molecular Neurogenetics)
- Ampicillin (100 mg/ml stock)
- Spectinomycin (50 mg/ml stock)
- LB (Luria-Bertani) medium (pH 7.0)
- LB/spectinomycine plates
- LB/ Ampicillin plates
- Agarose (SIGMA, Ca No. A9539)
- TBE buffer (89 mM Tris-borate / 2 mM EDTA)
- Ethidium bromid (MERCK)

miRNAs were designed and generated using the online tool by Life Technologies to target Car8.

| miRNA | Oligo | Sequence (5'-3') |
|---|---|---|
| mi327 | mi327-Top | TGC TGA CTT CAT ACA GCT CAA ACT CCG TTT TGG CCA CTG ACT GAC GGA GTT TGC TGT ATG AAG T |
| | mi327-Bottom | CCT GAC TTC ATA CAG CAA ACT CCG TCA GTC AGT GGC CAA AAC GGA GTT TGA GCT GTA TGA AGT C |
| mi616 | mi616-Top | TGC TGA AGA GGG TCT GGT AAT AAA GTG TTT TGG CCA CTG ACT GAC ACT TTA TTC AGA CCC TCT T |
| | mi616-Bottom | CCT GAA GAG GGT CTG AAT AAA GTG TCA GTC AGT GGC CAA AAC ACT TTA TTA CCA GAC CCT CTT C |
| mi686 | mi686-Top | TGC TGA TAT CCA GGT AAC TCC TTC GCG TTT TGG CCA CTG ACT GAC GCG AAG GAT ACC TGG ATA T |
| | mi686-Bottom | CCT GAT ATC CAG GTA TCC TTC GCG TCA GTC AGT GGC CAA AAC GCG AAG GAG TTA CCT GGA TAT C |

*Methods*

Each miRNA was generated by Microsynth and cloned into the BLOCK-iT™ Pol II miR RNAi expression vector (Invitrogen) according to the instructions of the manufacturer, briefly shown below.

- 5 µl Top strand DNA oligo (200 µM), 5 µl Bottom strand DNA oligo (200 µM), 2 µl 10 × Oligo Annealing Buffer and 8 µl DNase/RNase-Free Water were added in 1.5 ml tube.
- The mixture tubes were incubated at 95°C for 4 min.
- The tubes containing the annealing reaction were removed from the heat block and set on bench.
- To complete annealing, the reaction mixtures were put on the bench to cool to room temperature for 10 min.
- Reaction mixtures were centrifuged for 5 sec.
- 1 µl of the annealing mixture was removed and diluted 100-fold into DNase/RNase-free water to obtain a final concentration of 500 nM of ds oligo.
- Then vortexed to mix thoroughly.

- 500 nM ds oligo mixture was diluted 50-fold into Oligo Annealing Buffer as follows to obtain a final concentration of 10 nM. Then annealing was checked with Agarose Gel electrophoresis.
- To obtain the miRNA plasmid, set up a 20 µl ligation reaction at room temperature using the following reagents.
- The mixtures were incubated for 5 min at room temperature.
- The reaction tubes were placed on ice and proceeded to transforming to One Shot® TOP10 Competent E. coli and then sequenced (Microsynth).

Then pcDNA6.2-GW/miRNA expression vectors containing Car8 miRNAs were user for transfection to Hela cells. After choosing the best miRNAs with Hela transfection,

|  | sample | control |
|---|---|---|
| 5 × Ligation Buffer | 4 µl | 4 µl |
| pcDNA™6.2-GW/miR, linearized (5 ng/µl) | 2 µl | 2 µl |
| miR-ds oligo or miR-lacZ positive ds control oligo | miR-ds oligo 4 µl | miR-lacZ 4 µl |
| DNase/RNase-Free Water | 9 µl | 9 µl |
| T4 DNA Ligase (1 U/µl) | 1 µl | 1 µl |

pcDNA6.2-GW/miRNA expression vectors containing Car8 miRNAs were sub cloned to pL7 in order to transfect miRNA to Purkinje cells.

Restriction sites were added to the miRNA ds F primer and R primer, then proceeded as mentioned above.

Insert miRNA PCR (mi327 and mi616)

- PrimeSTAR® Max Premix (2×)          12.5 µl
- Forward Primer, 5 µM                1.0 µl
- Reverse Primer, 5 µM                1.0 µl
- Template 200 ng                     1.0 µl
- Sterile deionized $H_2O$ up to 25 µl    9.5 µl

PCR reaction was performed as following protocol.

- 98°C          10 sec

- 55°C         5 sec
- 72°C         30 sec/kb

The reaction was done for 35 cycles and PCR products were stored at 4°C.

Gel purification of the PCR products: To get the purified DNA fragment from the PCR product mixture, an Agarose gel was prepared as followed.

- Agarose         1.3 g
- 1 × TBE         130 ml
- Ethidium bromid    6.5 µl

PCR products were mixed with 5 × Sample buffer.

- 5 × Sample buffer    5 µl
- Marker or Sample    20 µl

Agarose Gel electrophoresis was done with 150 V for 1 hour.

After Agarose Gel electrophoresis, purification of DNA fragments from gels were done with QIAquick Gel Extraction Kit (Qiagen).

These purified PCR products and L7-GFP vector were then incubated in the presence of the restriction enzymes, *bgl2* (New England BioLabs) in New England 3.1 buffer. After 30 min incubation at 37°C, DNA fragment and linearized vector were fused with T4 ligase (New England BioLabs).

T4 ligase reaction: The following reaction was set up in a microcentrifuge tube on ice.

| COMPONENT | |
|---|---|
| 10 × T4 DNA Ligase Buffer | 2 µl |
| Vector DNA | 1 µl |
| Insert DNA | 3 µl |
| DNase/RNase-Free Water | 13 µl |
| T4 DNA Ligase | 1 µl |

- The reaction components were gently mixed by pipetting up and down followed by brief microcentrifuge.
- Tubes were incubated for 2 hours on bench.
- Heat inactivation was done at 65°C for 10 min.

45

- Tubes were placed on ice and proceeded to transforming One Shot® TOP10 Competent E. coli. Then sequenced (Microsynth).

Plasmid containing miRNA were amplified using E.coli and purified with QIAGEN Endfree Maxiprep (Qiagen), then they were used for transfection.

The structure of the plasmid pL7 with miRNA is shown in Fig. 8.
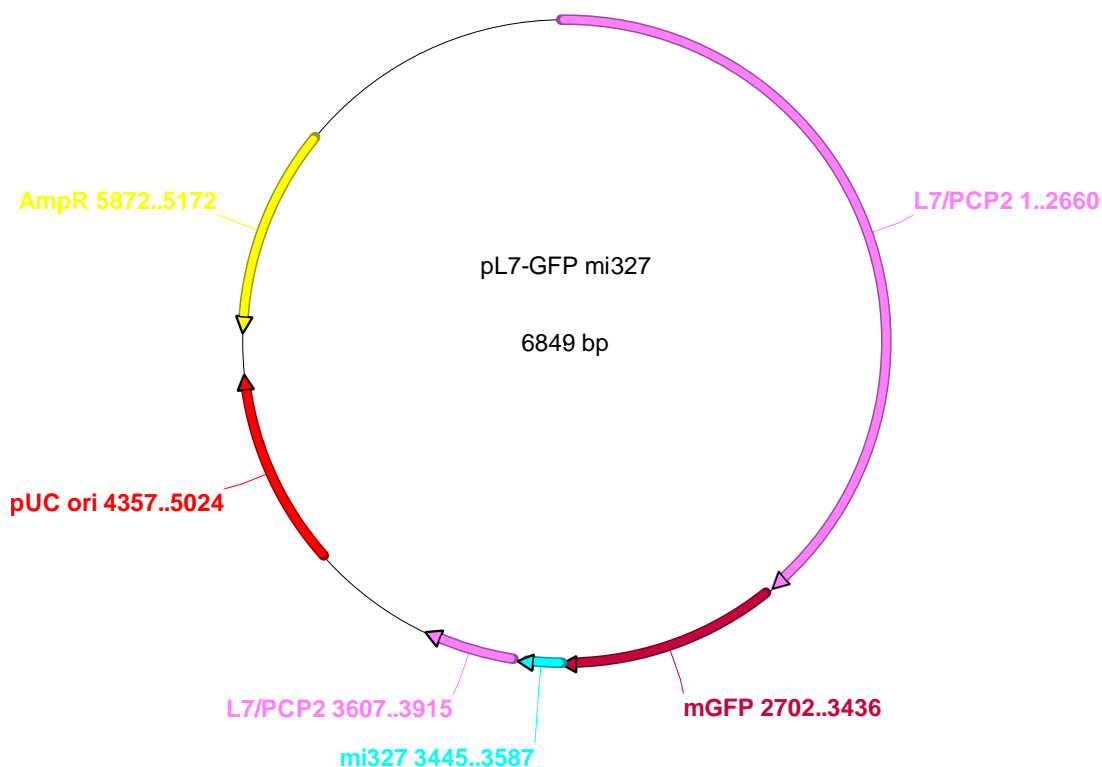


**Fig. 8 Structure of plasmid pL7 with miRNA**
Schematic of plasmid pL7-mGFP with miRNA. The L7 DNA fragment (shown in pink) contains a promoter sequence, as well as all of the exons and introns that comprise the small L7 structural gene. miRNA (miCont, mi327 and mi616) were inserted downstream of mGFP in order to ensure that transfection is visualize with fluorescence.

### 3.2. Plasmid transfection to Hela cells

In order to test the knockdown efficacy, three type of miRNA vectors (mi327, mi616, mi686) were transfected into HeLa cells together with a Car8 expression vector using Lipofectamin 2000 (Life Technologies, Zug, Switzerland).

### 3.2.1. Materials

Ingredients for 200 ml culture medium

- 180 ml Dulbecco's modified Eagle medium (Gibco)
- 20 ml FBS (GIBCO)
- 1N NaOH or 1N HCl to adjust pH to 7.2-7.4

75 cm$^2$ flask (FALCON, Ca No. 353136)

6 well cell culture plate (FALCON, Ca No. 353046)

Tripsin

Lipofectamine™ 2000 (Life Technologies)

Plasmid (mentioned above)

### 3.2.2. Procedure

- HeLa cells were cultured with 10% FBS containing culture medium.
- The day before transfection, $2.5 \times 10^5$ HeLa cells were plated in 2.5 ml of growth medium without antibiotics so that cells will be 90-95% confluent atthe time of transfection.
- Hela wells in a 6-well plate were transfected using Lipofectamine™ 2000 reagent with 100 ng Car8-GFP plasmid and co-transfected with 100 ng of miRNA expression vectors.
- Cell lysates were prepared 48 hours after transfection and assayed by Western Blotting and immunostaining.

## 3.3. Real time qPCR

### 3.3.1. cDNA reverse transcription

Total RNA was extracted as described.

Template for cDNA reverse transcription is showed below.

| 1 µg total RNA | 1.0 µl |
|---|---|
| H$_2$O | 12.2 µl |
| 10 × randam hexmer | 2.0 µl |
| 10 × Buffer | 2.0 µl |
| Protector RNase Inhibitor, 40 U/µl | 1.0 µl |

| 25 × dNTP 10 mM | 0.8 µl |
|---|---|
| TranscriptorReverse Transcriptase 10 U/tube | 1.0 µl |
| Final volume | 20.0 µl |

PCR reactions were run on PCR cycler (Mastercycler gradient, Eppendorf) under the following reaction conditions.

25°C 10 min→ 37°C 120 min→ 85°C 5 min

### 3.3.2. Quantitative real-time PCR

Quantitative real-time PCR reactions were conducted in a total volume of 20 µl as described.

| cDNA, 100 ng/µl | 0.3 µl |
|---|---|
| F primer, 5 µM | 0.5 µl |
| R primer, 5 µM | 0.5 µl |
| Mastermix with SYBR green | 10.0 µl |
| ultrapure water | 8.5 µl |

Real-time PCR reactions were run on a 48-well format with One step real-time detector (Applied Biosystems) under the following reaction conditions.

- 1 cycle 95°C for 10 min
- 40 cycles of 94°C for 15 sec → 65°C for 60 sec
- 1 cycle of 95°C for 15 sec → 72°C for 30 sec → 95°C for 15 sec

Oligonucleotide primers were designed using the Primer 3 software (http://frodo.wi.mit.edu/primer3/).

Primer sequences were described in Plasmid construction part.

### 3.4. SDS-PAGE

3.4.1. Materials

Tris (AppliChem, Ca No. A1086)

Glycine (SIGMA, Ca No. G7126)

SDS (BIORAD, Ca No. 161-0301)

TritonX-100 was from (Fluka, Ca No. 93148)

Electrophoretic apparatus was from BIORAD

10 × RIPA buffer

- 0.5 M Tris-HCl, pH 7.4
- 1.5 M NaCl
- 2.5% Sodium Deoxycholate
- 10% NP-40
- 10 mM EDTA

After making 1 × RIPA buffer, add following inhibitors

- phosphatase inhibitor (phosphor STOP, Roche)
- protease inhibitor (complete, Roche , Ca No. 11697498001)

Running gel solution (10% Acrylamide)

- 7.5 ml 1.5 M Tris-HCl, pH 8.8
- 0.15 ml 20% (w/v) SDS
- 9.9 ml Acrylamide/Bis-acrylamide (30%/0.8% w/v)
- 12.3 ml $H_2O$
- 0.15 ml 10% (w/v) ammonium persulfate (APS) (BIORAD, Ca No. 161-0700 )
- 0.02 ml TEMED (AppliChem, Ca No. A1148)

Stacking gel solution (4% Acrylamide)

- 1.25 ml 0.5 M Tris-HCl, pH 6.8
- 0.025 ml 20% (w/v) SDS
- 0.67 ml Acrylamide/Bis-acrylamide (30%/0.8% w/v)
- 3.075 ml $H_2O$
- 0.025 ml 10% (w/v) ammonium persulfate (APS)
- 0.005 ml TEMED

1 × Running buffer (25 mM Tris, 192 mM glycine, 0.1% SDS)

- 3.02 g Tris
- 14.4 g glycine
- 1 g SDS
- 1000 ml $H_2O$

1 × Transfer buffer (25 mM Tris, 192 mM glycine, 20% methanol)

- 3.02 g Tris
- 14.4 g glycine
- 200 ml methanol
- 800 ml $H_2O$

1 × TBS solution (10 mM Tris-Cl, pH 7.4-7.6; 150 mM NaCl)

- 8.76 g NaCl
- 1.21 g Tris
- Add HCl and adjust pH to pH 7.4-7.6
- Add $H_2O$ fill to 1000 ml

Blocking buffer

- 5% BSA (GIBCO) in TBS

T-TBS

- 950 ml 1 x TBS Solution
- 50 ml 10% TritonX-100

3.4.2. Procedure

- Cells were harvested with cell scraper.
- Samples were then homogenized in RIPA buffer with phosphatase inhibitor and protease inhibitor.
- Homogenates were sonicated for 5 sec a total of 5 times and cleared by centrifugation at 14,000 × g for 15 min at 4°C.
- Protein concentrations were determined with Nano drop or BCA kit (BioRad).
- 100 µg of each sample mixed with $H_2O$ and 2 × sample buffer.
- Samples were denatured at 95°C for 5 min.
- Running gel was filled and stacking gel solution was made, and comb was put on the Stacking gel.
- Then the comb was removed and the gel was clamped to the electrophoretic apparatus.
- The electrolyte compartment was filled with running buffer.
- After checking for leaks the bottom compartment was filled.

- With a plastic Pasteur pipette, thoroughly rinse each well in the stacking gel with running buffer.

- The samples were applied by using a micropipette to carefully add 10 µl of protein in a well.

- The electrical connections were checked.

- Samples were run at 120 V for 2 hours.

- The gel was carefully removed and was transferred in transfer buffer.

- Filter papers were placed onto the semi dry blotter.

- These are then wetted with transfer buffer

- The gel is put onto the filters and a pre wetted nitrocellulose filter was put on top of the gel.

- Then three more wetted filters should be placed on top of the pile, again taking great care not to have any air bubbles in the pile. The top of the apparatus and was fixed by tightening the screws. Proteins in transfer buffer were negative in charge mostly due to residual SDS.

- After blotting, membranes were blocked with 5% BSA in TBS for 1 hour and incubated with appropriate Primary antibodies.

- After washing with TBS-T, 3 times for 10 min, membranes were incubated with HRP-labelled secondary antibodies for 1 hour.

- After washing 3 times with TBS-T, the membrane was gently shaken with ECL2 Western blotting substrate (PIERCE, 80196).

- Immunoreactive bands were visualized in X-ray film (FUJI) or C-DiGit Western blot scanner and software (LI-COR Biosciences).

### 3.5. Immunoprecipitation

3.5.1. Materials

- Protein G (Pierce) or Pierce cross link Immunoprecipitation kit (Pierce)
- Protein samples

3.5.2. Procedure

- Cells were harvested in the tubes.

- Cells were then homogenized in RIPA buffer with phosphatase inhibitor and protease inhibitor.

- Homogenates were sonicated for 5 sec a total of 5 times and cleared by centrifugation at 14,000 x g for 15 min at 4 °C.

- Protein concentrations were determined with Nano drop.

- 100 µg of each sample were used for immunoprecipitation.

For immunoprecipitation with the kit, the following procedure was done

- Protein G was washed for two times at 12000 x g 10 sec with PBS

- Lysate was incubated with 50 µl Protein G for 30 min at 4 °C.

- Lysate was washed twice at 12000 x g 10 sec with PBS

- 1µg antibody, 50 µl beads and 50 µl PBS were mixed at RT for 1 hour.

- Mixture was centrifuged 4°C for 2 min at 3000g

- The antibody binding Protein G was washed with 1ml PBS 4°C for 2 min at 3000 x g

- The antibody binding Protein G was washed with 1ml PBS 4°C for 2 min at 3000 x g

- 20 µl sample were mixed with 20 µl sample buffer.

- Samples were denatured at 95°C for 5 min.

- Then proceeded as the same way as mentioned in SDS-PAGE.


### 3.6. Cerebellar slice culture

3.6.1. Materials

Ingredients for 200 ml preparation medium

- 100 ml minimal essential medium (MEM) (Gibco, Ca No. 11012), in twofold concentration

- 98 ml Aqua bidest

- 1 ml Glutamax  (Gibco, Ca No. 35050)

- 1 N NaOH or 1 N HCl to adjust pH to pH 7.2-7.4

Ingredients for 100 ml Incubation medium

- 25 ml MEM (Gibco, Ca No. 11012), in twofold concentration

- 23.5 ml Aqua bidest

- 25 ml Basal Medium Eagle, with Earl's salt, without glutamine (Gibco, Ca No. 21400)

- 25 ml horse serum, heat-inactivated (Gibco, Ca No. 26050)

- 1 ml Glutamax (Gibco, Ca No. 35050)

- 700 µl of a 10% glucose solution

- 1 N NaOH or 1 N HCl to adjust pH to pH 7.2-7.4

Ingredients for 100 ml Neurobasal medium

- 97 ml Neurobasal A medium (Gibco, Ca No. 10888)

- 2 ml B27 supplement (Gibco, Ca No. 17504)

- 1 ml Glutamax (Gibco, Ca No. 35050)

- 1 N NaOH or 1 N HCl to adjust pH to pH 7.2-7.4

Dishes and plates

- 6 well plates (BD Falcon, Ca No. 353046)

- 35 mm dishes (Greiner, Ca No. 627102)

- Millicell CM tissue culture Inserts (Millipore, Ca No. PICM 03050)

*Preparation*

- A sterilized razorblade was installed on a tissue chopper (McIllwain).

- Petri dishes (Greiner) were half-filled with ice-cold preparation medium and kept at 4°C, 2-3 dishes per mouse pup were required.

- 750µl of incubation medium or Neurobasal medium was pipetted in each well of a tissue culture plate (6 well plates). The plate was placed in an incubator providing a humidified atmosphere with 5% $CO_2$ at 37°C. One plate holds cultures from 3 mice placed on 6 culture inserts.

- Surgical instruments were sterilized and placed in the working area.

### 3.6.2. Procedure

Animal experiments were carried out in accordance with the EU Directive 2010/63/EU for animal experiments and were reviewed and permitted by Swiss authorities. Cultures were prepared from CB6 mice or mutant PKCγ transgenic mice at postnatal day 8 (P8) as described previously (Metzger and Kapfhammer, 2003; Kapfhammer, 2005, 2010) and incubated according to the static method (Stoppini et al., 1991). All

steps were carried out in the aseptic environment of a horizontal laminar flow workbench.

- A P8 mouse pup was decapitated.

- The skull was carefully opened in the sterile workbench.

- The brain was removed from the skull and placed in a 35 mm dish containing $4°C$ cold preparation medium. All further steps were carried out under a stereomicroscope (Zeiss, Stemi 2000).

- The cerebellum was isolated by cutting the cerebellar peduncles and the meninges were removed from the surface of the cerebellum.

- The cerebellum was placed on the tissue chopper and sagittal slices (350 µm) were cut.

- The cerebellar slices were placed in a fresh dish with cold preparation medium and the slices were separated from each other.

- The bottom membranes of two tissue culture inserts (Millipore) were moistened with preparation medium.

- Individual slices were transferred to the cell culture insert and placed on top of the membrane.

- The culture inserts were placed in the pre-arranged tissue culture plate and incubated immediately.

*Maintenance and experimental treatments of the cultures*

- The medium was changed every 2-3 days. Fresh medium was pre-warmed to 37°C and the pH was adjusted to 7.2-7.4, if necessary.

- Pharmacological compounds were added to the culture medium after every medium change. (e.g. PMA = Phorbol 12-myristate 13-acetate, Tocris, Ca No. 1201). Stock solutions were prepared in 50% EtOH / 50% DMSO (EtD) and were kept at -20°C.

*Immunocytochemistry*

- At the end of the culture period cultures were fixed in 4% paraformaldehyde in 100 mM phosphate buffer (PB) overnight at 4°C.

- The slices were washed with PB 3 times for 10 min.

- The plastic feet at the culture inserts were cut off to limit the required amount of antibody solution to 1000 µl.
- The 1st antibody solution was prepared in PB as follows:
  - 0.5% Triton X-100
  - 3% normal goat serum
  - rabbit anti-Calbindin D-28K (Swant) 1:1000
- The slices were incubated in 1st antibody solution at 4°C overnight.
- The slices were washed with PB with 0.1 % Triton X-100, 3 × for 10 min.
- The 2nd Antibody solution was prepared in PB as follows:
  - 0.1 % Triton X-100
  - goat anti-rabbit Alexa 488 (Molecular Probes, Invitrogen) 1:500
- The slices were incubated in 2nd antibody solution at room temperature for 2 hours.
- The slices were washed with PB for 3 times for 10 min.
- Stained slices were mounted on glass slides (Thermo Scientific Menzel-Gläser Superfrost Plus, Art. No. J1800AMNZ) and coverslipped with Mowiol.
- Cultures were viewed on an Olympus AX-70 microscope equipped with a Spot digital camera.
- Recorded images were adjusted for brightness and contrast with Photoshop image processing software

## 3.7. Dissociated cerebellar cultures

3.7.1. Materials

Ingredients for 100 ml DFM medium

- 97 ml 1:1 mixture of Dulbecco's modified Eagle medium and F–12 nutrients (DFM; Gibco, Ca No. 12400)
- 1 ml N-2 Supplement (100 ×), Liquid (GIBCO, Ca No. 17502-048)
- 1 ml Glutamax (Gibco, Ca No. 35050)
- 1 N NaOH or 1 N HCl to adjust pH to 7.2-7.4

Ingredients for 1000 ml Hank's Balanced Salt Solution

- 1000 ml Aqua bidest

- HBSS; 5.333 mM KCl, 0.441 KH2PO4, 137.931 mM NaCl, 0.336 mM Na$_2$HPO$_4$•7H$_2$O, and 5.556 mM d-glucose (HBSS, SIGMA, Ca No. H2387)
- 1 N NaOH or 1 N HCl to adjust pH to pH 7.2-7.4

Papain solution (HBSS containing 20 U/ml papain)

- Papain 20 U/ml, 5 ml vial, (Warthington, Ca No. 3176)
- HBSS, 5 ml

DNase solution (-20°C stock)

- DNase1, 0.2 mg (0.2 mg/ml) (0.02%), (SIGMA, Ca No. D5025)
- MgSO$_4$, 1.43 mg (11.88 mM), (SIGMA, Ca No. M-2643)
- HBSS, 1 ml

180 µm filter (Millipore, Ca No. SLGV 025 LS)

BD Poly-D-Lysine Laminin culture slide (BD, Ca No. 354688)

### 3.7.2. Procedure

- Dissociated cerebellar cultures were prepared from mice essentially as described (Linden et al., 1991; Tabata et al., 2000 )
- The cerebellum from every mouse was treated separately, resulting in one culture from one cerebellum. Newborn mouse pups (P0) were obtained from CB6 or mPKCγ transgenic mice.
- Each mouse was then decapitated and the cerebellar primordium was dissected free and transferred into a sterile 1.5 ml tube containing 250 µl ice-cold HBSS kept on ice.
- The isolated cerebellar primordia were minced in the tubes to obtain chunks of~1 mm size.
- Subsequently, the cerebellar tissues were digested by adding 250 µl of freshly prepared, ice-cold papain solution (HBSS containing 20 U/ml papain, Worthington 3176) to each tube, followed by incubation in a 33°C water bath for 30 min.
- To stop the digestion, 1 ml HBSS pre-warmed to room temperature (RT) was added to each tube.

- After gentle mixing by inverting the tube, the cells were harvested by centrifugation at RT for 4 min at 0.6 g. All subsequent steps were carried out at RT under the hood.

- After all supernatants were removed, 300 µl of freshly prepared DNase solution was added to each of the harvested cerebellar cell pellets.

- Each cell pellet was then triturated carefully by pipetting up and down ~40 times using a Gilson Pipetman P1000 equipped with a sterile 1000 µl tip.

- The triturated cells were then passed through a nylon mesh, collected in a fresh 1.5 ml tube, and harvested by centrifugation (at RT for 4 min at $0.6 \times g$).

- The cells were then washed twice by re-suspending them (via inverting the tube several times) in 1 ml of HBSS at RT and harvesting them by centrifugation (at RT for 4 min at $0.6 \times g$).

- DFM medium with 10% (v/v) fetal bovine serum (FBS) was added to the cells and transferred to a 14 mm diameter glass bottom culture dish that had been coated with poly-l-ornithine.

- The dish was then placed in a 37°C incubator (5%$CO_2$, 97% humidity).

*Experiments and maintenance of the cultures*

- The medium was changed at the second day after starting culture. Fresh medium without serum was pre-warmed to 37°C and the pH was adjusted to 7.2-7.4, if necessary.

- Then, every 3-4 days, half of medium was changed.

- Pharmacological compounds were added to the culture medium after every medium change.

*Immunocytochemistry*

- At the end of the culture period cultures were fixed in 4% paraformaldehyde in 100 mM phosphate buffer (PB) for 1 hour at 4°C.

- The cells were washed with PB for at least 3 times for 10 min.

- The 1st antibody solution was prepared in PB as follows:
  - 0.5%  Triton X-100,
  - 3% normal goat serum

- o rabbit anti-Calbindin D-28K (Swant) 1:1000
- The cells were incubated in 1st antibody solution at RT for 1 hour.
- The cells were washed with PB containing 0.1% Triton X-100, 3 times for 10 min.
- The 2nd Antibody solution was prepared in PB as follows:
  - o 0.1% Triton X-100
  - o goat anti-rabbit Alexa 488 or 568  (Molecular Probes, Invitrogen) 1:500
- The cells were incubated in 2nd antibody solution at room temperature for 1 hour.
- The cells were washed with PB for 3 times for 10 min.
- Stained cells on glass slides were covered with Mowiol.
- Cultures were viewed on an Olympus AX-70 microscope equipped with a Spot digital camera.
- Recorded images were adjusted for brightness and contrast with Photoshop image processing software.

### 3.8. Biolistic transfection

### 3.8.1. Materials

All ingredients were sterile and mixed in a laminar flow work bench.
Helios Gene Gun Kit (Biorad):

- Helios Gene Gun (Biorad, shown in Fig. 9)
- Tubing Prep Station (Biorad)
- Gold microcarriers (Biorad)
- Helium tank
- Nitrogen tank
- Nitrogen regulator
- Polyvinylpyrollidone, MW = 360,000
- 100% ethanol
- Spermidine (Sigma, Ca No. S-0266)
- Calcium chloride ($CaCl_2$)
- Plasmid DNA
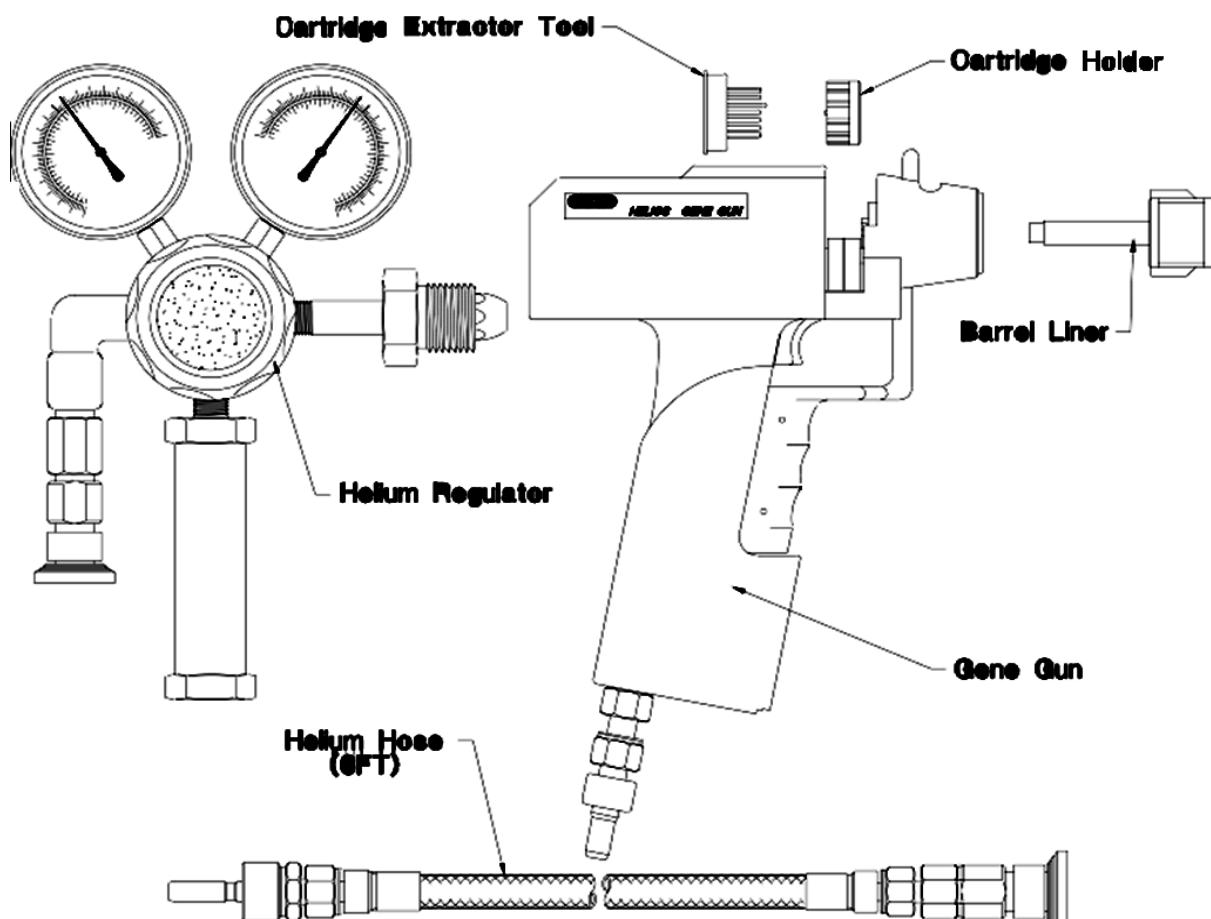
**Fig.9 Gene gun (from Biorad manual)**

The Helios (Bio-Rad) gene gun is a small portable instrument that enables efficient transportation of plasmid or dyes into cells.

3.8.2. Procedure

*Preparation of DNA-Coated gold particles for Slice culture*

- 15 mg gold particles and 30 µl spermidine stock solution were added to a 1.5 ml microfuge tube.

- Vortexed for 5 sec.

- 30 µl of plasmid DNA (0.5 mg/ml) were added to the microfuge tube and vortexed for 5 sec.

- 30 µl of $CaCl_2$ stock solution were added dropwise.

- Incubate the gold and plasmid DNA at room temperature for 10 min, flicking the tube periodically to mix the contents.

- Then spin the tube for 5 sec at 1,000 rpm to pellet the gold.

- The supernatant was removed and stored as a sample.

- The gold particles were washed three times with 1 ml of 100% EtOH.

- Then the gold pellet was re-suspended in 200 µl PVP working solution from a 3.5 ml aliquot, and the suspension was transferred to a 5 ml tube. This transfer was repeated with 200 ml aliquots of PVP until all the gold particles had been transferred, and then the remaining PVP solution was added.

Based on this reference (Wellmann et al., 1999), we first set the conditions below and changed several factors depending on the results.

| |
|---|
| 1.6 µm GOLD, 15 mg |
| 30 µl, 0.05 M Spermidine |
| 30 µl,  Plasmid (0.5 mg/ml) |
| 30 µl, 2 M $CaCl_2$ |
| 2 ml, PVP |

*Tubing Preparation (This step done according the manufacturer's manual)*

- Tubing was cut to the length of the tubing prep station, then inserted from the right end into the tubing prep station, and pushed in until it slipped through the O-ring on the left side

- The tube was dried for 20 min with $N_2$ at 0.3 – 0.4 lpm, then it was taken out from the tubing prep station and connected to a syringe with tubing

- The coated particle solution was sonicated, vortexed and then drawn up, it is important to leave some empty space at each end of tubing.

- Let the solution settle for 5 min, no turning of tubing.

- The solution was then slowly (1.5-3 cm/sec) withdrawn, leaving the gold particles on the bottom of the tubing.

- Then the tubing was rotated 90°, stopped for 5 sec, rotated for 180°, stopped again for 5 sec and rotated for 30 sec.

- Rotated under $N_2$ flow (0.4 lpm) for 5 min.

- The tubing was removed from the tubing prep station; the coating could be seen as a brownish film.

- Finally the coated area of the tubing was cut with the cutting machine to get the bullets.

*Bombardment*

- Cerebellar slice cultures were prepared as mentioned.
- Battery was inserted into the Helios Gene Gun.
- The Helios Gene Gun was connected to a Helium Source.
- To activate the Gene Gun: turn on the flow of helium to the desired pressure and with an empty cartridge holder in place, make 2–3 "pre-shots" by engaging the safety interlock and firing the trigger.
- The cartridges with tubes containing DNA-coated gold particles were prepared and cartridges were loaded into the cartridge holder and then placed in the Gene Gun.
- The lid of 6 well culture plate was opened and culture inserts were the target for bombardment.
- For bombardment: engage the safety interlock and press the firing trigger.
- As soon as possible, slice culture plates were returned to the incubator.

## 3.9. Magnetofection

### 3.9.1. Materials and Methods

Ingredients for 100 ml DFM medium

- 97 ml 1:1 mixture of Dulbecco's modified Eagle medium and F–12 nutrients (DFM; Gibco, Ca No. 12400)
- 1 ml N-2 Supplement (100 ×), Liquid (GIBCO, Ca No. 17502-048)
- 1 ml Glutamax (Gibco, Ca No. 35050)
- 1 N NaOH or 1 N HCl to adjust pH to 7.2-7.4

Ingredients for 1000 ml Hank's Balanced Salt Solution

- 1000 ml Aqua bidest
- HBSS; 5.333 mM KCl, 0.441 KH2PO4, 137.931 mM NaCl, 0.336 mM Na$_2$HPO$_4$•7H$_2$O, and 5.556 mM d-glucose (HBSS, SIGMA, Ca No. H2387)
- 1 N NaOH or 1 N HCl to adjust pH to pH 7.2-7.4

Papain solution (HBSS containing 20 U/ml papain)

- Papain 20 U/ml, 5 ml vial, (Warthington, Ca No. 3176)
- HBSS, 5 ml

DNase solution (-20°C stock)

- DNase1, 0.2 mg (0.2 mg/ml) (0.02%), (SIGMA, Ca No. D5025)
- $MgSO_4$, 1.43 mg (11.88 mM), (SIGMA, Ca No. M-2643)
- HBSS, 1 ml

180 µm filter (Millipore, Ca No. SLGV 025 LS)

BD Poly-D-Lysine Laminin culture slide (BD, Ca No. 354688)

NeuroMag kit (OZ BIOSCIENCES)

Plasmid mentioned above.

### 3.9.2. Procedure

*Preparation of DNA/NeuroMag complexes*

- The appropriate amount of NeuroMag reagent (4 µg) was vortexed in a microtube.
- For DNA preparation, the indicated quantity of plasmid DNA was diluted in 200 µl of culture medium without serum and supplement.
- The DNA solution was added to the NeuroMag solution (4 µg plasmid DNA + 14 µl Neuromag) and vortexed, then incubated at room temperature for 15 to 20 min.

*Cells*

- Dissociated cerebellar cultures were prepared from mice essentially as described (Linden et al., 1991; Schilling et al., 1991; Tabata et al., 2000), and explained above.

*Transfection*

- NeuroMag / DNA complexes were added onto cells drop by drop and the dish was gently rocked to ensure a uniform distribution. The cell culture dishes were incubated on the magnetic plate during 15 min.
- Then the magnetic plate was removed.
- The dish was then placed in a 37°C incubator (5% $CO_2$, 97% humidity).

*Maintenance of the cultures*

- Every 3-4 days, half of medium was changed. After one to two weeks cells were fixed and stained as described.


## 3.10. Effectene

### 3.10.1. Materials

All ingredients were sterile and mixed in a laminar flow work bench.
Effectene Kit:
- Buffer EC
- Enhancer

Ingredients for 100 ml DFM medium

- 97 ml 1:1 mixture of Dulbecco's modified Eagle medium and F–12 nutrients (DFM; Gibco, Ca No. 12400)

- 1 ml N-2 Supplement (100 x), Liquid (GIBCO, Ca No. 17502-048)

- 1 ml Glutamax (Gibco, Ca No. 35050)

- 1 N NaOH or 1 N HCl to adjust pH to 7.2-7.4

Ingredients for 1000 ml Hank's Balanced Salt Solution
- 1000 ml  Aqua bidest

- HBSS; 5.333 mM KCl, 0.441 KH2PO4, 137.931 mM NaCl, 0.336 mM $Na_2HPO_4 \bullet 7H_2O$, and 5.556 mM d-glucose (HBSS, SIGMA, Ca No. H2387)

- 1 N NaOH or 1 N HCl to adjust pH to pH 7.2-7.4

Papain solution (HBSS containing 20 U/ml papain)

- Papain 20 U/ml, 5 ml vial, (Warthington, Ca No. 3176)

- HBSS, 5 ml

DNase solution (-20°C stock)

- DNase1, 0.2 mg (0.2 mg/ml) (0.02%), (SIGMA, Ca No. D5025)

- $MgSO_4$, 1.43 mg (11.88 mM), (SIGMA, Ca No. M-2643)

- HBSS, 1 ml

180 µm filter (Millipore, Ca No. SLGV 025 LS)

BD Poly-D-Lysine Laminin culture slide (BD, Ca No. 354688)


Plasmids were mentioned above.

63

### 3.10.2. Procedure

- 0.4 µg plasmid (400 ng/ml plasmid 1 µl), 99 µl Buffer EC and 3.2 µl Enhancer were mixed in a 1.5 ml microtube.

- Vortexed for 1sec.

- Microtubes were incubated for 5 min at RT.

- 10 µl Effectene transfection regent was added to the plasmid mixture and pipetted up and down 5 times, then incubated for 5 min at RT.

- During the incubation, the medium of dissociated cerebellar cultures plate was changed and replaced with 1.6 ml fresh medium.

- 600 µl medium was added to the complex, and then the solution was added to the cultures.

- The dish was then placed in a 37 °C incubator (5% $CO_2$, 97% humidity).

- Cultures were maintained for 24 hours and fixed, stained with anti-GFP and anti-Calbindin antibody, mentioned above.

# *4.* *Results*

## **4.1. Mouse model of spinocerebellar ataxia 14**

**Increased protein kinase C gamma activity induces Purkinje cell pathology in a mouse model of spinocerebellar ataxia 14**

*Jingmin Ji; Melanie L Hassler; Etsuko Shimobayashi; Nagendher Paka; Raphael Streit; Josef P. Kapfhammer*

*Anatomical Institute, Department of Biomedicine Basel, University of Basel, Pestalozzistr. 20, CH - 4056 Basel, Switzerland.*

The following section is based on the work published in the Neurobiology of Disease, 2014, Volume 70, October 2014, Pages 1–11. Figure legend numbering and title numbering were modified to fit this thesis. The abstract and the introduction are unchanged from the publication, for Materials and methods, Results and Discussion the parts shown are limited to the experiments performed by myself.

### 4.1.1. Abstract

Spinocerebellar ataxias (SCA) are hereditary diseases leading to Purkinje cell degeneration and cerebellar dysfunction. Most forms of SCA are caused by expansion of CAG repeats similar to other polyglutamine disorders like Huntington's disease. In contrast, in the autosomal dominant SCA-14 the disease is caused by mutations in the protein kinase C gamma (PKCγ) gene which is a well characterized signaling molecule in cerebellar Purkinje cells. The study of SCA-14, therefore, offers the unique opportunity to reveal the molecular and pathological mechanism eventually leading to Purkinje cell dysfunction and degeneration. We have created a mouse model of SCA-14 in which PKCγ protein with a mutation found in SCA-14 is specifically expressed in cerebellar Purkinje cells. We find that in mice expressing the mutated PKCγ protein the morphology of Purkinje cells in cerebellar slice cultures is drastically altered and mimics closely the morphology seen after pharmacological PKC activation. Similar morphological abnormalities were seen in localized areas of the cerebellum of juvenile transgenic mice in vivo. In adult transgenic mice there is evidence for some localized

loss of Purkinje cells but there is no overall cerebellar atrophy. Transgenic mice show a mild cerebellar ataxia revealed by testing on the rotarod and on the walking beam. Our findings provide evidence for both an increased PKCγ activity in Purkinje cells in vivo and for pathological changes typical for cerebellar disease thus linking the increased and dysregulated activity of PKCγ tightly to the development of cerebellar disease in SCA-14 and possibly also in other forms of SCA.

Key words:

Spinocerebellar ataxia type 14, protein kinase C gamma, Purkinje cell dendritic development, transgenic mouse model.

### 4.1.2. Introduction

Spinocerebellar ataxias (SCAs) are hereditary diseases leading to Purkinje cell degeneration and cerebellar dysfunction. By now more than 30 different mutations have been identified as the underlying cause of this group of diseases (for a recent review see Matilla-Dueñas et al 2012). Most forms of SCA are caused by expansion of CAG repeats similar to other polyglutamine disorders like Huntington's disease. In contrast, in the autosomal dominant SCA-14 the disease is caused by mutations in the protein kinase C gamma (PKCγ) gene which is a well characterized signaling molecule in cerebellar Purkinje cells. The study of SCA-14, therefore, offers the unique chance to reveal the molecular and pathological mechanism eventually leading to Purkinje cell dysfunction and degeneration (Pandolfo and van de Warrenburg 2005). Genetic analysis has shown that the disease is caused by different point mutations in the PKCγ gene. Many, but not all, of the identified mutations are clustered in the regulatory C1b domain of the PKCγ gene (Chen et al., 2012). Clinically, the disease is characterized by a slowly progressive pure cerebellar ataxia with the age of onset ranging from 5 – 60 years. The dominant pathological finding is a mild to moderate cerebellar atrophy with a loss of Purkinje cells. Because of the dominant inheritance of the disease it is assumed that the mutated PKCγ protein must have a toxic action or may confer a gain of function phenotype eventually resulting in Purkinje cell dysfunction and death. When two of the mutations causing SCA-14 were characterized functionally by in vitro assays it was shown that they resulted in an increase of PKCγ catalytic activity (Verbeek et al.

2005) linking Purkinje cell degeneration to a potential gain of function phenotype of PKCγ. More recently, Adachi et al. (2008) studied the PKC activity of 20 spontaneous mutations found in the PKCγ gene of SCA-14 patients. 19 of the 20 mutations showed an increased constitutive activity of PKC and increased calcium levels in the cytoplasm when assayed in transfected cells. Furthermore, transfection of mutant PKCγ into cultured dissociated Purkinje cells resulted in increased apoptosis and in a reduction of dendritic growth (Seki et al., 2009). These findings are consistent with the concept that the disease phenotype in SCA-14 is related to increased PKC activity. Nevertheless, there are also indications that despite an increased basal activity of mutated PKCγ, there might be a deficit to recruit downstream targets resulting in a certain loss of function (Verbeek et al., 2008). After viral transfection of a mutated form of PKCγ in vivo LTD was shown to be impaired and there were indications that the mutant PKCγ may interfere with normal endogenous PKC activity in a dominant negative manner (Shuvaev et al., 2011). Furthermore, another typical feature of mutated PKCγ proteins is an increased protein aggregation which may cause Purkinje cell death by ER-stress (Seki et al., 2005, 2007). In a recent study it was shown that the disaccharide trehalose can inhibit PKCγ aggregation and improves survival and development of Purkinje cells in an in vitro model (Seki et al., 2010). Taken together, the mechanism by which the mutations in the PKCγ gene lead to Purkinje cell degeneration in SCA-14 are still rather unclear (Sakai et al., 2011). Until today, only one transgenic mouse model of SCA-14 has been published (Zhang et al., 2009). In these mice the H101Y mutation was transgenically expressed under the control of a universal CMV promoter. The authors report an altered morphology and loss of Purkinje cells, but the documentation of these findings in the article is incomplete. In this study we present a novel SCA-14 mouse model with Purkinje cell specific expression of the PKCγ mutation S361G which is located in the kinase domain and was shown to confer an increased constitutive activity as tested by in vitro assays (Adachi et al., 2008). We find that in PKCγ-S361G transgenic mice there is evidence for both an increased PKCγ activity in vivo and for pathological changes typical for cerebellar disease thus linking the increased and dysregulated activity of PKCγ tightly to the development of cerebellar disease.

### 4.1.3. Materials and Methods

*Real time quantitative PCR*

RNA was purified from the cerebellum of control and PKC-C mice at different ages using the RNeasy Mini-kit (Qiagen) following the instructions of the manufacturer. Real time quantitative PCR was performed on a StepOne real-time PCR system (Applied Biosystems, Zug, Switzerland) using the manufacturer's Syber green master mix. The following primers were used: human (transgenic) PKCγ, forward gaaacagaagacccgaacgg, reverse: cgccttgagcagctccgagacg; mouse (endogenous) PKCγ, forward: caaaacagaagacaaagacc, reverse: ggccttgagtagctctgagaca; GAPDH, forward: aactttggcattgtggaagg, reverse: acacattgggggtaggaaca. Reactions were quantified by relative standard curve system and the cycle threshold method using the SDS2.2 software (Applied Biosystems, Foster City, CA). A relative quantitation value (RQ) for each sample from the triplicates of that sample was calculated for each gene. The data were analyzed with GraphPad Prism software.

*Western blot analysis*

Control and PKC-C mice of different ages were sacrificed by an overdose of pentobarbital, then the cerebellum was quickly dissected and frozen in liquid nitrogen. Samples were homogenized in RIPA buffer (SigmaAldrich, Buchs, Switzerland) with phosphatase and protease inhibitors. Protein concentrations were determined using a NanoDrop instrument (ThermoScientific, Reinach, Switzerland) and 100 µg of each sample were subjected to SDS-PAGE. The separated proteins were transferred to a nitrocellulose membrane using a semidry blotting machine (Bio-Rad, Cressier, Switzerland). After blotting, membranes were blocked with 5% BSA in TBS for 1 h and incubated with appropriate primary antibodies. After washing with TBS-T membranes were incubated with HRP-labelled secondary antibodies for 1 h. After washing bound antibodies were visualized with ECL2 Western blotting substrate (Pierce, Thermo Scientific, Reinach, Switzerland) and quantified using a C-Digit Western Blot scanner and software (LI-COR Biosciences, Bad Homburg, Germany).

*Immunohistochemistry and Histology*

Immunohistochemistry was performed as described previously (Gugger et al., 2012). For the analysis of the cerebellar sections control and PKC-C transgenic mice were sacrificed by perfusion with 4% paraformaldehyde and the cerebellum was sectioned on a cryostat at 20μm. Sections were incubated free floating with the following antibodies: rabbit anti-calbindin D28K and mouse monoclonal anti-Parvalbumin (1:1000, Swant, Marly, Switzerland), mouse monoclonal anti-NeuN (1:500, Millipore, Zug, Switzerland), rabbit anti-GFAP (1:1000, Dako, Baar, Switzerland), rabbit anti vGlut1 (1:1000, Synaptic Systems,Heidelberg, Germany), rabbit anti-PKCγ (1:1000, Santa Cruz Biotechnology, Santa Cruz, CA), rabbit anti-GFP (1:500, Abcam, Cambridge, UK). Organotypic slice cultures were fixed after 9-11 days in vitro in 4% paraformaldehyde overnight at 4°C. All reagents were diluted in 100 mM phosphate buffer (PB), pH 7.3. Cryoections or slices were incubated in blocking solution (0.1 - 0.3% Triton X-100, 3% normal goat serum) for a minimum of 30 minutes in order to permeabilize the tissue and block non-specific antigen binding. Primary antibodies were added in fresh blocking solution and incubated overnight at 4°C. The staining was visualized with anti-mouse and anti-rabbit AlexaFluor 488 and 568 2nd antibodies (1:500, Molecular Probes, Eugene, OR). After washing in PB, secondary antibodies were added in PB containing 0.1% Triton X-100 in order to prevent non-specific antigen binding for at least 1 hour at room temperature. For cresyl violet staining cryostat sections were collected on Superfrost slides (Menzel, Braunschweig, Germany) and were stained with 0.125% cresyl violet to show the cellular pattern of the cerebellum. Stained slices or sections were mounted on glass slides and coverslipped with Mowiol (SigmaAldrich, Buchs, Switzerland). Cultures and sections were viewed on an Olympus AX-70 microscope equipped with a Spot digital camera. Recorded images were adjusted for brightness and contrast with Photoshop image processing software.

### 4.1.4. Results

*Transgene expression in PKCγ–S361G (PKC-C) transgenic mice*

We have aimed at creating a mouse model of SCA-14 by introducing a mutated human PKCγ gene carrying a mutation found in an affected family. We have chosen the S361G mutation (Chen et al., 2005) located in the kinase domain of the PKCγ gene. This mutation was shown to increase the kinase activity of PKCγ in a cell based assay

using CHO cells (Adachi et al., 2008). Five founders (for simplicity called PKC-C mice) were originally identified from 64 mice and were double tested by PCR genotyping with a second pair of primers (Fig. 10A). The identity and completeness of the transgene was checked and confirmed by DNA sequencing. In order achieve a Purkinje cell specific expression using the Tet-off system, the selected transgenic founder mice were crossed with Pcp2-tTA transgenic mice (Zu et al., 2004) which express the Tet-Transactivator under a Purkinje cell specific promoter. In the offspring double transgenic mice were identified by PCR genotyping (Fig. 10B). Expression of the transgene was indicated by the presence of the GFP reporter included in the transfected construct, and was only observed in mice double transgenic for Pcp2-tTA and PKC-C (Fig. 10C and 10D). The expression of the mutated PKCγ protein cannot be directly assayed because no antibody specific for human PKCγ protein is available. Therefore, we have analyzed the presence of the mutated human mRNA by real time quantitative PCR (qPCR), (Fig. 10E) and the amount of total PKCγ protein as detected by Western blotting with the polyclonal anti-PKCγ antibody (Fig. 10F). No signal was obtained in qPCR for the mutated human PKCγ mRNA confirming the specificity of the used primers. In PKC-C mice mRNA expression of the mutated human PKCγ mRNA was present but only reached approximately 50% of the value of the endogenous normal PKCγ mRNA in P12 postnatal animals. In adult animals expression of the mutated human PKCγ mRNA declined slightly compared to the GAPDH control but because the mRNA of the endogenous PKCγ mRNA became expressed much stronger the mutated mRNA only constituted 15-20% of the endogenous mRNA in adult animals (Fig. 10E). The findings from qPCR were confirmed by Western blot analysis of total PKCγ protein in the cerebellum of control and PKC-C mice (Fig. 10F). In P12 PKC-C mice, PKCγ protein was increased to approximately 175% of control mice, but this increase had disappeared in 3 month and 12 month old adult mice (Fig. 10F). These findings indicate that the human mutated PKCγ protein is specifically present in Purkinje cells of PKC-C mice but only constitutes about 30-50% of the total PKCγ protein in postnatal mice and much less in adult mice. The results shown in this manuscript are based on studies with founder 3 which had a solid GFP expression in Purkinje cells. Parts of the experiments were reproduced in founders 2 and 6 with very similar findings (data not shown).
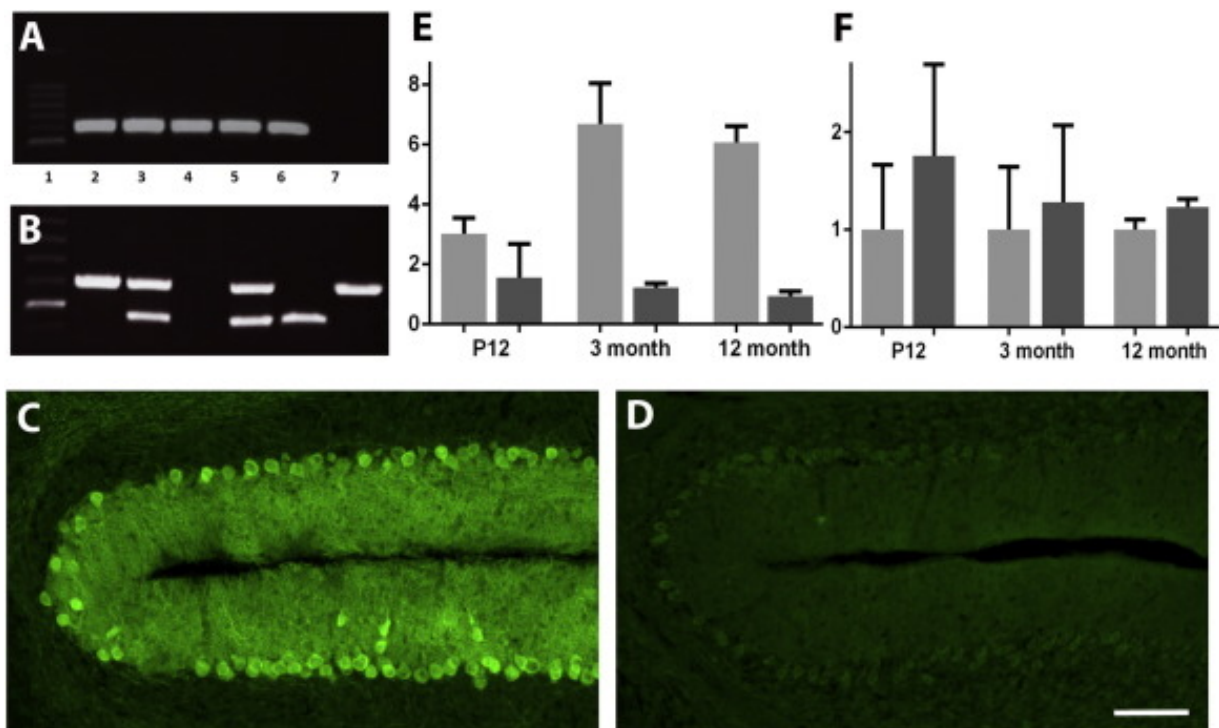
**Fig. 10 Generation of transgenic mice**

**A** The genotype of the founders was confirmed by PCR with a second pair of primers for human mutated PKC$\gamma$ transgenic mice. A 585bp band is detected in all positive founders but not in control.  1, DNA ladder; 2-6, 5 different founders; 7, negative control.
**B**  Double transgenic mice expressing the mutated PKC$\gamma$ protein were identified by PCR. These mice show the 585bp band for mutated PKC$\gamma$ and Pcp2-tTA (472bp) band. 1, DNA ladder; 2, PKC$\gamma$+, 3, PKC$\gamma$+ Pcp2-tTA +, 4, negative mouse, 5, PKC$\gamma$+ Pcp2-tTA +, 6, Pcp2-tTA +, 7, PKC$\gamma$+. **C, D** In double transgenic mice (C) the GFP marker was expressed specifically in Purkinje cells, while no GFP expression was found in control mice (D). Scale bar in D = 100 µm. **E** The expression of the mutated PKC$\gamma$ mRNA was analyzed by quantitative RT-PCR. Light grey bars: Expression of endogenous PKC$\gamma$ mRNA in PKC-C mice, dark grey bars: Expression of mutated human PKC$\gamma$ mRNA. In P12 postnatal animals the mutated PKC$\gamma$ mRNA constituted approximately 50% of the endogenous normal PKC$\gamma$ mRNA, in adult animals expression of endogenous mRNA became stronger and the mutated PKC$\gamma$ mRNA constituted only 15-20% of the endogenous PKC$\gamma$ mRNA. **F** Quantitation of Western blots for total PKC$\gamma$ protein in the cerebellum of control and PKC-C mice. Light grey bars: Expression of total PKC$\gamma$ protein in control mice, dark grey bars: Expression of total PKC$\gamma$ protein in PKC-C mice. In P12 postnatal PKC-C mice total PKC$\gamma$ protein was increased by approximately 75% compared to control mice, in adult PKC-C mice total PKC$\gamma$ protein expression was similar to control mice.

71

### 4.1.5. Discussion

We have generated a novel SCA-14 mouse model with Purkinje cell specific expression of the PKCγ mutation S361G. This mutation was identified in 2005 (Chen et al., 2005) and is located in the kinase domain of the PKCγ protein. In a cellular assay system, this mutation was shown to confer an increased constitutive PKC activity (Adachi et al., 2008). We find that in PKCγ-S361G transgenic mice (here called PKC-C mice) there is evidence for both an increased PKCγ activity in vivo and for pathological changes typical for cerebellar disease thus linking the increased and dysregulated activity of PKCγ tightly to the development of cerebellar disease.

In human patients affected with the SCA-14 mutation used in this study, the major clinical and neuroimaging findings were a cerebellar ataxia, dysarthria and a cerebellar atrophy confirmed by MRI scans (Chen et al., 2005). In contrast, we did not find an overt cerebellar atrophy in the PKC-C mice. There are several possible explanations for this apparent difference. First, the age of onset of symptoms and the cerebellar atrophy in the human patients was between 5 and 60 years of age, with a mean of 28 years of age. It may be difficult to replicate the cerebellar atrophy in the mouse with a life span of 1 to 2 years. Furthermore, the expression levels of the mutated transgenic PKCγ protein in the PKC-C mice are rather moderate. The expression level of the transgenic mRNA constitutes less than 50% of the mRNA of the normal endogenous PKCγ and a moderate increase of total PKCγ protein could only be found in young postnatal mice. Taken together these findings suggest that the fraction of the mutated PKCγ protein is around 30-50% of total PKCγ protein in young postnatal mice and will be less in older animals. In heterozygous SCA14 patients the expression of the transgene should be around 50% of the total protein throughout life and would be substantially higher compared to PKC-C mice. It is well conceivable that the expression level found in the PKC-C mice could be sufficient for causing functional changes in Purkinje cells but too low for causing Purkinje cell degeneration and death throughout the cerebellum.

### 4.2. Cerebellar slice culture and dissociated cerebellar culture

#### 4.2.1. Cerebellar slice culture

The model system of cerebellar slice cultures is extensively used in neurobiology and electrophysiology studies. Initially organotypic slice cultures were developed with explant cultures of various neuroanatomical origins (Gähwiler et al., 1997 ). Since then, slice cultures have become an attractive alternative in addition to acute slices, and the spectrum of possible culturing methods, as well as the type of applications with which they have been used, have been considerably expanded.

In organotypic slice cultures, a complete slice of tissue is kept in culture. This has the advantage that the natural microenvironment of the neurons with cell-cell interactions and the local neuronal networks is preserved (Dupont et al., 2006). This provides the possibility for various kinds of studies, like cellular development, synaptogenesis, repair after lesions, or electrophysiology. Slice cultures from the nervous system, however, can only be obtained from immature tissue, as survival of neurons critically depends on their stage of development. For example, Purkinje cells are extremely sensitive to axotomy at the age around P5 in mice and do not survive in slice cultures prepared during this period (Dusart et al., 1997). In general, slice cultures give best results when taken from developing nervous tissue before myelination.

Some special measures have to be taken to ensure a sufficient supply with nutrients and oxygen to all cells in the typically 0.3 – 0.5 mm thick slice cultures. In the technically simplest method, the static slice culture, which allows cerebellar slices to be cultured for several weeks, the slices are placed on top of a membrane which is permeable to all ingredients of the culture medium (Stoppini et al., 1991). The membrane is held by a culture insert and placed over the medium, which is drawn through the membrane into the slice culture by capillary forces. In this culture, the top of the culture is at the interface between culture medium and air, which allows both nutrients and oxygen to reach the whole culture (Kapfhammer and Gugger, 2012).

#### 4.2.2. Results of cerebellar slice culture

Organotypic cerebellar slice cultures were cultured for 7 days. Starting at the 3rd day in vitro, some of the cultures were treated with PMA (50 nM), a phorbol ester which is stimulating PKC, until the cultures were fixed. PMA has been shown previously to

inhibit and limit Purkinje cell dendritic development (Metzger F., 2000). As control we added EtOH/DMSO which was used for diluting PMA.

Purkinje cells in the slices were visualized by immunostaining with anti-Calbindin D28K which is a Purkinje cell marker (Fig. 11A).In the control slices, Purkinje cells developed large and highly branched dendritic trees. In Purkinje cells treated with PMA, the morphology of the dendritic tree was completely changed (Fig. 11B). The dendritic tree was very small and stunted, the branches appeared thickened with only few short side branches. The area covered by the dendritic tree was markedly reduced. A similar morphology was present in cultures derived from mPKCγ transgenic mice. The dendritic tree of the Purkinje cells from these mice was greatly reduced in size and the branching was markedly reduced (Fig. 11C). The morphology was very similar and indistinguishable from that of PMA treated control Purkinje cells suggesting that the mutated PKCγ-S361G from transgenic mice had an increased PKC activity. Moreover, when Purkinje cells derived from mPKCγ transgenic mice were treated with PMA, the dendritic tree of the Purkinje cells was further reduced in size and almost no branching could be detected (Fig. 11D). A quantitative analysis of Purkinje cell dendritic tree size is shown in Fig. 11E. For statistical analysis the area covered by the dendritic trees of at least 20 different Purkinje cells was measured. Statistical analysis of the data was done with Graph Pad Prism software. Results are typically presented as bar graphs. The statistical analysis showed clear statistically significant differences between the size of the dendritic tree of Purkinje cells from the control condition compared to PMA treatment or Purkinje cells derived from mPKCγ transgenic mice with or without PMA treatment (Fig. 11E). No statistically significant differences were found between control Purkinje cells treated with PMA and Purkinje cells from mPKCγ transgenic mice. Interestingly, the dendritic size of PMA-treated Purkinje cells from mPKCγ transgenic mice was further reduced compared to untreated Purkinje cells from mPKCγ transgenic mice or PMA-treated control Purkinje cells. This finding suggests that the mPKCγ does mediate a strong but not maximal stimulation of PKC activity, which can be further boosted by PMA treatment.
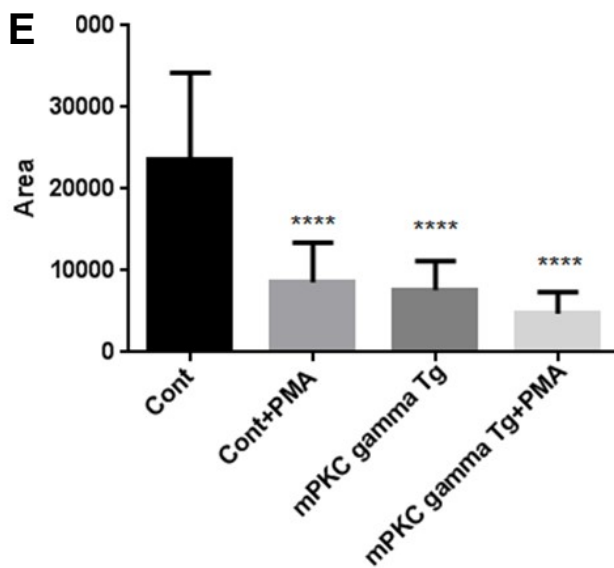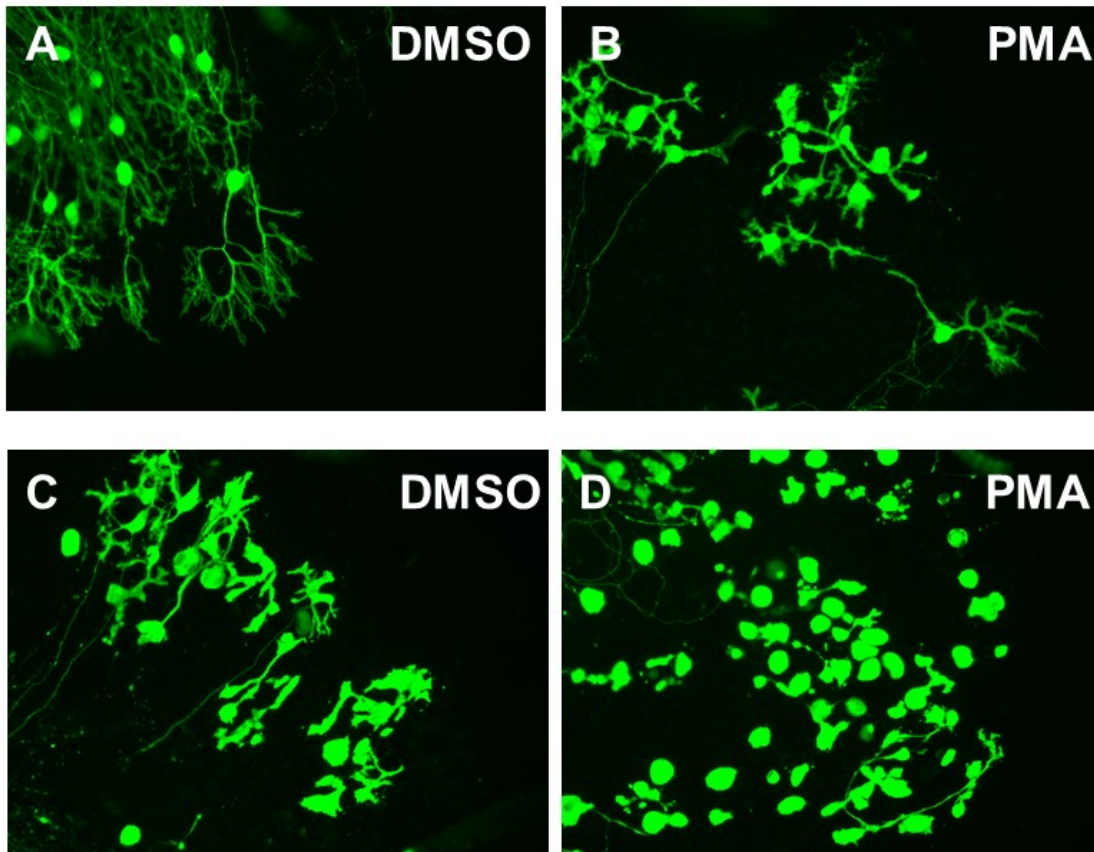
**Fig. 11 Purkinje cell morphology and dendritic size of mPKCγ transgenic mice and control mice**

(A) Immunofluorescence staining of cerebellar slice cultures after one week in vitro. Cultures from control mice showed expanded dendritic trees. (B) Purkinje cells from control cultures treated with the PKC activator PMA developed only very small dendritic trees. (C) The dendritic tree of Purkinje cells from mPKCγ transgenic mice was also small with few side branches. (D) PMA treatment of Purkinje cells from mPKCγ transgenic mice further compromised dendritic tree development. (E) Quantification of the total dendritic area of Purkinje cells. The reduction of dendritic size of Purkinje cells from mPKCγ transgenic mice and PMA-treated control cultures versus untreated control cultures was statistically significant with $p < 0.05$. Error bars indicate the SEM.

### 4.2.3. Dissociated cerebellar culture

In contrast to slice cultures, in dissociated cell cultures, cells are taken out of their tissue environment and can be studied in isolation. Dissociated Purkinje cells preparations maintained in an in vitro environment with simplified cellular and biochemical conditions can facilitate molecular analyses of neuronal development. Pharmacological manipulation of Purkinje cells is also possible in cultures maintained with a serum free, chemically defined medium. Because of these advantages, dissociated cultures of cerebellar neurons have been utilized for example in the search for granule neuron (GN)-derived trophic factors which support the survival of developing Purkinje cells (Baptista et al., 1994; Morrison et al., 1998).

A disadvantage of dissociated cerebellar cultures is the relatively low survival rate of Purkinje cells in serum free, hormone supplemented Eagle's basal medium, in particular as long term culture over two weeks and longer is needed. Furuya et al. (1995) found that the use of Dulbecco's modified Eagle medium : F-12 nutrient based medium (DFM) significantly improves the long term survival of dissociated rat Purkinje cells. Later, Tabata et al. (2000) further modified this method for mouse Purkinje cells. Mouse Purkinje cells cultured according to their method differentiated through several morphological and electrophysiological stages similar to those seen in Purkinje cells in vivo. Various aspects of Purkinje cell biology, including their morphological development, electrophysiological properties, sub-cellular organization, and relationships with other cell types have been investigated using these dissociated cerebellar cultures (Matsuda et al., 2010; Okubo et al., 2001 ; Tanaka et al., 2006; Uemura et al., 2010).

Recently, Wagner et al., (2011) showed that transfection by electroporation using a novel plasmid containing the promoter sequence of the Purkinje cell specific gene L7 provides an efficient and simple method to achieve the expression of multiple exogenous cDNAs in cultured Purkinje cells.

The dissociated cerebellar cultures are heterogeneous, containing granule neurons, interneurons and glial cells in addition to Purkinje cells. Remarkably, the expression of cDNAs with pL7 plasmids is highly specific for Purkinje cells. In contrast, expression from plasmids utilizing a β-Actin promoter is observed mainly in neurons other than Purkinje cells (Wagner et al., 2011). Similarly, CMV promoter-based plasmids led to

high level cDNA expression in cells other than Purkinje cells. These differences highlight the value of novel pL7-plasmids for achieving Purkinje cell transfection.

We obtained the pL7 plasmid from Dr. Wagner and established the transfection of Purkinje cells in dissociated cerebellar cultures in order to be able to evaluate the effects of different transfected genes for Purkinje cell dendritic development.

### 4.2.4. Results of dissociated cerebellar culture

*Purkinje cell dendritic development in dissociated cultures*

We observed the dendritic development of Purkinje cells in these cultures for 18 days. With this dissociated culture system, we could follow the development of Purkinje cells as a single cell. The time point for terminating the cultures can be chosen based on visualizing the living Purkinje cells and their dendritic trees.

At DIV 4, Purkinje cell dendrites start to develop but the cells still have multiple thin perisomatic processes. At DIV 8, Purkinje cells have formed a primary dendrite and start rapid dendritic expansion. At around DIV 14-18, Purkinje cells have developed a rather elaborated highly branched dendritic tree (Fig. 12). An advantage of this culture system is that we could follow the dendritic development of Purkinje cells over time and also we could maintain the cultures for more than 4 weeks.
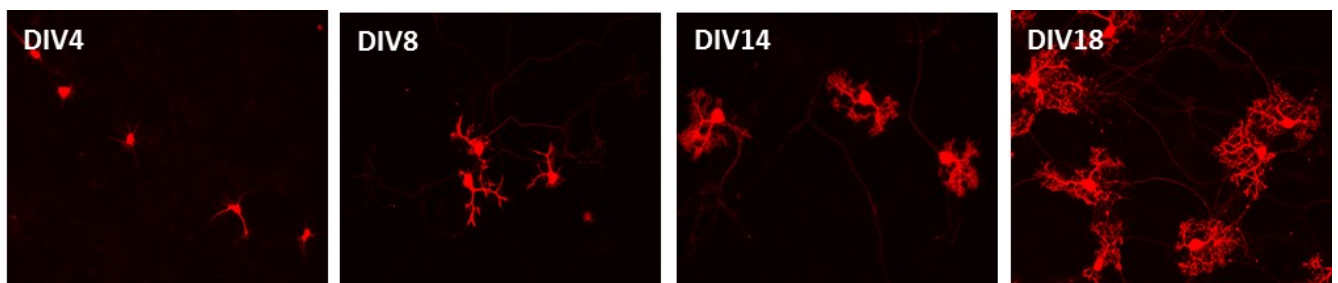


**Fig. 12 Development of Purkinje cell in Dissociated cerebellar culture**
Immunofluorescence staining of dissociated cerebellar cultures in each point in vitro. Cultures were stained with anti-Calbindin D-28K (1:1000).

*Purkinje cell dendritic development in dissociated cultures from mPKCγ transgenic mice*

As shown above, Purkinje cells from control mice developed elaborated branched dendritic arbors after a culture period of 14-18 days. In contrast, Purkinje cells from mPKCγ transgenic mice developed only very small dendritic trees.
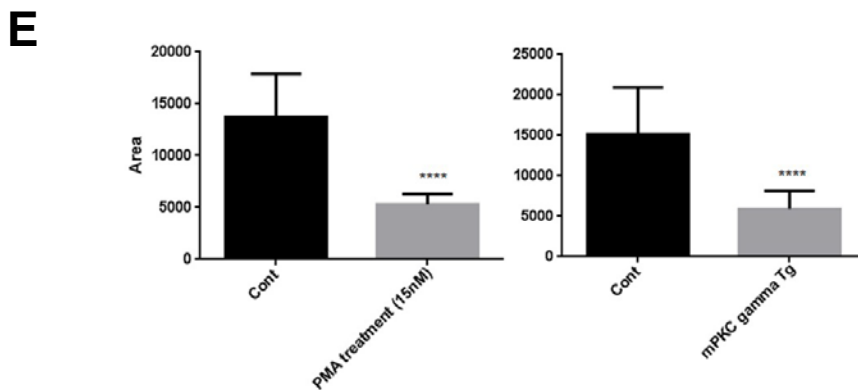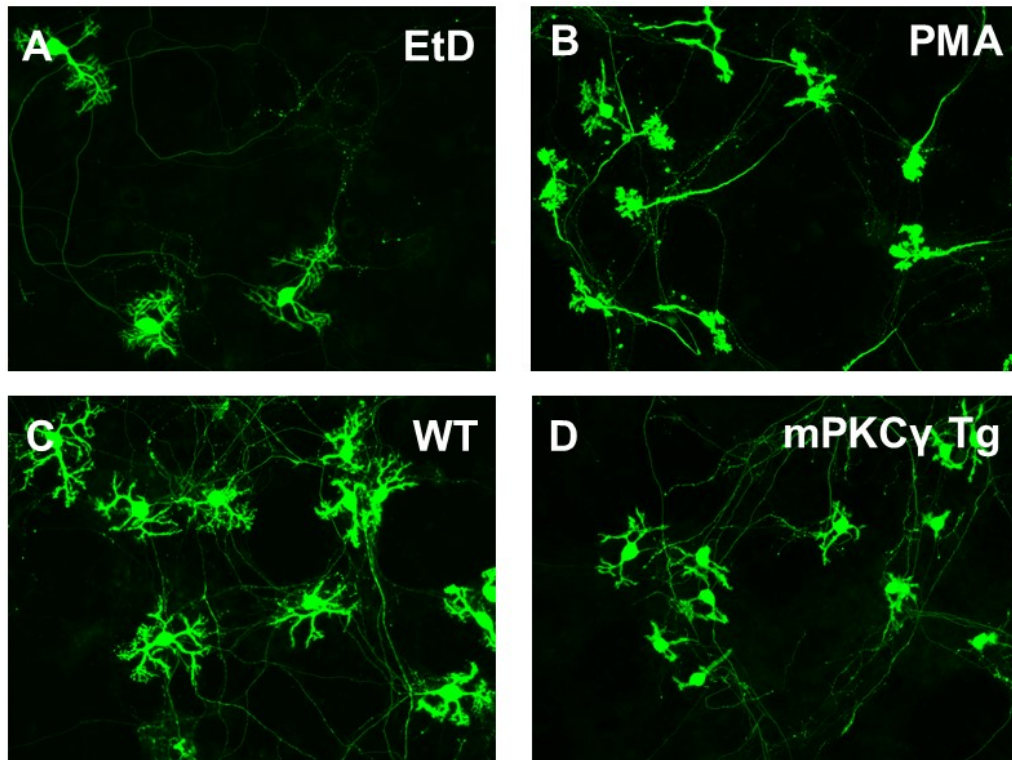
**Fig. 13 Immunofluorescence staining analysis of dissociated cerebellar culture of mPKCγ transgenic mice and control mice**

(A) Immunofluorescence staining of dissociated cerebellar culture after two weeks in vitro. Cultures from control mice treated with EtOH/DMSO showed expanded dendritic trees. (B) Purkinje cells from control cultures treated with the PKC activator PMA developed a small dendritic tree with only very few processes. (C) Cultures from control mice without any treatment showed large expanded dendritic trees. (D) The dendritic tree of Purkinje cell from mPKCγ transgenic mice was very small and very similar to the dendritic tree of PMA-treated control. (E) Quantification of the total dendritic area of Purkinje cells. The reduction of dendritic size of PMA-treated cultures or Purkinje cells from mPKCγ transgenic mice versus control cultures was statistically significant with $p < 0.05$. Error bars indicate the SEM.

These findings are comparable to those obtained in organotypic slice cultures. The morphology of Purkinje cells from mPKCγ transgenic mice was similar to that of control Purkinje cells treated with the PKC activator PMA (Fig. 13A-D, previous page). The statistical analysis showed clear statistically significant differences of the size of the dendritic tree of Purkinje cells between the control condition and PMA treatment or Purkinje cells derived from mPKCγ transgenic mice (Fig. 13E).

From these data two important conclusions emerge:

First, dissociated cultures yield exactly the same results with respect to the Purkinje cell dendritic tree as organotypic slice culture showing that this culture method is appropriate for studying Purkinje cell dendritic development.

Second, Purkinje cells from mPKCγ transgenic mice showed a gain of function phenotype of PKCγ biological activity. With the consistent results from these experiments, dissociated cerebellar cultures are proven to be an appropriate system to analyse Purkinje cell dendritic morphology after gene manipulation experiments.

### 4.3. Transfection approach for Purkinje cells

4.3.1. Biolistic transfection

In order to optimize the transfection parameters, we performed transfections with several conditions (Table. 1 and 2).

| Plasmid 1mg/ml | Gold | pressure | shooting day | transfected cell number | Purkinje cells |
|---|---|---|---|---|---|
| GFP | 1.6um B(12.5mg) | 200 Psi  wide barrel | DIV3 | 20<transfedted cells<40 | 3--8 |
| GFP | 1.6um B(12.5mg) | 200 Psi  wide barrel | DIV3 | 20<transfedted cells<40 | 3--8 |
| GFP | 1.6um B (6mg) | 80 Psi  narrow barrel | DIV3 | 20<transfedted cells<40 | 2 |
| GFP | 1.6um B (6mg) | 150 Psi  narrow barrel | DIV3 | 20<transfedted cells<40 | 1 |

**Table. 1 Condition of biolistic transfection 1**
The same GFP-vector was transfected with the different parameters at DIV 3 to cerebellar slices. Total transfected cell number and transfected Purkinje cell number are shown for 8 cerebellar slices on one culture insert transfected together with the same conditions.

| Plasmid 1mg/ml | Gold | pressure | shooting day | transfected cell number | Purkinje cells |
|---|---|---|---|---|---|
| GFP | 1.6um B(12.5mg) | 120 Psi narrow barrel | DIV4 | poor <5 | 0 |
| GFP | 1.6um B(12.5mg) | 120 Psi X2 narrow barrel | DIV4 | poor <20 | 0 |
| GFP | 1.6um B(6mg) | 120 Psi narrow barrel | DIV4 | 40<transfedted cells<80 | 2--5 |
| GFP | 1.6um B(6mg) | 120 Psi X2 narrow barrel | DIV4 | 60<transfedted cells<100 | 3--8 |
| GFP | 1.6um B(12.5mg) | 200 Psi wide barrel | DIV4 | 20<transfedted cells<40 | 1 |
| GFP | 1.6um B(12.5mg) | 200 Psi wide barrel | DIV4 | 20<transfedted cells<40 | 0 |
| GFP | 1.6um B(6mg) | 200 Psi wide barrel | DIV4 | 40<transfedted cells<80 | 2--5 |
| GFP | 1.6um B(12.5mg) | 120 Psi narrow barrel | DIV7 | 30<transfedted cells<60 | 1--3 |
| GFP | 1.6um B(12.5mg) | 120 Psi X2 narrow barrel | DIV7 | 30<transfedted cells<60 | 1 |
| GFP | 1.6um B(12.5mg) | 200 Psi wide barrel | DIV7 | 40<transfedted cells<60 | 2--5 |
| GFP | 1.6um B(12.5mg) | 200 Psi wide barrel | DIV7 | 40<transfedted cells<60 | 6--12 |

**Table. 2 Condition of biolistic transfection 2**
GFP-vector was transfected with different conditions at DIV 4 or DIV 7 to cerebellar slices. Transfected cell number and transfected Purkinje cells number are shown for 8 cerebellar slices on one culture insert transfected together with the same conditions.

We first used the original barrel provided by Biorad for bombardment ("wide barrel"), it's a rather wide barrel and makes it difficult to target a specific region on the culture insert. We also used another barrel which is narrower ("narrow barrel") and allows to target specific regions on the culture inserts (O'Brien and Lummis, 2006). Also we compared bombardments at different times in vitro (from DIV 3 to DIV 7) and with two different amounts of Gold particles. The results are shown Fig. 14 and 15. In some cases we could get several transfected Purkinje cells (Fig. 15) but it was rather rare and often we only got few transfected Purkinje cells per slice.

*Wide barrel VS Narrow barrel*

With the wide barrel (pressure 200 Psi), we got several transfected Purkinje cells in one well with 8 cerebellar slices (at DIV 3; 3-8 Purkinje cells, at DIV 4; 0-5 Purkinje cells, at DIV 7; 2-12 Purkinje cells). With the narrow barrel (80 Psi to 150 Psi), we got slightly fewer transfected Purkinje cell compared to the wide barrel (at DIV 3; 1or2 Purkinje cells, at DIV 4; 0-8 Purkinje cells, at DIV 7; 1-3 Purkinje cells), but the difference was small.

*Shooting day*

We did the transfections at DIV 3, DIV 4 and DIV 7 independently and could not see any difference in the transfection rate.

We also tried several types of Gold particles and again no clear difference was found for different particle sizes or particle types (data not shown).

In all the experiments we have done we could get only a small number of transfected Purkinje cells insufficient for doing an analysis of the size and morphology of the Purkinje cell dendritic tree. For this reason we did not further pursue this method for Purkinje cell transfection in slice cultures.
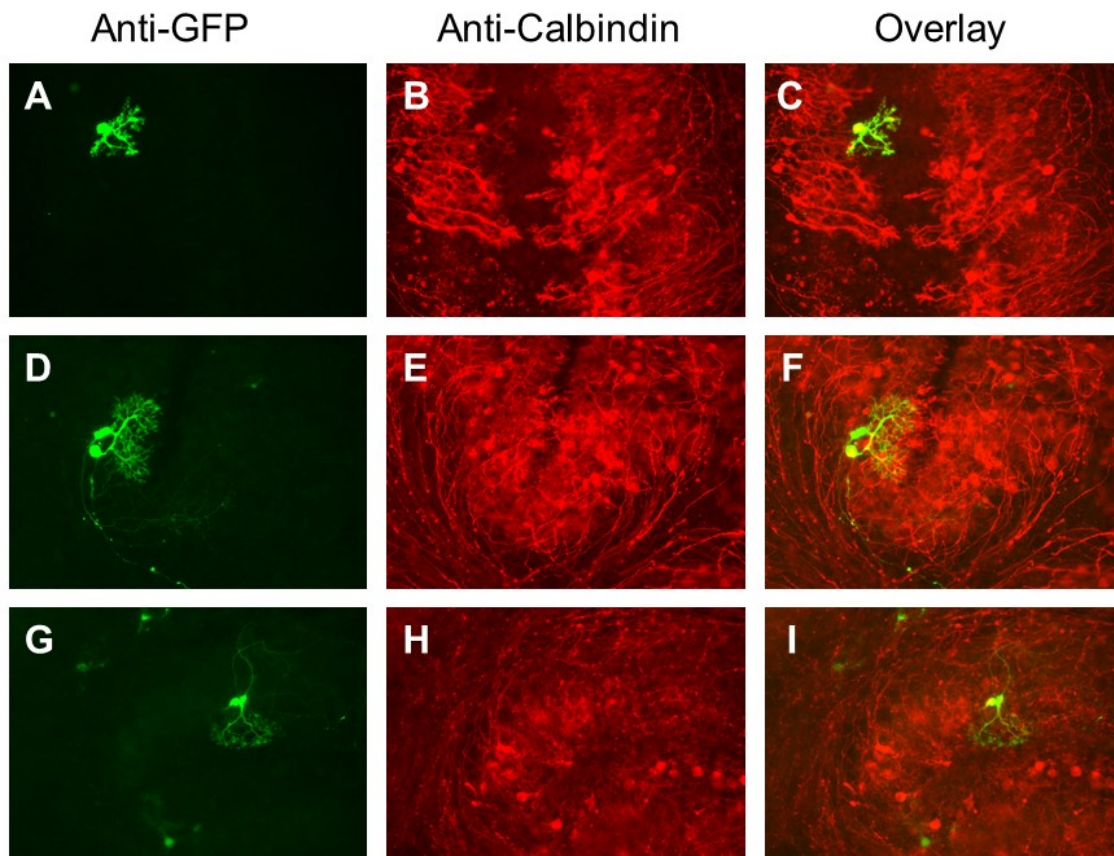
**Fig. 14 Immunostaining of GFP-transfected Purkinje cells**
Immunofluorescence staining of cerebellar slices after one week in vitro. After fixing, cerebellar slices were stained with anti-GFP and anti-Calbindin D28K antibodies. (A-C) Result with 1.6 µm (12.5 mg) Bio-Rad Gold, 200 Psi wide barrel at DIV 4. (D-F) Result with 1.6 µm (6.0 mg) Bio-Rad Gold, 80 Psi Narrow barrel at DIV 3. (G-I) Result with 1. 6 µm (6.0 mg) Bio-Rad Gold, 150 Psi Narrow barrel at DIV 3.
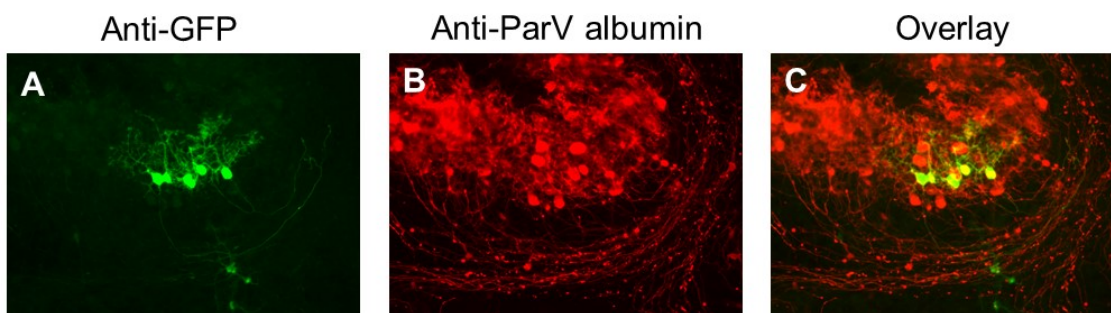


**Fig. 15 Immunostaining of GFP-transfected Purkinje cells**
Immunofluorescence staining of cerebellar slices after 9 days in vitro. After fixing, cerebellar slices were stained with (A) anti-GFP and (B) anti-Parvalbumin antibodies. Result with 1.6 µm (12.5 mg) Bio-Rad Gold, 200 Psi wide barrel at DIV 7.

### 4.3.2. Magnetofection

*Results*

In order to find the optimal conditions for transgene expression with Magnetofection (Buerli et al., 2007; Hughes et al., 2001; Krotz, 2003; Plank et al., 2003; Plank et al., 2011) we tested several time points of transfection as shown in Fig. 16.

We tested the transfection efficiency for transfections performed at DIV 5 or at DIV 14. At both time points, the magnetofection procedure didn't compromise the survival of the Purkinje cells (Fig. 16A-C). However, at both time points we only got few transfected cells, and only a very low number of transfected Purkinje cells. Furthermore, in the transfected cells the expression of the transgene was very weak as seen by the low intensity of GFP staining (Fig. 16D-I). Therefore, we didn't continue this method further.
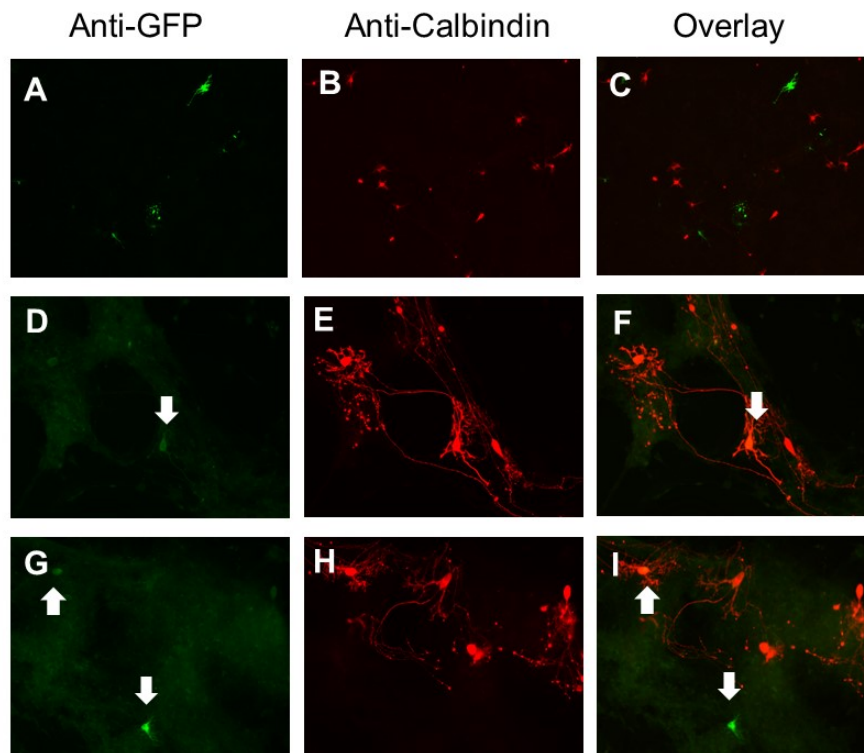


**Fig. 16 Immunostaining of GFP-transfected dissociated cerebellar cells**
(A-C) Immunofluorescence staining of dissociated cerebellar cells after 48 hours transfection with NeuroMag. Plasmid was transfected to dissociated cerebellar cells at DIV 5. At DIV 7, cells were fixed and stained with anti-GFP and anti-Calbindin D28K antibodies. (D-I) Immunofluorescence staining of dissociated cerebellar cells after 72 hours transfection with NeuroMag. Plasmid was transfected to dissociated cerebellar

cells at DIV 14. At DIV 17, cells were fixed and stained with anti-GFP and anti-Calbindin D28K antibodies.

### 4.3.3. Effectene

We tried transfections with Effectene at DIV 10 (Fig. 17A-F) and DIV12 (Fig. 17G-L). As a result of transfection at DIV 10, we found several transfected cells but no Purkinje cells (Fig. 17A-F). Very rarely we found GFP-transfected Purkinje cells (Fig. 17J-L) but the transfection rate was very low and transgenic GFP expression was weak. We therefore decided not to use this method for further experiments.
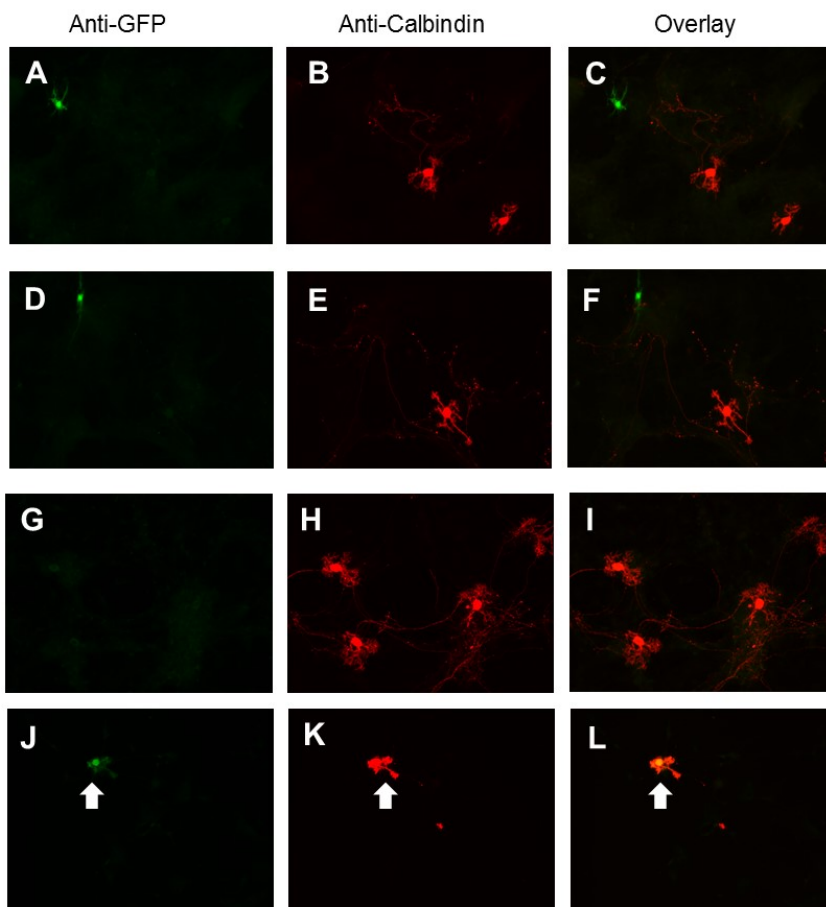


**Fig. 17 Immunostaining of dissociated cerebellar cells**

(A-F) Immunofluorescence staining of dissociated cerebellar cells after 24 hours transfection with Effectene. Plasmid was transfected to dissociated cerebellar cells at DIV 10. At DIV 11, cells were fixed and stained with anti-GFP and anti-Calbindin D28K antibodies. (G-I) Immunofluorescence staining of dissociated cerebellar cells without any transfection after 24 hours treated with Effectene. (J-L) Plasmid was transfected to dissociated cerebellar cells at DIV 12 with Effectene. At DIV 13, cells were fixed and stained with anti-GFP and anti-Calbindin D28K antibodies.

### 4.3.4. Conclusion

We tried 3 different transfection methods using various commercially available reagents. Using these three methods, we could obtain a certain number of transfected Purkinje cells. The best results were obtained using the Gene gun but still the achieved transfection efficiency was not sufficient for evaluating the dendritic development of transfected cells.

A possible explanation for the poor transfection efficiency might be that the CMV promoter contained in the expression plasmid does not support gene expression in Purkinje cells very well. Therefore, we had to reconsider the expression vector itself. Recently, Wagner et al. showed that with a Purkinje cell specific expression vector based on the L7 promoter long term transfections of Purkinje cells could be achieved after electroporation (Wagner et al., 2011). Therefore, we decided to try electroporation with the vector based on the L7 promoter from Wagner (Wagner et al., 2011).

## 4.4. Phenotype of other PKC gamma mutations

The following section contains unpublished results.

### 4.4.1. Transgenic mice which carry human PKCγ S361G mutation (mPKCγ) showed severe inhibition of dendritic in dissociated cerebellar culture

In a previous study, we have reported that the catalytic domain mutation caused severe inhibition of Purkinje cell dendritic development in organotypic cerebellar slice culture and in vivo (Ji et al., 2014). In order to confirm that a similar inhibition of Purkinje cell dendritic development could be seen in dissociated cerebellar cultures we made such cultures from mPKCγ transgenic mice. The cultures were fixed at DIV14 and stained with Calbindin-D28K, a marker protein for Purkinje cells. As expected, Purkinje cells from mPKCγ transgenic mice had small dendritic tree with few branch points, similar to Purkinje cells treated with the PKC activator PMA (Fig. 18). We performed PMA treatment during either from P4-P11 or from P7-P14, both showed a similar morphology (data not shown). These findings in dissociated cerebellar cultures correlate well with those in organotypic cerebellar slice cultures and demonstrate that an increased PKC activity caused inhibition of Purkinje cell dendritic development in in the dissociated cerebellar culture system. Using dissociated cerebellar cultures, we now tested whether mutant PKCγ constructs expressed via a L7 promoted-based vector would inhibit dendritic development in Purkinje cells.
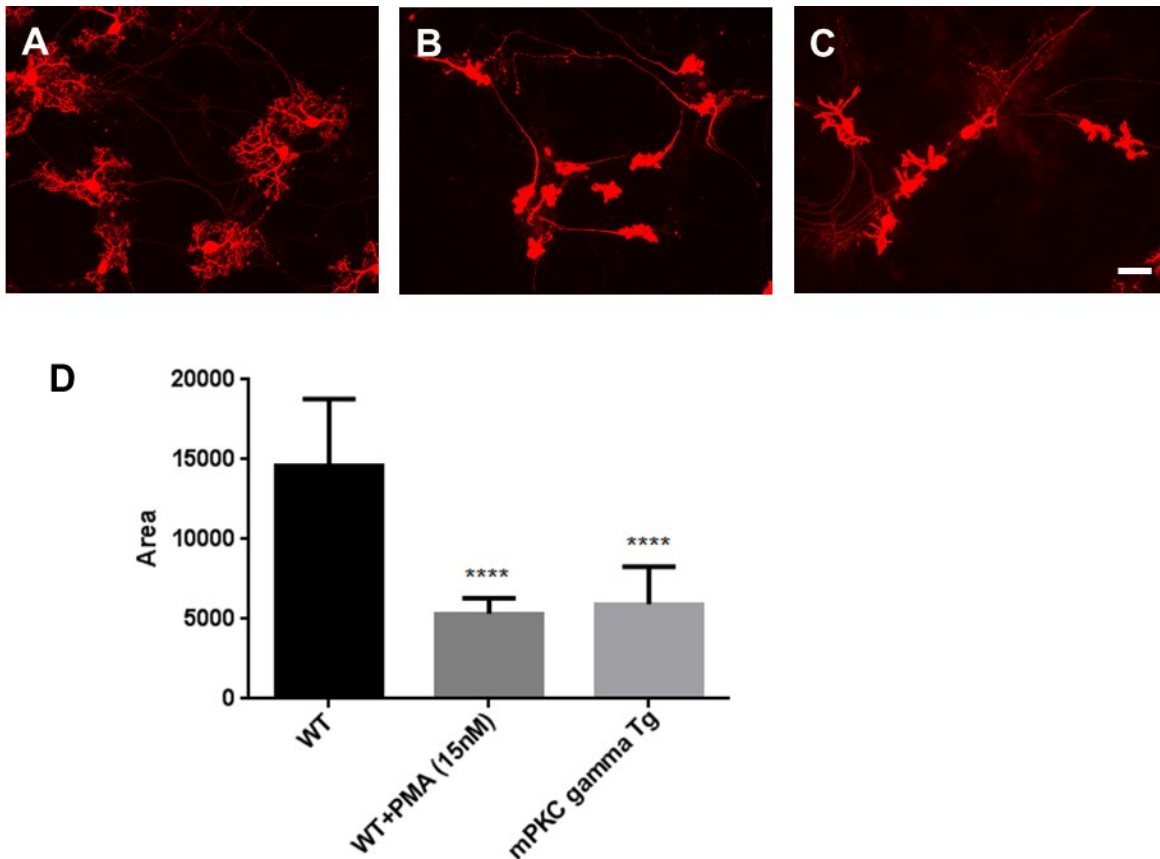
**Fig. 18 Increased PKC activity reduces Purkinje cell dendrites in dissociated primary culture.**
(A) Purkinje cells with normal dendritic expansion in dissociated primary culture. (B) PMA (15 nM, 10 days) treated Purkinje cell with greatly reduced dendrites. (C) Purkinje cells from mPKCγ transgenic mice also have greatly reduced dendrites. Scale bar in H = 50 μm. (D) Quantitative analysis of Purkinje cell dendritic tree size. Data are shown as the mean ± S.D of at least 20 Purkinje cells.

*SCA14 mutations for expression in Purkinje cells*

To date, over 30 mutations in PKCγ have been found in SCA14 families (Fig. 19A). Many of them are concentrated on C1B domain while some mutations are found throughout the coding regions of the PRKCG gene. In order to study the effects on Purkinje cell dendritic morphology of mutations in different domains of PKCγ , we constructed plasmids containing three C1B mutations, one deletion in the C2 domain (which is not reported in a SCA14 family but thought to be constitutive active (Rotenberg et al., 1998)) and two mutations in the  catalytic domain (Fig. 19B).

We have used a L7-based plasmid (a gift of Dr. Wolfgang Wagner in Hamburg) for the subsequent experiments because it allows expression of the transgene selectively in Purkinje cells (Baader et al., 1998; Wagner et al., 2011; Zhang et al., 2001). In order to observe the transfection and expression of PKCγ easily, the mutated PKCγ constructs are constructed as GFP fusion proteins (Fig. 19C).
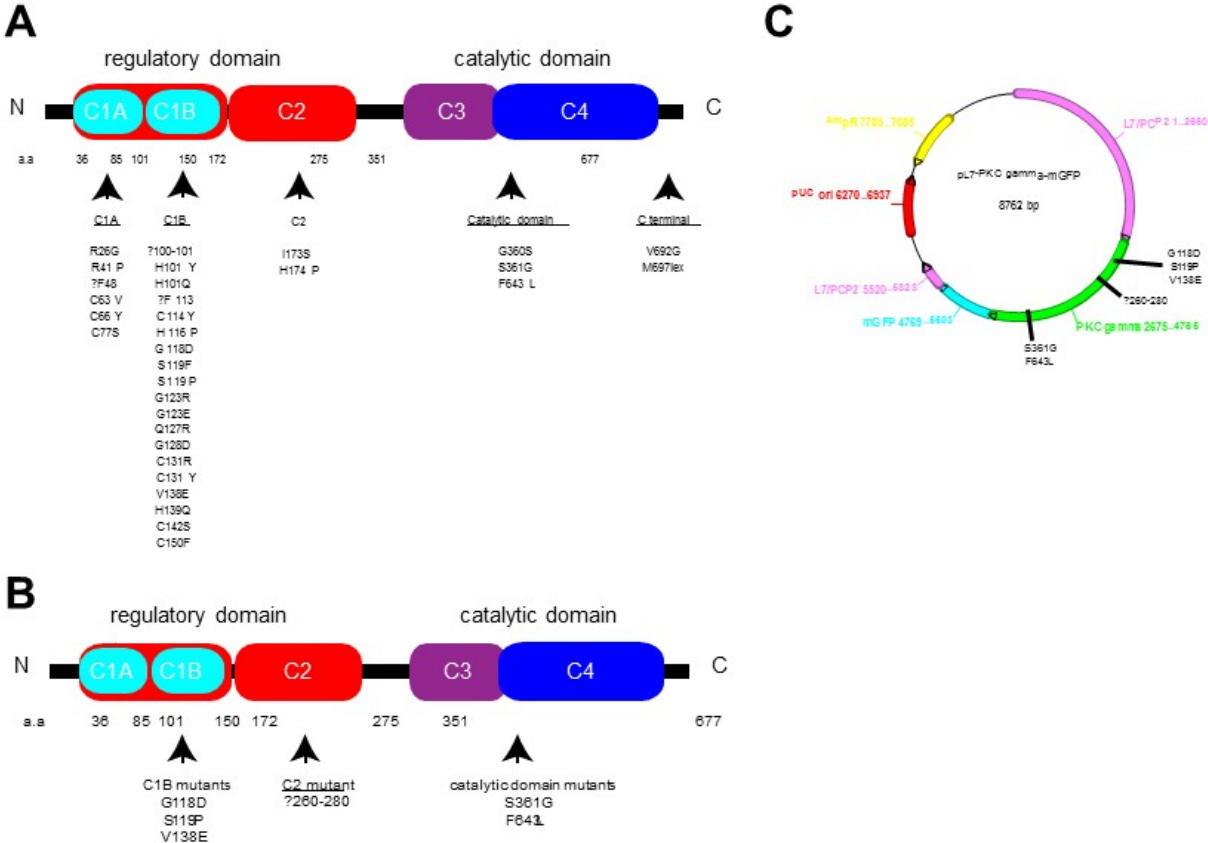


**Fig. 19 PKCγ protein domains with SCA14 mutations and the construct used for the experiments**

(A)Thirty two point mutations and deletions which were found in SCA14 families. (B)Five point mutations and one deletion which we chose for experiments. (C)Plasmid for expression of exogenous genes in Purkinje cells. Each mutation or deletion was constructed as GFP fusion protein.

### 4.4.2. Purkinje cells transfected with PKCγ carrying C1 or C2 domain mutations developed normal dendritic trees

First, in order to see the effect of a transgenic expression of wild type PKCγ (WT PKCγ), a WT PKCγ-GFP fusion plasmid was transfected to dissociated cerebellar cells. The transfection resulted in the continuous presence of the WT PKCγ–GFP fusion protein over several days as seen by GFP fluorescence. In the transfected Purkinje cells we found a small change of dendritic morphology with a thickening of the dendrites. However, quantitative analysis only showed a slight reduction of the dendritic tree size which didn't reach statistical significance. The amount of WT PKCγ–GFP fusion protein overexpression achieved with the L7-based vector is thus sufficient to have a small inhibitory effect on Purkinje cell dendritic development (Fig. 20A, F).
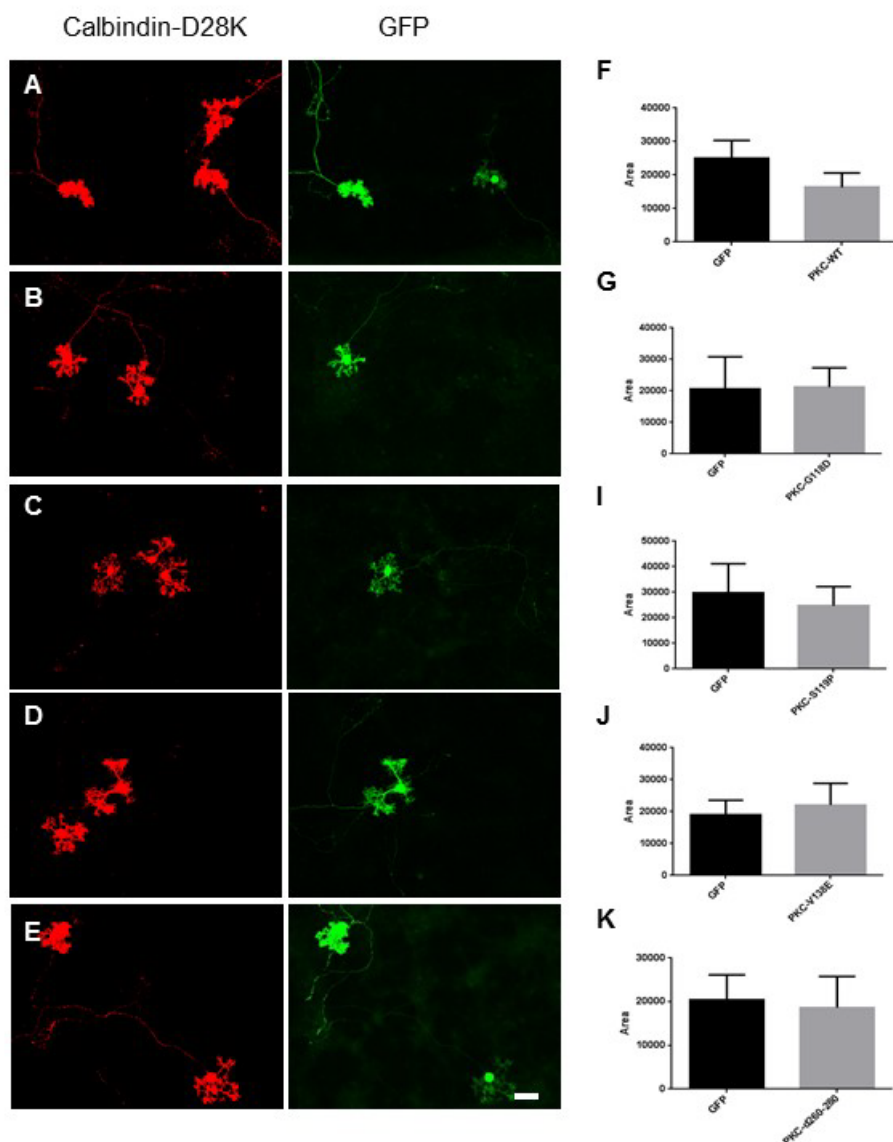
**Fig. 20 Purkinje cells transfected with PKCγ WT or C1B and C2 mutant constructs**

(A) Purkinje cells transfected with WT PKCγ in dissociated primary culture. At DIV 14, cells were fixed and stained by anti-CalbindinD28K (red) and anti-GFP antibodies (green). (B) Purkinje cells transfected PKCγ G118D. (C) Purkinje cells transfected PKCγ S119P. (D) Purkinje cells transfected PKCγ V138E. (E) Purkinje cells transfected PKCγ Δ260-280. Scale bar in H = 50 μm. (F-K) Purkinje cell dendritic area was measured with image J and statistically analyzed with Graph pad prism. Data are shown are the mean ± S.D of at least 20 Purkinje cells.

It can serve as a reference to see whether the other constructs would confer an increased biological activity compared to the WT PKCγ construct.

Next, three of C1B mutations and one deletion in C2 domain were transfected by the same procedure as for WT PKCγ. Fig. 20B-E and Fig. 20G-K show the Purkinje cell morphology for all C1B and C2 mutations. None of these mutant constructs had a strong effect on dendritic tree development in Purkinje cells. C1B mutations transfected cells showed almost the same morphology compared to that of GFP control transfected cells (data not shown), i.e. there were not even the small qualitative changes present that were seen with transfection of WT PKCγ. This observation would be compatible with a reduced biological activity of the C1B mutations. The Purkinje cells transfected with the C2 mutation were more like WT PKCγ transfected Purkinje cells and also showed some thickening of the dendrites (Fig. 20E). Statistical analysis showed no significant changes of the dendritic area, similar to transfections of WT PKCγ.

### 4.4.3. Purkinje cells transfected with PKCγ carrying catalytic domain mutations showed inhibition of dendritic development

As shown above, Purkinje cells in dissociated cultures from PKCγ S361G transgenic mice show a sever reduction of dendritic development. When we transfected Purkinje cells with a construct carrying the same S361G mutation they developed again only a very small dendritic tree with few side-branches (Fig. 21A) identical to that of mPKCγ *S361G* transgenic mice (Fig. 18). We tested another mutation in the catalytic domain, F643L which causes SCA14 with cognitive decline and atrophy of the vermis in human (Stevanin et al., 2004). Purkinje cells transfected with the F643L construct also showed a strong reduction of dendritic development with few side branches (Fig. 21B). On quantitative evaluation, the reduction of dendritic size was less pronounced compared to S361G but still dramatic and highly significant (Fig. 21C and 21D). These results indicate mutations in the catalytic domain of PKCγ have a higher PKC activity compared to WT PKCγ and negatively regulate dendritic growth of Purkinje cells.
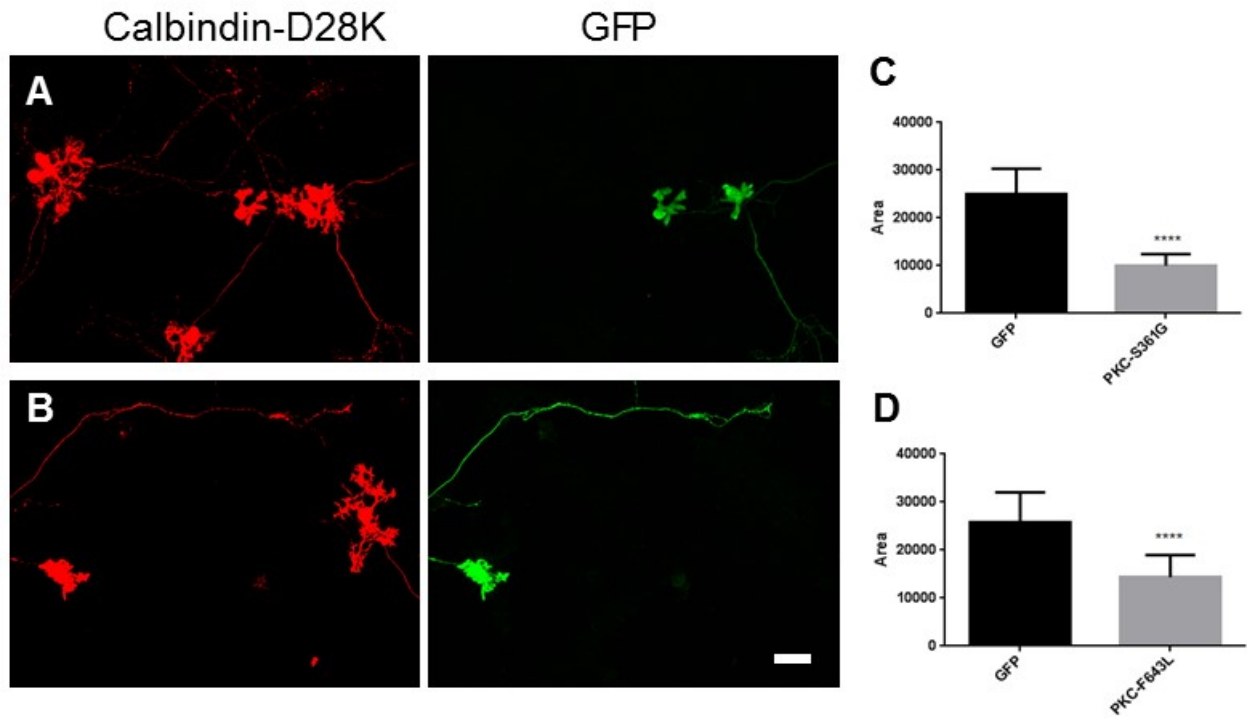
**Fig. 21 Purkinje cells transfected with PKCγ catalytic domain mutants.**
(A) Purkinje cells transfected with PKCγ S361G in dissociated primary culture. (B)
Purkinje cells transfected with PKCγ F643L. Scale bar in H = 50 µm. (C and D)
Purkinje cell dendritic area was measured with image J and statistically analyzed with
Graphpad prism. Data are shown as the mean ± S.D of at least 20 Purkinje cells.

### 4.5. Mutant PKC gamma signalling related proteins

The following section is based on the work published in the Molecular Neurobiology, 2015, Print ISSN 0893-7648, DOI; 10.1007/s12035-015-9444-3. Some text, figures, figure legend numbering and title numbering were modified to fit this thesis. All the experiments described in the manuscript were carried out E.S., and the writing of the manuscript was done together with J.P.K., W.W. provided the L7-based expression plasmid,

## Carbonic anhydrase 8 expression in Purkinje cells is controlled by PKCγ activity and regulates Purkinje cell dendritic growth

Etsuko Shimobayashi[1], Wolfgang Wagner[2] and Josef P. Kapfhammer[1]

1) Anatomical Institute, Department of Biomedicine Basel, University of Basel, Pestalozzistrasse 20, CH - 4056 Basel, Switzerland
2) Department of Molecular Neurogenetics, Center for Molecular Neurobiology Hamburg (ZMNH), University Medical Center Hamburg-Eppendorf, Falkenried 94, D - 20251 Hamburg, Germany.

### 4.5.1. Abstract

Purkinje cell dendritic development is severely compromised after chronic activation of protein kinase C (PKC). In a recent transgenic mouse of model spinocerebellar ataxia 14, the S361G mutation of the PKCγ-gene was expressed in Purkinje cells. Purkinje cells from these mutant mice in organotypic slice cultures have the same stunted dendritic tree as Purkinje cells after pharmacological activation of PKC. Because the transgene is exclusively present in Purkinje cells, cerebellar tissue from these mice is an attractive starting material for searching genes which might be interacting with PKCγ in Purkinje cells for inducing the stunted dendritic growth. We have performed a micro array analysis and identified several candidate genes with an increased mRNA expression in the PKCγ-S361G transgenic Purkinje cells. Out of these candidates we have further studied carbonic anhydrase 8 (CA8). We show here that CA8 mRNA and protein expression is strongly induced in PKCγ-S361G transgenic Purkinje cells.

Overexpression of CA8 in Purkinje cells in dissociated cultures strongly inhibited Purkinje cell dendritic development and produced a dendritic phenotype similar to PKCγ-S361G. There was no evidence for a direct binding of CA8 to either PKCγ or the type 1 IP3 receptor. Knock-down of CA8 with miRNA did not alter Purkinje cell dendritic development and did not protect Purkinje cells in dissociated cultures from the stunted dendritic growth induced by PKCγ-S361G or by PKC activation. Our results indicate that CA8 is a novel important regulator of Purkinje cell dendritic development and that its expression is controlled by PKCγ activity.

### 4.5.2. Introduction

The signalling molecule PKC plays an important role for long term depression of Purkinje cells (Ito et al., 2014) and has a strong negative impact on Purkinje cell dendritic growth and development (Kapfhammer, 2004; Metzger and Kapfhammer, 2003; Schrenk and Kapfhammer, 2002). Increased PKC activity is likely to affect the long term calcium equilibrium of the Purkinje cells. Blockade of voltage gated calcium channels could partially protect Purkinje dendrites cells from the stunted growth seen with increased PKC activity (Gugger et al., 2012) and Purkinje cells from *Moonwalker (Mwk)* mutant mice with increased calcium influx through TRPC3 channels also show a stunted dendritic morphology (Becker et al., 2009). Similarly, inhibition of the Plasma Membrane calcium-ATPase 2 (PMCA2) affected Purkinje cell dendritic growth (Huang et al., 2010; Sherkhane and Kapfhammer., 2013). These findings demonstrate the involvement of the calcium equilibrium for regulating Purkinje cell dendritic growth but still very little is known about the downstream molecular interactions after PKC activation in Purkinje cells leading to the reduced dendritic growth. Interestingly, one form of spinocerebellar ataxias, SCA 14, is caused by point mutations in the PKCγ gene (Chen et al., 2012; Pandolfo et al., 2005) and that at least some of the missense mutations may confer a gain of function phenotype with a constitutive activation of PKCγ (Adachi et al., 2008; Verbeek et al., 2005). We have recently created a transgenic mouse model of SCA 14 by introducing a transgene carrying the S361G mutation of the PKC-gene specifically into Purkinje cells. This mutation is located in the catalytic domain (Chen et al., 2005) and was shown previously to confer an increased catalytic activity as tested by in vitro assays (Adachi et al., 2008). PKCγ-

S361G transgenic mice have pathological changes typical for cerebellar disease and have an increased PKCγ activity *in vivo* reflected by the reduced dendritic development typically seen with increased PKC activity (Ji et al., 2014). Purkinje cells from these mutant mice thus show both an increased PKCγ activity and a severe dendritic reduction. Because the transgene is exclusively activated in Purkinje cells, cerebellar tissue from these mice is an attractive starting material for searching other genes which might be interacting with PKCγ for inducing the stunted dendritic growth. We have performed a gene chip micro array analysis and identified several candidate genes with an increased mRNA expression in the PKCγ-S361G transgenic Purkinje cells. Out of these candidate genes we have further studied CA8 which was shown previously to be involved in Purkinje cell function and cerebellar disease (Hirasawa et al., 2007; Jiao et al., 2005). We show here that CA8 mRNA and protein expression is strongly induced after PKC activation and that overexpression of CA8 in cultures of dissociated Purkinje cells strongly inhibits Purkinje cell dendritic development. However, we found no evidence of a binding of CA8 to either PKCγ or the type 1 IP3 receptor. Knock-down of CA8 protein expression by miRNA transfection did not protect Purkinje cells in dissociated cultures from the stunted dendritic growth after increased PKCγ activity. Our results indicate that CA8 is an important regulator of Purkinje cell dendritic development and that its expression is controlled by PKCγ activity.

### 4.5.3. Materials and Methods

*Plasmid Construction*

Plasmid L7-GFP was previously described (Wagner et al., 2011). CMV-CA8 and CMV-PKCγ plasmids were from Origene (Rockville, MD, USA). Restriction sites were added to the CA8 and PKCγ genes by polymerase chain reaction (PCR) using the following primers: Forward primer for CA8: 5'CAG GAT CCA GCG GCC GCA TGG CTG ACC TGA GCT TC3', Reverse primer for CA8: 5'CCC TTG CTC ACC ATG GCC TGA AAG GCC GCT CGG A3', Forward primer for PKCγ: 5'CAG GAT CCA GCG GCC GCA TGG CTG GTC TGG GCC CC 3', Reverse primer for PKCγ: 5'CCC TTG CTC ACC ATG GCC ATG ACG GGC ACA GGC A3'. These PCR products were incubated with the L7-GFP vector in the presence of the restriction enzymes, *NotI* and *NcoI* (New England BioLabs, Massachusetts, USA) in suitable buffer. After 30min incubation at

37°C, DNA fragment and linearized vector were fused using in-Fusion HD Cloning Kits (Clontech, Mountain View, CA). The constructed expression vectors were confirmed by DNA sequencing (Microsynth, Balgach, Switzerland).

*Organotypic Slice Cultures*

Animal experiments were carried out in accordance with the EU Directive 2010/63/EU for animal experiments and were reviewed and permitted by Swiss authorities. Cultures were prepared from B6CF1 (CB6) mice or PKCγ-S361G transgenic mice as described previously (Kapfhammer JP, 2010). Briefly, mice were decapitated at postnatal day 8 (P8), their brains were aseptically removed and the cerebellum was dissected in ice-cold preparation medium (minimal essential medium (MEM) with 1% glutamax (Life Technologies, Zug, Switzerland), pH 7.3). Sagittal sections 350 µm thick were cut on a McIllwain tissue chopper under aseptic conditions. Slices were separated, transferred onto permeable membranes (Millicell-CM, Merck-Millipore, Zug Switzerland) and incubated on a layer of Neurobasal medium (97% Neurobasal medium, 2% B27 supplement, 1% glutamax, pH 7.3) in a humidified atmosphere with 5% $CO_2$ at 37°C. The medium was changed every 2-3 days for a total of 5 days for microarray analysis and of 7 days for protein analysis and immunostaining.

*Microarray analysis*

Starting material for the microarray analysis were cerebellar slice cultures from PKCγ-S361G transgenic mice versus control mice. After 5 days in vitro (DIV 5), organotypic cerebellar slices were washed, harvested and submerged in RNAlater (Life Technologies, Zug, Switzerland) solution for storage. The slices from one litter deriving from 3-4 mouse pups were collected and used for RNA purification. Purified total RNA was amplified by in-vitro transcription and converted to sense-strand cDNA. Fragmented cDNA samples were then hybridized to GeneChip Mouse Gene 1.0 ST Arrays (Affymetrix, Santa Clara, CA, USA). Procedures were carried out as described by the manufacturers and the analysis was done in the LSTF core facility of the University of Basel by Dr. Philippe Demougin. Raw data were processed and analyzed using Partek Genomics suite (version 6.12.0907). Transcripts were considered to be changed if the p-value was smaller than 0.05. After filtering, 1045 genes were retained.

We then set the threshold at a fold change exceeding 1.25 for being specifically expressed and 98 genes were retained.

*Reverse transcriptase-quantitative PCR (RT-qPCR)*

Total RNA was extracted from organotypic cerebellar slices harvested at DIV 5-7 and cDNA was synthesized with RT-qPCR using oligo (dT) primers (Applied Biosystems, Foster City, CA). For gene expression analysis, RT-qPCR reactions were conducted in a total volume of 20 µl comprising 10 µl of Mastermix with SYBR green (Applied Biosystems, Foster City, CA), 0.5 µl of each primer (1.0 µM), 0.3 µl of sample cDNA, and 8.5 µl ultrapure water. Real-time PCR reactions were run on a Real time PCR system (Applied Biosystems, Foster City, CA) under the following reaction conditions: 1 cycle of [95°C for 10 min], 40 cycles of [94°C for 15 s → 65°C for 60 s], and 1 cycle of [95°C for 15 s → 72°C for 30 s → 95°C for 15 s]. Oligonucleotide primers were designed using the Primer3 software (http://bioinfo.ut.ee/primer3/). The primer sequences are given in supplementary methods. Reactions were quantified by relative standard curve system and the cycle threshold (Ct) method using the SDS2.2 software (Applied Biosystems, Foster City, CA). A relative quantitation value (RQ) for each sample from the triplicates of that sample was calculated for each gene. The data was analyzed as RQ for the gene of PKCγ transgenic mice/ RQ for control mice. For each comparison a minimum of 3 independent experiments were done with unrelated RNA samples.

*Western Blot analysis*

Tissue slices were harvested with a cell scraper. Samples were then homogenized in RIPA buffer with phosphatase inhibitor (phosphor STOP, Roche, Basel Switzerland) and protease inhibitor (cOmplete Protease Inhibitor Cocktail Tablets, Roche, Basel Switzerland). Homogenates were sonicated for 5 seconds a total of 5 times and cleared by centrifugation at 14,000 × g for 15 min at 4 °C. Protein concentrations were determined with Nano drop (ThermoScientific, Reinach, Switzerland). Western blotting analysis was performed by standard protocols. Membranes were blocked with 5% BSA in TBS for 1 hour and incubated with appropriate Primary antibodies. Rabbit anti-

ITPR1 (Cell signaling, Massachusetts, USA 1:1000), Rabbit anti-CA8 (Novus Biologicals, Colorado, USA 1:2000), Rabbit anti-PKCγ (Santa Cruz Biotechnology, Santa Cruz, CA, 1:1000), Rabbit anti-Fam40b (AVIVA, San Diego, USA, 1:1000), Rabbit anti-Plekhd1 (Thermo Scientific, Reinach, Switzerland, 1:1000), Rabbit anti-Homer3 (Abgent Inc., San Diego, CA, USA 1:1000) , mouse anti-mGluR1 (BD Biosciences, Franklin Lakes, NJ, USA 1:1000) or anti-βActin (Millipore Zug Switzerland, 1:1000) was used. After washing with TBS-T, membranes were incubated with HRP-labelled secondary antibodies for 1 hour. After washing, bound antibodies were visualized with ECL2 Western blotting substrate (Pierce, Thermo Scientific, Reinach, Switzerland) and quantified using a C-Digit Western Blot scanner and software (LI-COR Biosciences, Bad Homburg, Germany). For each comparison a minimum of 3 independent experiments were done with unrelated protein samples.

*Immunoprecipitation*

Cerebellar slice cultures at DIV 7 were used as starting material. Slice cultures were harvested with a cell scraper. Samples were then homogenized in RIPA buffer with phosphatase inhibitor and protease inhibitor as described in Western Blot analysis. Homogenates were sonicated for 5 sec a total of 5 times and cleared by centrifugation at 14,000 × g for 15 min at 4°C and protein concentrations were determined and 100 µg of each sample were used for immunoprecipitation. Before using, Protein G was washed twice at 12000 × g for 10 sec with PBS. Lysate was incubated with 50 µl Protein G for 30 min at 4°C and lysate was washed twice at 12000 × g for 10sec with PBS. 1 µg antibody, 50 µl pre-washed Protein G and 50 µl PBS were added to the lysate and rotated at 4°C for overnight. Tubes were then centrifuged at 4°C for 2 min at 3000 × g and washed with 1ml PBS 4°C for 2 min at 3000 × g four times. SDS-PAGE and Western blot were done as described. A minimum of 3 independent immunoprecipitation experiments with unrelated protein samples were done per condition.

*Immunohistochemistry*

At DIV 7, slices were fixed in 4% paraformaldehyde overnight at 4°C. All reagents were diluted in 100 mM phosphate buffer (PB), pH 7.3. Slices were incubated in blocking solution (0.5% Triton X-100, 3% normal goat serum) for 1 hour at room temperature. Two different primary antibodies were simultaneously added to the slices in fresh blocking solution and incubated overnight at 4°C. After washing in PB, secondary antibodies were added to the slices in PB containing 0.1% Triton X-100 for 2 hours at room temperature. For the analysis of protein expression in Purkinje cells, mouse anti-Calbindin D-28K (Swant, Marly, Switzerland 1:1000) and polyclonal Rabbit anti-GFP (Abcam, Cambridge, UK 1:1000), Rabbit anti-CA8 (Novus Biologicals, Colorado, USA 1:2000), mouse anti-ITPR1 (Abcam, Cambridge, UK 1:100), rabbit anti-ITPR1 (Millipore, Zug Switzerland, 1:2000) or Rabbit anti-PKCγ (Santa Cruz Biotechnology, Santa Cruz, CA, 1:1000) were used as primary antibodies and goat anti-mouse Alexa 568 (Molecular Probes, Eugene, OR, 1:1000) and goat anti-rabbit Alexa 488 (Molecular Probes, Eugene, OR, 1:1000) were used as secondary antibodies to visualize Purkinje cells. Stained slices were mounted on cover slips with Mowiol (Sigma-Aldrich, Buchs, Switzerland). Cultures were viewed on an Olympus AX-70 microscope equipped with a Spot digital camera. Recorded images were adjusted for brightness and contrast with Photoshop image processing software.

*Histology*

Mice were deeply anesthetized, perfused through the aorta with 4% paraformaldehyde and cryoprotected with 30% sucrose overnight. Brains were embedded in tissue freezing medium (OCT), frozen and sectioned using a Leica cryostat CM1900. Sagittal sections (25 µm) were examined by immunohistochemical staining.

*Plasmid transfection of Purkinje cells in dissociated cerebellar cultures*

Dissociated cerebellar cultures were prepared from mice essentially as described (Wagner et al., 2011) except that the cells were obtained from postnatal day 0 (P0) mice. The transfection of the cells was performed using a Nepa21 electroporator (NEPAGENE, Japan) according to manufacturer's instructions. 100 µl of the Opti-MEM (Life Technologies, Zug, Switzerland)

solution was mixed with the plasmid DNA to be transfected. This mixture was then used to suspend the cerebellar cell pellet. The cell suspension was transferred into one of the cuvettes provided in the kit and subjected to the optimized electroporation program. After transfection, cells were plated in glass chambers that had been coated with poly-L-lysine containing 90% v/v DFM, 1% N-2 Supplement, 1% Glutamax and 10% v/v FBS (all from Life Technologies, Zug, Switzerland), pH was adjusted to 7.2-7.4. Two hours after transfection, 0.8 ml DFM, containing 1% N-2 Supplement, 1% Glutamax at 37°C was added to each dish. After that, half of medium was changed once or twice a week. After 14-18 days, cells were fixed in 4% paraformaldehyde for 1 hour at 4°C and processed for immunohistochemistry as described. A minimum of 3 independent transfection experiments using different dissociated cultures were done for each plasmid.

*Knockdown of CA8 expression*

miRNAs were designed and generated by Life Technologies, Zug, Switzerland to target CA8 (for details see supplementary methods). Each miRNA was cloned into the BLOCK-iT™ Pol II miR RNAi expression vector according to the instructions of the manufacturer and then sequenced (Microsynth, Balgach, Switzerland). In order to test the knockdown efficacy, the different miRNA vectors together with a CA8 expression vector were transfected into HeLa cells using Lipofectamin 2000 (Life Technologies, Zug, Switzerland). The most efficient pcDNA6.2-GW/miRNA expression vectors containing CA8-specific miRNAs were sub cloned to pL7 in order to transfect miRNA to Purkinje cells. In order to monitor miRNA transfection, a GFP reporter was included in the miRNA vectors. Dissociated cerebellar cultures cells were electroporated using Nepa21 (NEPAGENE, Japan) according to manufacturer's instructions and cultured as described. A minimum of 3 independent transfection experiments using different dissociated cultures were done for each plasmid.

*Statistical analysis of Purkinje cell dendritic tree size*

The quantification of Purkinje cell dendritic tree size and counting of branch points from organotypic slice cultures or dissociated Purkinje cell cultures was done as previously

described (Gugger and Kapfhammer., 2012). Purkinje cells which had a dendritic tree isolated from its surroundings were selected for analysis. An image analysis program (Image Pro Plus or ImageJ) was used to trace the outline of the Purkinje cell dendritic trees yielding the area covered by the dendritic tree. Over 20 cells per experimental condition originating from at least 3 independent experiments were acquired and analysed using GraphPad Prism software (San Diego, USA). The statistical significance of differences in parameters was assessed by a non-parametric Mann-Whitney's test. Confidence intervals were 95%, statistical significance was assumed when $p<0.05$.

### 4.5.4. Results

*Up-regulated genes in* PKCγ-S361G *transgenic mice identified by Gene chip analysis*
We have previously reported that PKCγ-S361G mice carrying a human SCA 14 allele with Purkinje cell specific expression showed an increased PKCγ activity in Purkinje cells leading to abnormal morphology of Purkinje cells, a phenotype which is very similar to the one found after pharmacological treatment of PKC stimulator. In contrast to pharmacological stimulation, the increased PKC activity in PKCγ transgenic is Purkinje cell specific, offering the possibility to search for downstream targets of PKCγ-S361G signaling which might be involved in the inhibition of Purkinje cell dendritic growth.

In order to search for transcripts with altered expression in Purkinje cells of PKCγ-S361G transgenic mice we used the Affymetrix Gene Chip Mouse Gene 1.0 ST Array comparing samples of cerebellar slice cultures from PKCγ transgenic mice to control mice. The micro array analysis was performed twice using 2 independent samples from different culture experiments. We could identify 98 genes which were up-regulated and 17 genes which were down-regulated in PKCγ-S361G transgenic mice based on a change of more than 1.25 fold (the complete microarray data sets are available from the authors on request). The rather moderate changes in expression of most transcripts could be explained by the fact that the Purkinje cells population is very small and only comprises around 0.1% of the total cells of the cerebellum of adult rodents (Tomomura et al., 2001). We focused on up-regulated genes because our previous

studies had shown that PKCγ-S361G transgenic mice had an increased activity of PKC and we searched for candidates which might be involved in PKC signaling.

Out of the 98 up-regulated genes, we selected eight genes for further analysis based on their expression level in Purkinje cells in situ and their presumed function (Table. 3). A brief description of the main features of the eight candidate genes is given in the Supplementary Table 1. The expression of the mRNA of the eight candidate genes was verified using the Allen brain atlas. The in situ hybridisation data from the Allen Brain Atlas (http://mouse.brain-map.org/) confirm that all of the 8 selected candidate genes are strongly expressed in Purkinje cells. For several of these genes an important role for Purkinje cell differentiation and function has already been suggested (Supplementary Table. 1).

| Gene | p-value | Fold change |
|---|---|---|
| Bcl11a | 0.036643 | 1.412 |
| CA8 | 0.023265 | 1.63062 |
| Chn1 | 0.011644 | 1.47505 |
| Fam40b | 0.045992 | 1.92428 |
| Klhl4 | 0.025187 | 1.9327 |
| Lhx1 | 0.007259 | 1.36811 |
| Plekhd1 | 0.000103 | 1.38 |
| Ywhah (14-3-3eta) | 0.024979 | 1.29995 |

**Table. 3 Gene chip micro array results of candidate genes.**
For the 8 selected candidate genes the induction of mRNA expression in PKCγ-S361G transgenic mice compared to control mice (Fold change) and the p-values of for the significance of the change are shown.
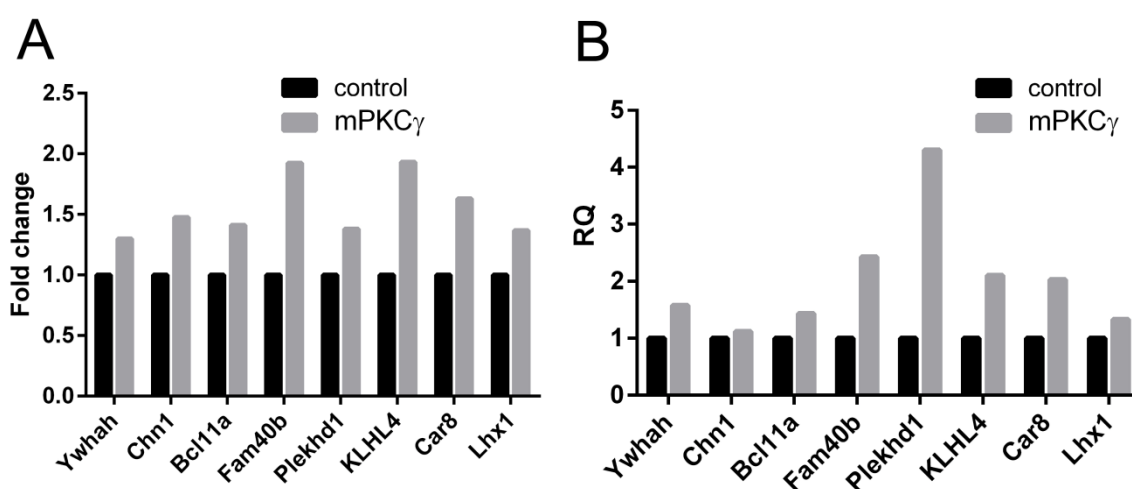


**Fig. 22 Gene chip and quantitative RT-PCR data for cerebellum of PKCγ-S361G transgenic mice and control mice**
(A) Induction of the expression of the 8 selected candidate genes as found in the gene chip assay (B) Quantitative RT–PCR confirmed that all candidates are up-regulated in PKCγ-S361G transgenic mice.

*RT-qPCR analysis and Western blotting confirms the upregulation of candidate genes*

In order to confirm the GeneChip micro array results (Fig. 22A), we performed RT-qPCR assays using cerebellar slice cultures. As expected, all of the candidate genes were up-regulated in the cerebellar slice cultures from PKCγ-S361G transgenic mice (Fig. 22B). In order to confirm the increased expression of candidates on the protein level, we performed Western blot analysis. After 7 days of culture (DIV 7), cerebellar slice cultures of control mice and PKCγ-S361G transgenic mice were collected and candidate proteins were detected with Western Blotting. At DIV7 there is a strong reduction of the dendritic expansion of Purkinje cells in slice cultures from PKCγ-S361G transgenic mice (Ji et al., 2014). In PKCγ-S361G transgenic mice, the PKCγ-S361G protein expression level is higher than that of control (Fig. 23A). Notably, fold change of PRKCG gene in GeneChip micro array was around 1.6 (data not shown). Within the candidates, the protein expression of CA8, Fam40b and Plekhd1 was induced in PKCγ-S361G transgenic mice (Fig. 23B, C). CA8 was more than 5 times up-regulated while Fam40b and Plekhd1 were only slightly up at around 1.3 of control levels. As for the other candidates, either we could not see a strong difference in protein expression or no antibody suitable for Western blot analysis is available so far. Therefore, further analysis was restricted to CA8, Fam40b and Plekhd1.

*RT-qPCR analysis and Western blotting confirms the upregulation of candidate genes*

In order to confirm the GeneChip micro array results (Fig. 22A), we performed RT-qPCR assays using cerebellar slice cultures. As expected, all of the candidate genes were up-regulated in the cerebellar slice cultures from PKCγ-S361G transgenic mice (Fig. 22B). In order to confirm the increased expression of candidates on the protein level, we performed Western blot analysis. After 7 days of culture (DIV 7), cerebellar slice cultures of control mice and PKCγ-S361G transgenic mice were collected and candidate proteins were detected with Western Blotting. At DIV7 there is a strong reduction of the dendritic expansion of Purkinje cells in slice cultures from PKCγ-S361G transgenic mice (Ji et al., 2014). In PKCγ-S361G transgenic mice, the PKCγ-S361G protein expression level is high er than that of control (Fig. 23A).

**Fig. 23 Western Blot analysis of cerebellum of PKCγ-S361G transgenic mice and control mice**

(A) Protein expression of PKCγ is increased in the cerebellum of PKCγ-S361G transgenic mice. βActin was used as a loading control. (B) Western Blot results of CA8, Fam40b and Plekhd1. βActin as loading control. (C) Quantitation of Western Blot data. Signal intensity of each candidate was normalized with βActin. Data were from three independent experiments and signal intensity of samples from control mice was set to one.

Notably, fold change of PRKCG gene in GeneChip micro array was around 1.6 (data not shown). Within the candidates, the protein expression of CA8, Fam40b and

*CA8 is specifically and strongly expressed in Purkinje cells*

To determine the expression pattern of CA8 in brain, we performed immunohistochemical analysis on mid-sagittal brain sections of P14 wild-type mice and PKCγ-S361G transgenic mice. Purkinje cells were identified by staining for Calbindin-D28K together with CA8. We found that CA8 was specifically expressed in Purkinje

cells and that the staining intensity was higher in PKCγ-S361G transgenic mice (Fig. 24A, B). Further we performed immunostaining in organotypic slice cultures. CA8 was again most strongly expressed in cultures derived from PKCγ-S361G transgenic mice (Fig. 24C, D). These results suggest that CA8 is specifically expressed in Purkinje cells and that the expression level is induced by the PKCγ-S361G transgene.
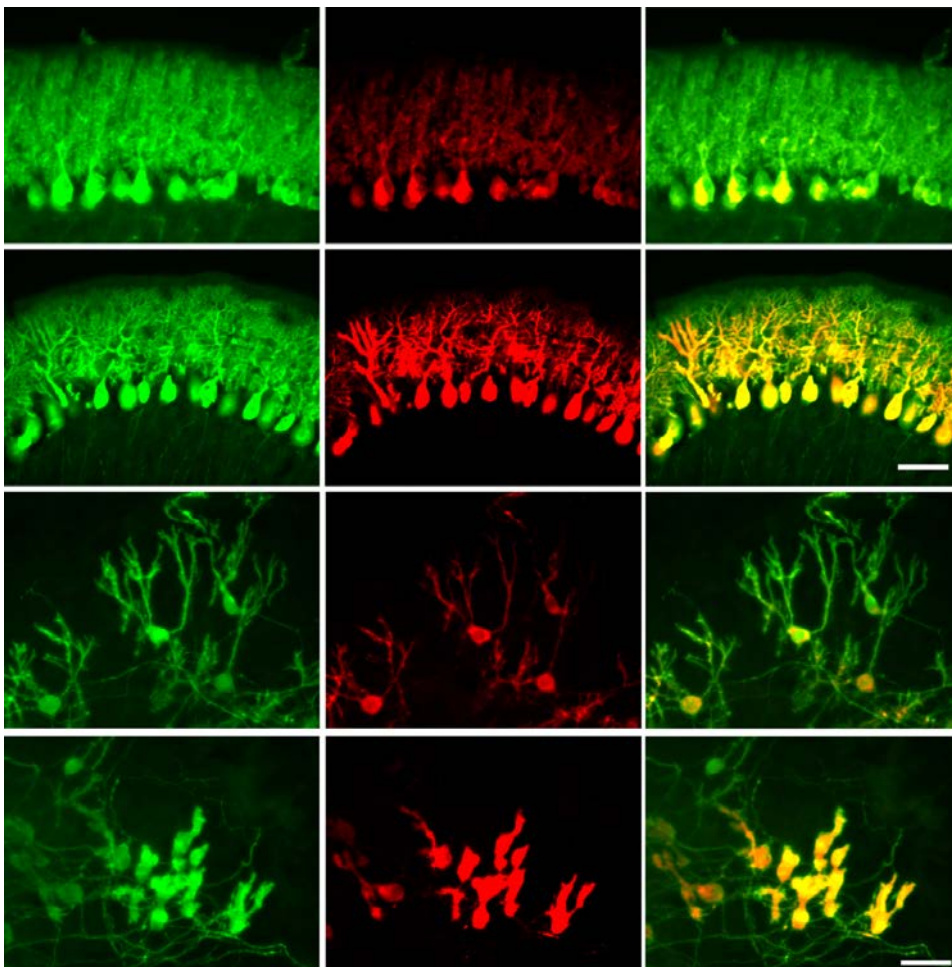


**Fig. 24 Immunofluorescence staining analysis of cerebellum of PKCγ-S361G transgenic mice and control mice**

(A-F) Immunofluorescence staining of frozen section from P14 control mice in A-C and from PKCγ-S361G mice in D-F with anti-Calbindin-D28K (A, D) and with anti-CA8 (B, E). Merged images in (C, F).

(G-L) Immunofluorescence staining of cerebellar slice cultures after one week in vitro. Cultures from control mice in G-I and from PKCγ-S361G mice in J-L stained with anti-Calbindin-D28K (G, J) and with anti-CA8 (H, K). Merged images in (I, L).

Note the strong induction of anti-CA8 immunostaining in PKCγ-S361G cerebellum. Scale bar in H = 50 μm.

Immunostaining for Fam40b and Plekhd1 with commercially available antibodies did not give satisfactory results and showed either no staining or only poor staining intensity on sections or organotypic cerebellar slice cultures. Therefore, we didn't further analyze these candidates and focused on CA8.

*The inositol 1, 4, 5-trisphosphate receptor 1 (ITPR1) is also induced in PKCγ-S361G transgenic mice*

CA8, 10, and 11 are called CARPs because they lack classical carbonic anhydrase enzymatic activity due to the missing catalytic zinc coordinating residues (Sjöblom et al., 1996). Thus their biological functions are still unclear. Hirota et al. showed that
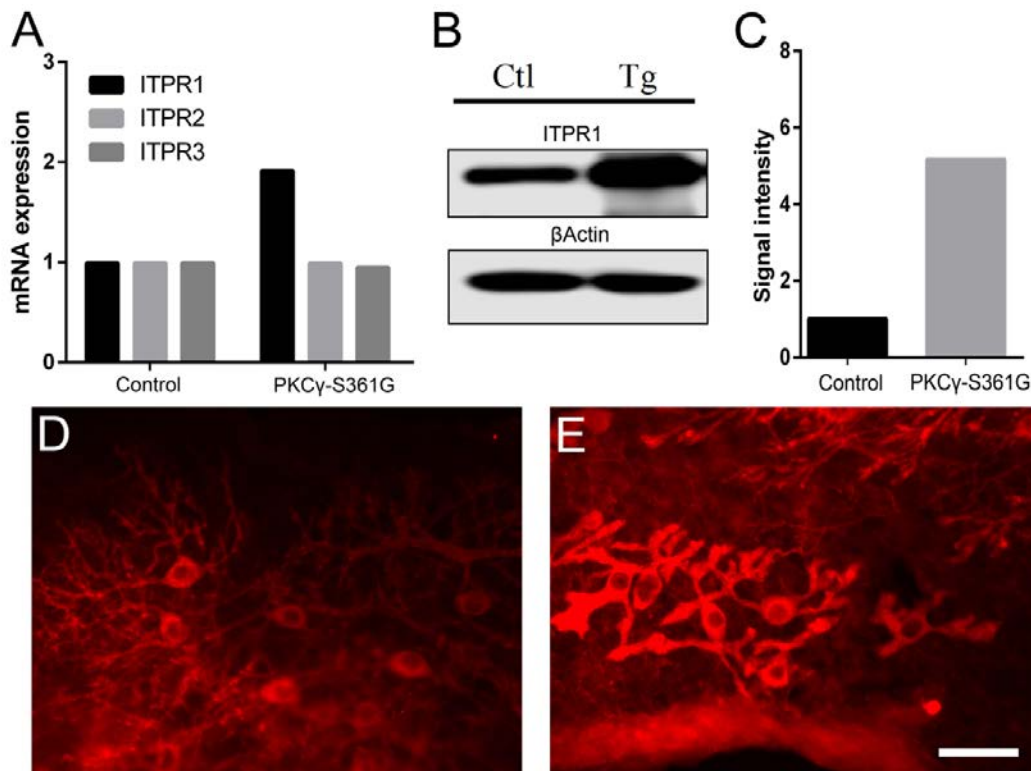


**Fig. 25 ITPR1 is induced in PKCγ-S361G transgenic mice**

(A) Quantitative RT–PCR showing upregulation of ITPR1 but not ITPR2 and ITPR3 in PKCγ-S361G. (B) Western Blot results of ITPR1 from cerebellum of control and PKCγ-S361G transgenic mice. βActin as loading control. (C) Quantitation of Western Blot data. Signal intensity was normalized with βActin. (D, E) Anti-ITPR1 immunostaining of cerebellar slice cultures after one week in vitro. Note the strong induction of anti-ITPR1 immunostaining in PKCγ-S361G slices (E) versus control slices (D).  Scale bar in E = 50 μm.

CARPs bind to ITPR1 using a yeast hybrid system and also found abundant co-expression and co-localization of CARP and ITPR1 in Purkinje cells (Hirota et al., 2003). The ITPR1 functions as a ligand-gated ion channel that releases $Ca^{2+}$ from intracellular stores (Banerjee and Hasan, 2005). We analyzed the ITPR1 expression level in PKCγ-S361G transgenic mice. Although we had not identified ITPR1 as a candidate in our GeneChip micro array because the p-value was above 0.05 (p-value 0.052 and fold change was 1.42), ITPR1 mRNA was induced in PKCγ-S361G transgenic mice when tested with RT-qPCR (Fig. 22A). Western Blotting analysis confirmed that ITPR1 protein is strongly up-regulated in PKCγ-S361G transgenic mice (Fig. 25B, C). Immunofluorescence staining results showed specific expression in Purkinje cells which was increased in PKCγ-S361G transgenic mice (Fig. 25D, E).

*No evidence for a binding between CA8 and ITPR1 in cerebellar Purkinje cells*

The co-expression of ITPR1 and CA8 in Purkinje cells and the induction of both proteins by increased PKCγ activity raise the question about a direct interaction of ITPR1 and CA8 in Purkinje cells. Binding of CA8 to ITPR1 has been previously shown using a GST pull-down assay with recombinant proteins but it is not known whether such an interaction also occurs endogenously in Purkinje cells. In order to identify an interaction in Purkinje cells, we have carried out co-immunoprecipitation using lysates from cerebellar slice cultures. Using this assay, we were unable to detect an interaction between ITPR1 and CA8 (Fig. 26) in cerebellar tissue.

Furthermore, no interaction of CA8 and ITPR1 was detected using the Duo-link proximity ligation assay (data not shown). Our data do not support the idea of an interaction of CA8 and ITPR1 in cerebellar Purkinje cells.

*CA8 overexpression in Purkinje cells inhibits Purkinje cell dendritic development*

In order to characterize the functions of CA8 on dendritic development of Purkinje cells, we performed transfection experiments in dissociated cerebellar cell cultures with a Purkinje cell specific expression vector based on the L7 promoter (Wagner et al., 2011). The L7 promoter plasmid was transfected by electroporation and efficiently and selectively mediated expression of the transfected genes in Purkinje cells at a high rate and with a continued expression for more than three weeks.
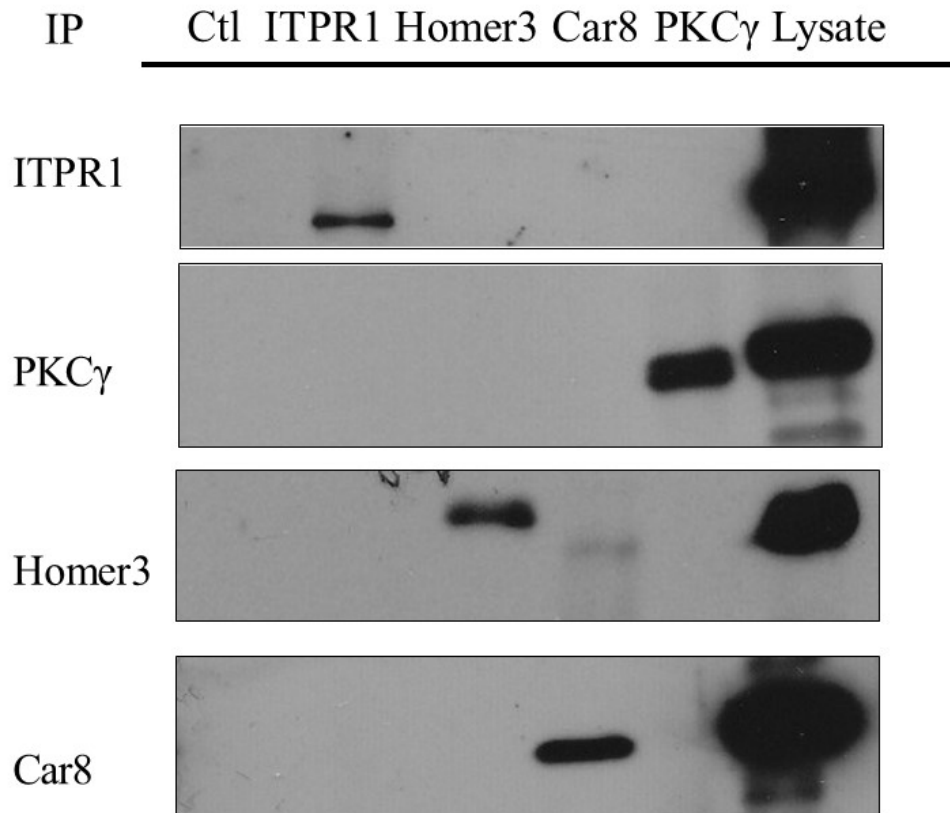
**Fig. 26 Co-Immunoprecipitation for CA8, ITPR1, PKCγ and Homer3.**
At DIV7, cerebellar slices were lysed (see Methods) and subjected to co-immunoprecipitation analysis. Western blots with the antibodies indicated at the left margin of co-immonoprecipitates from the antibodies indicated in the top line. Immunoprecipitation was only observed for the protein of the antibody used, and no co-immunoprecipitation of other proteins was found.

We first transfected a plasmid containing the mutated PKCγ-S361G construct that was used for the generation of the PKCγ-S361G transgenic mice (Ji et al., 2014). Control Purkinje cells in these cultures transfected with a GFP plasmid showed a well-developed branched dendritic tree (Fig. 27C) which was indistinguishable from that of non-transfected Purkinje cells (Fig. 27A). In contrast, Purkinje cells transfected with the PKCγ-S361G plasmid developed only very small dendritic trees with little branching (Fig. 27D). This morphology was indistinguishable from that of Purkinje cells derived from m PKCγ transgenic mice (Fig. 27B). This finding confirms that the dissociated cultures are useful for studying some aspects of Purkinje cell dendritic development and that the PKCγ mediated inhibition of Purkinje cell dendritic growth is present in the dissociated cultures. We then transfected a plasmid containing the CA8 gene inducing
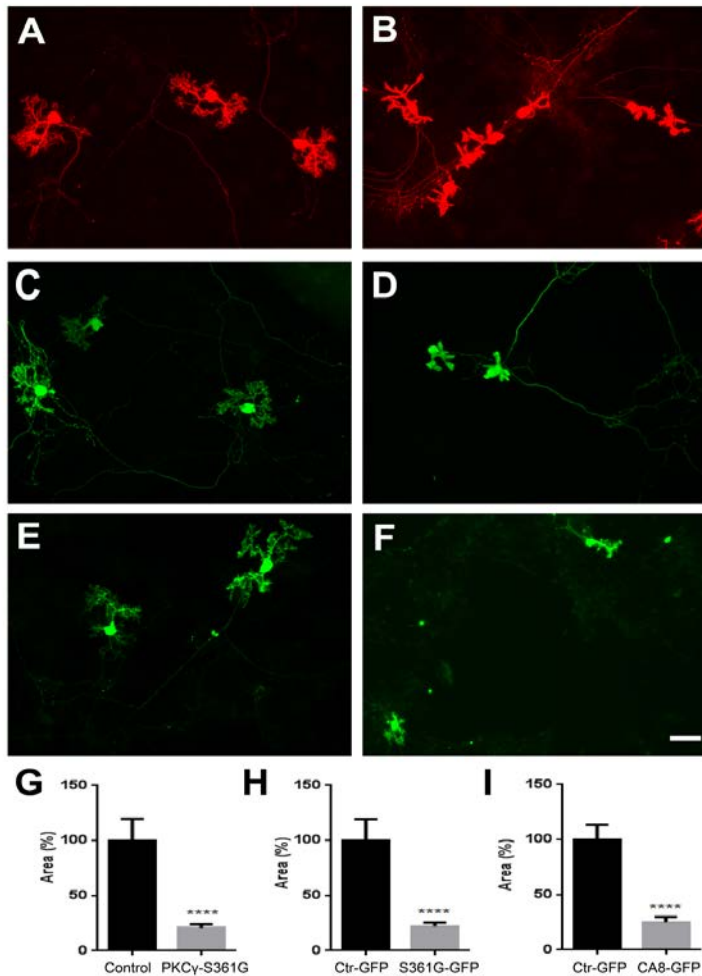
**Fig. 27 Morphology of Purkinje cells after PKCγ-S361G and CA8 transfection after 2 weeks in vitro. Immunostaining with anti-Calbindin-D28K (A, B) or anti-GFP (C-F).**
(A) Purkinje cells from control mice in dissociated culture with expanded dendritic trees. (B) Purkinje cell from PKCγ-S361G transgenic mice with very small dendritic trees. (C) Purkinje cells transfected with a control GFP vector with normal dendritic expansion. (D) Purkinje cells transfected with a PKCγ-S361G-GFP vector with small dendritic trees similar to those of PKCγ-S361G transgenic mice. (E) Purkinje cells transfected with a control GFP with normal dendritic expansion. (F) Purkinje cells transfected with a CA8-GFP vector also with small dendritic trees. Scale bar in H = 50 μm. (G-I) Quantification of the total dendritic area of Purkinje cells in the transfection experiments. The analysis shows that Purkinje cells transfected with PKCγ-S361G (H) or CA8 (I) had very small dendritic trees similar to those of Purkinje cells from PKCγ-S361G transgenic mice (G). The number of measured cells (n) was 20 for all experiments, and the results were statistically significant with p<0.0001 in all conditions. Error bars represent the SEM.

an overexpression of CA8 in the transfected Purkinje cells. CA8 overexpression resulted in a strong inhibition of Purkinje cell dendritic development compared to control Purkinje cells (Fig. 27E) with a morphology of the dendritic tree in transfected cells (Fig. 27F) very similar to that after transfection of the PKCγ-S361G containing plasmid (Fig. 27D). Quantitative measurements of the size of the Purkinje cell dendritic tree with the different transfections confirm that both PKCγ-S361G and overexpression of CA8 lead to a severe and similar reduction of the size of Purkinje cell dendritic trees (Fig. 27G-I). Our findings show that CA8 overexpression has similar effects on Purkinje cell dendritic development as a strong activation of PKCγ and suggests that PKCγ and CA8 may be acting in the same or related signaling pathways within Purkinje cells.

*miRNA-mediated suppression of CA8 protein does not protect from reduction of dendritic growth by increased activity of PKC*

Our finding that overexpression of CA8 reduces dendritic growth raises the question whether CA8 might be part of a signaling complex which converts increased PKC activity into reduced dendritic growth. We have therefore aimed at suppressing the expression of CA8 protein in Purkinje cells by miRNA transfection. In order to knock down CA8 protein expression in Purkinje cells, we used two different miRNAs, mi327 and mi616, which were selected based on their knockdown efficiency in HeLa cells and which were cloned into the L7 promoter plasmid together with a GFP reporter (for details see supplementary methods). mi327 and mi616 transfected Purkinje cells showed a greatly reduced CA8 expression as revealed by immunohistochemistry (Fig. 28D, F, H) compared to control miRNA transfected (Fig. 28A) or non-transfected cells. Purkinje cells with a CA8 knockdown displayed a rather normal morphology with no significant reduction of the size of the dendritic tree (Fig. 28C). When CA8 knockdown was combined with stimulation of PKC activity with phorbol-12-myristate-13-acetate (PMA), the CA8 knock down didn't provide any protection from the reduction of the dendritic tree seen under these conditions (Fig. 28E, F). A similar result was obtained when CA8 knockdown was done in Purkinje cells from PKCγ-S361G transgenic mice. The CA8 knockdown did not rescue the dendritic tree form the severe reduction typical for this condition (Fig. 28G, H). A quantitative evaluation of the dendritic tree sizes is

111

shown in Fig. 28I confirming the qualitative findings. These data indicate that the signaling from PKCγ to the control of dendritic growth in Purkinje cells does not require a strong contribution of CA8 protein function.
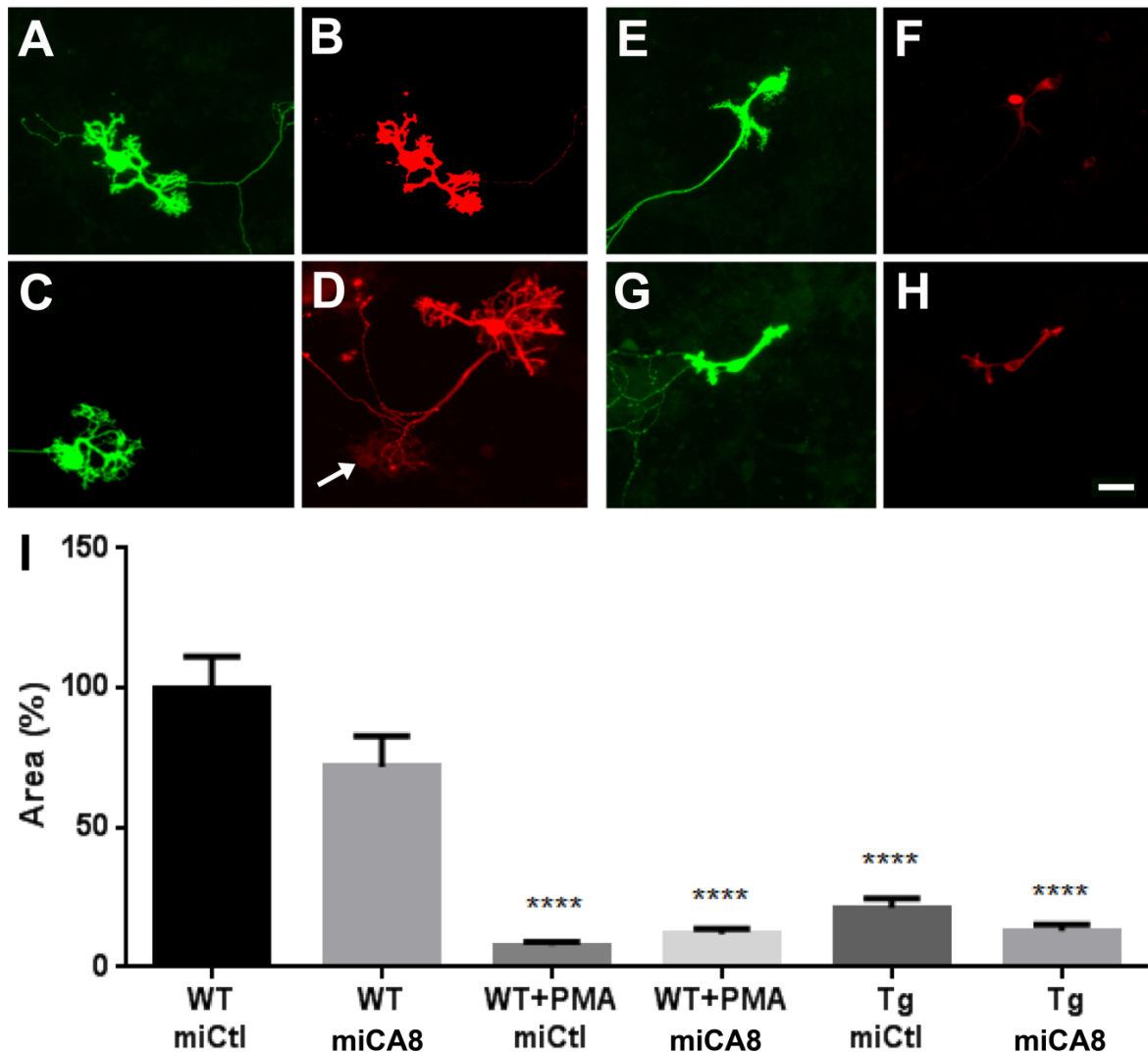


**Fig. 28 Morphology of Purkinje cells after CA8 miRNA-mediated knockdown after 2 weeks in vitro.**

Immunostaining with anti-GFP (A, C, E, G, I, L) or anti-CA8 (B, D, F, H, K, M). (A, B) Control miRNA-GFP-transfected Purkinje cells express the GFP reporter (A), show normal CA8 immunostaining (B) and a normal morphology. (C, D) A Purkinje cell transfected with CA8 miRNA-GFP expresses GFP and shows a normal morphology (C). A non-transfected Purkinje cell is well stained in the anti-CA8 immunostaining whereas the CA8 miRNA-GFP-transfected Purkinje cell (arrow) is almost not visible. (E, F) Treatment with the PKC stimulator PMA dramatically reduced dendritic growth. (E) Anti-GFP immunostaining, (F) Anti-CA8

immunostaining. Transfection with CA8 miRNA-GFP strongly reduced the CA8 immunostaining but did not protect from the PMA-induced dendritic reduction.
(G, H) Purkinje cell from a PKCγ-S361G transgenic mouse with strongly reduced dendrites. (G) Anti-GFP immunostaining, (H) Anti-CA8 immunostaining. Transfection with CA8 miRNA-GFP strongly reduced the CA8 immunostaining but did not protect from the dendritic reduction. Scale bar in H = 50 μm.
(I) Quantification of the dendritic area of Purkinje cells in the CA8 miRNA-GFP transfection experiments. The analysis shows that transfection with CA8 miRNA-GFP could not rescue the dendritic tree size after stimulation with PMA (labeled WT+PMA) or in PKCγ-S361G transgenic Purkinje cells (labeled Tg). The data include control experiments with transfections of a control miRNA-GFP plasmid for which no images are shown in (A-H). The number of measured cells (n) was 20 for all experiments, and the reduction of the dendritic tree in the experiments with either PMA treatment or PKCγ-S361G transgenic mice was statistically significant with $p < 0.0001$ in all conditions irrespective of the presence of miRNA. Error bars represent the SEM.

### 4.5.5. Discussion

Using a transgenic mouse model expressing a constitutive active form of PKC specifically in Purkinje cells, we have identified several candidate genes which might be involved in the stunted dendritic growth of Purkinje cells seen after PKC activation. One of these candidate genes, CA8, has a greatly increased mRNA and protein expression after PKC activation. Overexpression of CA8 in cultures of dissociated Purkinje cells strongly inhibited Purkinje cell dendritic development. Knock-down of CA8 protein expression by miRNA transfection did not protect Purkinje cells in dissociated cultures from the stunted dendritic growth after increased PKCγ activity. Our results show that CA8 is an important regulator of Purkinje cell dendritic development and that its expression is controlled by PKCγ activity.

*Genes with increased mRNA expression in Purkinje cells with activated PKCγ*
Increased activity of PKC in Purkinje cells results in a dramatic reduction of dendritic outgrowth and in the formation of a greatly reduced dendritic tree. The downstream signalling events converting the activation of PKC to reduced dendritic growth are still very unclear. We have used a transgenic mouse model expressing a mutant PKCγ with increased catalytic activity specifically in Purkinje cells resulting in stunted dendritic growth (Ji et al., 2014) as starting point for searching for genes with an

increased expression in such Purkinje cells using a gene chip approach. We have identified many candidate molecules although the observed upregulation was typically only in the range of 1.5 -1.2 x the original expression. The rather moderate changes in expression of most transcripts could be explained by the fact that the Purkinje cell population is very small and only comprises around 0.1% of the total cells of the cerebellum of adult rodents (Tomomura et al., 2001). When we confirmed the increased expression of some of the candidates by RT-qPCR we actually found factors of 2 and more (Fig. 22). All of the selected candidate molecules are expressed in Purkinje cells and have the potential to be involved in PKC signaling and Purkinje cell dendritic development (see supplementary table. 1). We decided to focus the further analysis on CA8 because it was the only candidate molecule for which commercially available antibodies gave satisfactory results in Western blotting and immunohistochemistry, both of which was required for further analysis of a potential function in Purkinje cell dendritic development.

CA8 is a carbonic anhydrase lacking enzymatic activity (Sjöblom et al., 1996). In the *wdl* mouse, mutant with a 19-base-pair deletion in CA8 gene, the loss of function of CA8 results in ataxia (Jiao et al., 2005) and synaptic changes in the cerebellum (Hirasawa et al., 2007) which are associated with alterations in calcium signalling (Lamont et al., 2015). CA8 knockdown in zebrafish resulted in abnormal cerebellar development and ataxia (Aspatwar A,2013). Mutations in the human CA8 gene were identified which are associated with cerebellar ataxia and mild cognitive retardation (Kaya et al., 2011; Türkmen et al., 2009) and antibodies directed against CA8 have been identified as a cause of Purkinje cell degeneration and cerebellar ataxia in paraneoplastic syndromes (Höftberger et al., 2014). While through these studies there is a strong association of CA8 mutations with Purkinje cell death and cerebellar ataxia only little is known about CA8 function in Purkinje cells. Our finding that CA8 mRNA is approximately two-fold increased and that its protein shows a 6-fold increase in Purkinje cells of PKCγ-S361G transgenic mice suggests that it may be involved in the signalling events downstream of PKC activation. In view of the reported interaction between CA8 and ITPR1 (Hirota et al., 2003), we have now shown that ITPR1 is strongly induced in Purkinje cells from PKCγ-S361G transgenic mice. Mutations in ITPR1 are causing spinocerebellar ataxia (Schorge et al., 2010; van de Leemput et al.,

2007) linking the final outcome of disturbances of PKCγ, CA8 and ITPR1 and suggesting that these proteins may interact functionally for the control of Purkinje cell synaptic function and dendritic development.

PKCγ, *CA8 and ITPR1 do not co-immunoprecipitate*

CA8 was previously identified as a protein binding to ITPR1 in a yeast two hybrid screen and the interaction was confirmed with a GST-pulldown assay (Hirota et al., 2003). In a recent report CA8 was shown to modulate pain sensation in sensory neurons by inhibiting ITPR1-mediated signalling and calcium release (Zhuang et al., 2015). Although the ITPR1 was not originally identified as being upregulated in our gene chip screening (because the p-value was slightly above 0.05) we have confirmed that it is also increased with an almost 5-fold increased protein expression in Purkinje cells with activated PKC. In the classical signalling pathway, both PKCγ and the ITPR1 are activated in parallel via DAG and IP3. It is an interesting finding that a chronic activation of PKC induces a strong induction of the protein expression of ITPR1 and the presumed interacting protein CA8. The activation of the PKC pathway thus induces an induction of its parallel pathway which is activated by IP3. This could mean that these pathways are not only linked by the common activation by DAG and IP3 but that PKC activation by itself can recruit the parallel IP3 pathway. The exact mechanism of this interaction still needs to be determined. It is well known that the IP3 receptor is a target of PKC phosphorylation and that phosphorylation changes the IP3-induced calcium release (Vermassen et al., 2004). Our finding suggest that PKC-mediated phosphorylation of the ITPR1 may eventually increase the protein expression of this receptor.

Despite the parallel rise of protein expression of ITPR1 and CA8 in Purkinje cells of PKCγ-S361G transgenic mice and the finding that an interaction between these two proteins was identified in a yeast two hybrid screen and by a GST-pulldown assay (Hirota et al., 2003) we could not show a co-immunoprecipitation of CA8 and ITPR1 in Purkinje cells. Neither ITPR1 nor PKCγ co-immunoprecipitated with CA8. Similarly, in the Duolink proximity assay no evidence for a close interaction was found (data not shown). Of course we cannot exclude that this failure to demonstrate a direct binding was due to technical limitations, but both proteins are solidly expressed and we have

tried different immunoprecipitation protocols, none of which was showing co-immunoprecipitation (data not shown). Therefore, the exact nature of the interaction between PKCγ, CA8 and ITPR1 in Purkinje cells still needs to be studied further.

*CA8 and Purkinje cell dendritic development*

The strong upregulation of CA8 with activation of PKCγ raises the possibility that CA8 is directly or indirectly involved in the stunted growth of the Purkinje cell dendritic tree seen with constitutive activation of PKCγ in PKCγ-S361G transgenic mice. We have addressed this issue by overexpressing CA8 in dissociated Purkinje cell cultures. The dissociated culture system is of course less complex and more artificial compared to organotypic slice cultures, but it allows to reliably transfect Purkinje cells by electroporation and the use of an L7-based Purkinje cell specific expression vector (Wagner et al., 2011). Purkinje cells derived from PKCγ-S361G transgenic mice show a much reduced dendritic development in such cultures, and also transfection of a PKCγ-S361G plasmid resulted in a strong reduction of dendritic outgrowth (Fig. 27) indicating that the dissociated culture does indeed reflect the changes of dendritic outgrowth originally seen in organotypic slice cultures. When Purkinje cells were transfected with a CA8 plasmid resulting in CA8 overexpression a similar stunted dendritic growth was observed as seen after overexpression of PKCγ or of the mutated PKCγ-S361G (Fig. 27). This finding shows that CA8 function does have an inhibitory effect on Purkinje cell dendritic growth and that it is likely that PKCγ and CA8 are both part of a common or related signalling pathway eventually controlling dendritic outgrowth and retraction. If CA8 was a downstream effector of PKC activation a loss of function of CA8 should reduce the effects of PKCγ on the Purkinje cell dendrites. To this end we have used transfection of miRNA in order to suppress CA8 expression. After transfection with miRNA, protein expression of CA8 was reduced to a degree that cells were only weakly detected by immunohistochemistry (Fig. 28) confirming an efficient suppression of CA8 protein expression by the miRNA. Despite this marked reduction of CA8 expression, activation of PKC with PMA still showed the typical stunted dendritic growth indicating that CA8 is not required for this effect. There was also no rescue of the stunted dendritic tree by CA8 knockdown in Purkinje cells derived from PKCγ-S361G transgenic mice. While these findings leave open the possibility that

the small residual amount of CA8 protein present in Purkinje cells with CA8 knockdown is sufficient for mediating the effects of PKCγ activation they make it very unlikely that CA8 is the dominant mediator of PKCγ activation. They leave open the possibility that CA8 may be more loosely associated with PKCγ signalling or that its function might be redundant with another yet to be identified mediator of PKCγ activation.

Conclusions

In this study we have identified CA8 and the ITPR1 as two genes with strongly increased expression in Purkinje cells with chronic activation of PKCγ. We could not find evidence for a direct interaction of CA8 with the ITPR1 but show that overexpression of CA8 in Purkinje cells results in a phenotype with stunted dendritic growth similar to that seen after activation or overexpression of PKCγ. Although CA8 is probably not a direct mediator of PKCγ for the effects on dendritic growth, it is likely to be part of a larger signalling network including PKCγ and the ITPR1 which controls synaptic function and dendritic growth of Purkinje cells.

**Supplementary material for**

Carbonic anhydrase related protein 8 expression is controlled by PKCγ activity and regulates Purkinje cell dendritic growth

Etsuko Shimobayashi, Wolfgang Wagner and Josef P. Kapfhammer

**Supplementary methods:**

*Primer sequences for RT-qPCR*

The following primer sequences were used:

Chn1 (forward: tcagccatgtgactttgagc, reverse: tccatcgtcctgattcttcc),

Klhl4 (forward: ttgctccaggctttctgact, reverse: caacagcatctcgaggaaca),

CA8 (forward: tcagttgagttcaggcaacg, reverse: tgcttggaaaaactgcctct),

Bcl11a (forward: tcccatcgagatgaaaaagg, reverse: gctgctgggctcatctttac),

Fam40b (forward: gtacagcctcccccagtaca, reverse: cacgtcaatgcctagcttca),

Lhx1 (forward: tagcccgcttgagactgatt , reverse: gagcgacagggcaattagag)

Plekhd1 (forward: ggcctcctatctttccttgg, reverse: tacaaccatccacgactcca) and

Ywhah (forward: ggctctgcttgacaagttcc, reverse: gcctcagaagcttcaaccac).

As endogenous control GAPDH was selected.

GAPDH (forward: aactttggcattgtggaagg, reverse: acacattgggggtaggaaca)

*Supplementary Table 1*

| B-cell CLL/lymphoma 11A (Bcl11a) | Bcl11 (also known as Evi9, Ctip1) encodes a C2H2 zinc finger transcription factor that acts as a transcriptional regulator (John et al., 2012). Bcl11 is involved in neuronal differentiation and the formation of sensory circuits (Jiao et al., 2005). |
|---|---|
| Carbonic anhydrase-related proteins 8 (CA8) | CA8 is a carbonic anhydrase which is lacking the enzyme activity of carbonic anhydrase. A 19 bp deletion of CA8 in waddles (*wdl*) mice causes an ataxic phenotype with a side-to-side" waddling gait (Lim et al.,1992). CA8 is strongly expressed in Purkinje cells. |
| Chimerin (chimaerin) 1 (Chn1) | Chn1 belongs to Rho GTPase-activating protein family and within the cerebellum the mRNA of Chn1 was detected only in Purkinje neurons (Andrews et al., 2007). Chn1 is a member of the "Duane's retraction syndrome 2 related genes" in which mutations cause familial isolated Duane syndrome (Buttery et al., 2006). The diacylglycerol-binding protein alpha1-chimaerin (Chnα1) regulates dendritic morphology (Goudreault et al., 2009). |
| family with sequence similarity 40, member B (Fam40b) | Fam40b as well as Fam40a have recently been isolated as part of a striatin-interacting phosphatase and kinase (STRIPAK) complex contains the PP2A catalytic (PP2Ac) and scaffolding (PP2A A) subunits (Bai SW, 2011). Interestingly, Fam40a and Fam40b are well conserved from fungi and amoebae to humans and involved in cell cytoskeletal organization and migration in human cells (Chen et al., 2008). Their detailed function is not yet known. |
| Kelch-like family 4 (Klhl4) | Klhl4 belongs to actin-binding protein (ABP) Kelch-like family. Klhl1 is involved in T-type Ca-channels and SCA-8 (Aromolaran et al., 2010; He et al., 2006) and |

| | Klhl4 is a constitutive neuronal ABP localized to the soma and dendritic arbors. Its deletion in Purkinje neurons results in dendritic atrophy and motor insufficiency (Hayes et al., 2001). The exact function of Klhl4 is yet unknown. |
| --- | --- |

| | |
| --- | --- |
| LIM homeobox protein 1 (Lhx1) | Lhx1 encodes a LIM-homeo domain transcription factor. Lhx1 and the closely related protein Lhx5 previously have been detected in Purkinje cells in rodents (Zhao et al., 2007). Recently, Lhx1 and Lhx5 were shown to play essential roles in the differentiation of neurons throughout the developing central nervous system. Mutant mouse embryos lacking the function of these genes showed a defective Purkinje cell differentiation in the developing cerebellum (Rippey et al., 2013). |
| pleckstrin homology domain containing, family D (Plekhd1) | Plekhd1 is an uncharacterized gene that has an N-terminal Pleckstrin homology (PH) domain (Meuillet et al., 2011). PH domains are generally involved in intracellular signaling by binding to phospho-tyrosine and polyproline sequences, $G_{\beta\gamma}$ subunits of heterotrimeric G proteins, and phosphoinositide (PI) and recruitment of their target proteins to the cell membrane (Martin et al.,1994). According to data from the Allen Brain Atlas Plekhd1 mRNA in the cerebellum is strongly and specifically expressed in Purkinje cells. |
| Tyrosine 3-monooxygenase/tryptophan 5-monooxygenase activation protein, eta (Ywhah) | Ywhah encodes 14-3-3 protein eta chain gene. 14-3-3 is abundant in the brain and it is known that 14-3-3 proteins participate in neuronal development and cell growth control (Ubl et al., 2002). 14-3-3 eta chain might be involved in preventing neuronal cell death in several ways (Metzger and Kapfhammer, 2000; Wetsel et al., 1992). |

| miRNA | Oligo | Sequence (5'-3') |
|---|---|---|
| mi327 | mi327-Top | TGC TGA CTT CAT ACA GCT CAA ACT CCG TTT TGG CCA CTG ACT GAC GGA GTT TGC TGT ATG AAG T |
| | mi327-Bottom | CCT GAC TTC ATA CAG CAA ACT CCG TCA GTC AGT GGC CAA AAC GGA GTT TGA GCT GTA TGA AGT C |
| mi616 | mi616-Top | TGC TGA AGA GGG TCT GGT AAT AAA GTG TTT TGG CCA CTG ACT GAC ACT TTA TTC AGA CCC TCT T |
| | mi616-Bottom | CCT GAA GAG GGT CTG AAT AAA GTG TCA GTC AGT GGC CAA AAC ACT TTA TTA CCA GAC CCT CTT C |
| mi686 | mi686-Top | TGC TGA TAT CCA GGT AAC TCC TTC GCG TTT TGG CCA CTG ACT GAC GCG AAG GAT ACC TGG ATA T |
| | mi686-Bottom | CCT GAT ATC CAG GTA TCC TTC GCG TCA GTC AGT GGC CAA AAC GCG AAG GAG TTA CCT GGA TAT C |

**Table. 4 Sequence of miRNA oligomer**

**A**
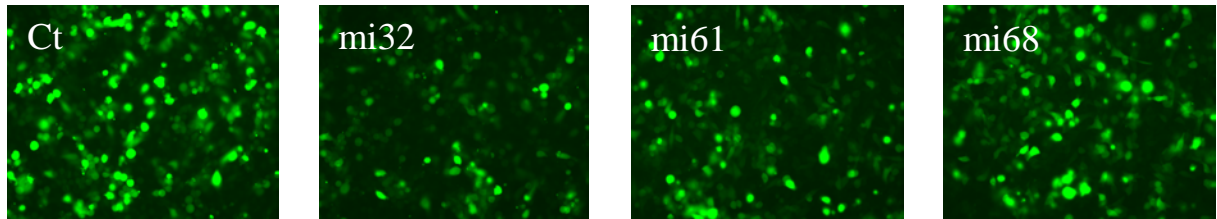


**B**
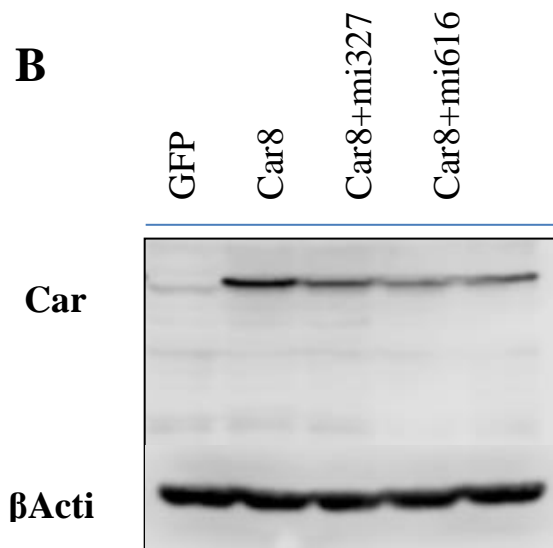


**C**
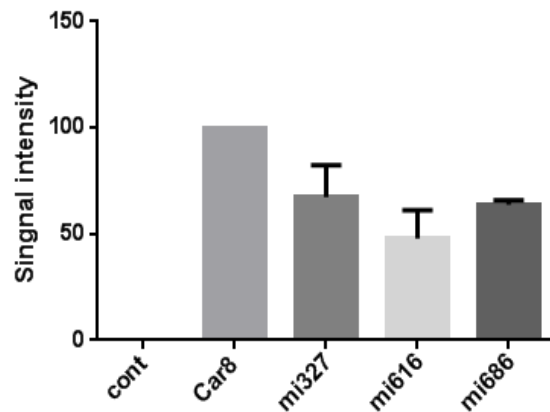


**Fig.29 Immunofluorescence staining analysis and Western Blotting analysis of Car8miRNA transfected Hela cells.**
(A) Control is Car8-GFP transfected Hela cells. mi327, mi616 and mi686 are transfected with Car8-GFP. Cells were fixed after 72hr transfection. (B) WB results showed Car8 expression level was reduced in miRNA transfected cells. (C) Each Car8 expression was calculated and analyzed with Graphpad prism.

# 5. *Discussion*

## 5.1. Gene transfection of Purkinje cells with electroporation

In the study with several point mutations in PKCγ, we have analyzed the effect of several PKCγ mutations on the dendritic growth of Purkinje cells. To achieve Purkinje cell transfection with the different mutant constructs, we first performed lipofection, magnetofection (Jenkins et al., 2011 ; Sapet et al., 2011) and biolistic gene transfection with gene gun (Haag et al., 2012; Smith-Hicks et al., 2010). Although these transfection systems worked well for cell lines or some neural cells, we couldn't get satisfying transfection rates for Purkinje cells. Thus we performed electroporation for cerebellar cells in dissociated cultures. When we used expression plasmids with the CMV promoter, we did get a good overall number of transfected cells in the culture, but only very few transfected Purkinje cells. Only when we used with the plasmid with the L7 promoter (Wagner et al., 2011), we got a sufficient number of transfected Purkinje cells and no transgene expression in cells other than Purkinje cell. Furthermore, in our experiments the L7 promoter-plasmid yielded adequate expression levels for more than two weeks, which helped to investigate the effects of PKCγ mutants throughout Purkinje cell dendritic development.

The morphology of Purkinje cell dendrites changes drastically during postnatal cerebellar development (Armengol et al., 1991; Tanaka et al., 2006). In the first postnatal week, Purkinje cells have several primary dendrites. In the second postnatal week, most Purkinje cells lose all of their primary dendrites except one, which rapidly elongates and branches in the sagittal plane to elaborate the typical dendritic tree (Sotelo et al., 2009) which forms numerous synapses with climbing fibers and parallel fibers (Rossi et al.,1995). Previous research showed that the final morphology of Purkinje cell dendrites is achieved both through extension and through retraction of dendritic processes (Tanaka et al., 2006). Therefore, our approach made it possible to observe the influence of several types of mutant PKCγ proteins on extension and retraction of Purkinje cell dendrites from postnatal 0 to the second and third postnatal week. In our experiments, we always use P0 mice because when we used cerebella

from P1 or older mice, the dendritic development of Purkinje cells was reduced and more variable.

## 5.2. The domain location of SCA14 mutations determines their effect on dendritic growth of Purkinje cells

We had expected that most PKCγ mutants would have a similar effect on dendritic growth of Purkinje cells as most PKCγ mutants have an increased enzymatic activity in cell based assays (Adachi et al., 2008; Verbeek et al., 2005). Earlier studies have shown that activation of PKCγ negatively regulates the development of the Purkinje cell dendritic tree in rodent cerebellar slice cultures (Metzger et al., 2003; Schrenk et al., 2002). Our previous finding that Purkinje cells in S361G PKCγ transgenic mice have shown a strong reduction of dendritic development is a proof for a biologically relevant activation of PKC (Ji et al., 2014). Therefore, it is conceivable that every PKCγ mutation which have an increased enzymatic activity would negatively regulate dendritic development of Purkinje cells similar to S361G mutant. However, we found that none of several tested PKCγ mutations located in the C1B domain showed an inhibitory effect on dendritic growth of Purkinje cells although increased enzymatic activities of these PKCγ mutants (S119P, G128D and V138E) were demonstrated before (Adachi et al., 2008; Seki et al., 2009). On the other hand, there are indications that the C1B domain PKCγ mutants H101Y, S119P and G128D could disrupt the association of endogenous PKCγ with other binding proteins, such as 14-3-3 proteins, resulting in an inactivation of endogenous PKCγ (Lin D et al., 2007). Recently, Jezierska et al. (2014) suggested that alterations in the conformation of the C1B domain might affect PKCγ mutant autophosphorylation levels and might lead to a decreased kinase activity. In addition, Adachi et al. had shown that 14 types of C1B mutants failed to regulate $Ca^{2+}$ influx into CHO cells while the catalytic domain mutants S361G and F643L had an increased inhibitory effect of $Ca^{2+}$ entry compared to WT PKCγ (2008). This finding is in agreement with our results that S361G and F643L mutants have an increased biological activity compared to WT PKCγ. Our results suggest that the catalytic domain mutants S361G and F643L have an increased catalytic activity resulting in dendritic growth inhibition of Purkinje cells while C1B

mutants didn't show increased biological activity probably due to inactivation of endogenous PKCγ or decreased kinase activity. In the C2 domain deletion, we found the same minor morphological changes as with transfection of WT PKCγ. Further investigations with SCA14 mutants in the C2 domain are needed in order to better understand the consequences of mutations in this domain for PKCγ biological activity. Taken together, our results suggest that SCA14 is likely not to be caused by a simple pathological mechanism but that several different pathways may be involved depending on the position of the point mutations or deletions. In this study, we found that SCA14 mutations could be divided into two types, one type with a point mutation in the kinase domain (S361G and F643L) which has an increased biological activity resulting in reduced Purkinje cell dendrites, the other type with a point mutation in the C1B domain has normal or decreased biological activity (perhaps by inactivation of endogenous PKCγ), and has no effect on Purkinje cell dendritic development. Further experiments are necessary to investigate that how these different effects on biological activity are involved in the pathogenesis of SCA14 and cerebellar dysfunction.

## 5.3. General discussion

### 5.3.1. PKC isoforms expressed in Purkinje cells

As stated in the introduction, PKC has several isoforms and PKCγ is the dominant classical isoform in Purkinje cells. However, the α- and β-isoform might be also be expressed in Purkinje cells. PKCα is ubiquitously expressed in all cerebellar cells whereas PKCβ was reported to be mostly present in granule cells (Hirono et al., 2001) but may also be expressed Purkinje cells (Gundlfinger et al., 2003).

Do all isoforms have the same function on dendritic development of Purkinje cells? There are some evidences about the role of the different PKC isoform for dendritic development of Purkinje cells. Gundlfinger et al (2003) showed that PKCα is expressed in Purkinje cells while PKCβ is not expressed in Purkinje cells under normal culture conditions. PKCα deficient mice showed rather normal dendritic development. The lack of PKCα might be compensated by PKCγ because PKCγ is dominantly expressed in Purkinje cells. On the other hand, Purkinje cells from PKCγ deficient mice showed a slightly more complex dendritic tree (Schrenk et al., 2002)

indicating that PKCγ has a dominant effect on dendritic tree development. But if PKCα is activated by phorbol ester treatment it does inhibit dendritic development in the absence of PKCγ (Gundlfinger et al., 2003). These findings are best explained by assuming that under normal conditions PKCγ is the functional relevant isoform and that PKCα is rather forming a reserve pool. Taken together, in Purkinje cells PKCγ and PKCα are expressed and PKCγ is the major isoform responsible for dendritic development under normal conditions.

PKC is also well known as a key protein for the induction of cerebellar long term depression (LTD). LTD is produced by associative activation of PF and CF (Kim and Thompson,1997), which results in co-activation of AMPA receptor and PLCβ in Purkinje cells (Linden and Connor,1995). Co-activation of AMPA receptors and mGluR1 activate phospholipase Cβ (PLCβ) coupled to heterotrimeric G-proteins Gq/G11, leading to hydrolysis of phosphatidylinositol 4, 5-bisphosphate (PIP2) to inositol 1, 4, 5-trisphosphate (IP3) and diacylglycerol (DAG). This will result in an increased intracellular $Ca^{2+}$ concentration by release of $Ca^{2+}$ from IP3R-mediated stores and TRPC3-mediated $Ca^{2+}$ influx. Increased $Ca^{2+}$ concentration in the cytoplasm and DAG activate PKC (Ohtani et al., 2014). There are several PLCβ isoforms in Purkinje cells (dominantly PLCβ1, 3 and 4) and within PLCβ isoforms PLCβ3 and PLCβ4 are crucial for mGluR1 induced LTD (Hirono et al., 2001). There are some studies about the relevant PKC isoform for the expression of LTD. In a first publication no change was seen in LTD in PKCγ deficient mice (Chen et al., 1995), which indicates that PKCγ is less important for LTD compared to other PKC isoforms. Furthermore, PLC (β3 and β4) activation caused translocation of PKCα and PKCβ but not PKCγ (Hirono et al., 2001). In further studies it was shown that the PDZ ligand in PKCα is of crucial importance for the induction of LTD (Leitges et al., 2004). On the other hand, as mentioned in the introduction, the PKC inhibitor peptide (PKC 19-36) completely blocks LTD in wild-type mice but not in PKCγ deficient mice (Hémart et al., 1995). While it is evident that PKCγ is not required for the induction of LTD, it may still have a modulatory role.

### 5.3.2. SCA14 mutations and inhibition of Purkinje cell dendritic development

In this thesis I have focused on mutant PKCγ and Purkinje cell dendritic development. The findings that on the one hand PKCγ deficient mice have an enlarged dendritic tree and on the other hand PKC activation causes severe dendritic growth inhibition indicate that PKC has a negative influence on dendritic development. This links increased PKC activity to Purkinje cell dysfunction and SCA14.

An important question to answer will be whether SCA14 mutations will cause dendritic growth inhibition and pathogenesis by the same mechanisms?

There is some evidence that many or even all SCA14 related mutant PKCγ proteins might have increased kinase activity (Adachi et al., 2008; Verbeek et al., 2005). But there are also data showing that mutant PKCγ failed to recruit downstream targets resulting in a certain loss of function (Verbeek et al., 2008). In order to study the biological relevance of SCA14 and PKCγ mutations for Purkinje cells dendritic development, we generated transgenic mice expressing a mutated PKCγ with the S361G point mutation from SCA14. We found that this mutant PKCγ caused severe dendritic reduction of Purkinje cells in organotypic slice cultures. Furthermore, these transgenic mice showed mild ataxia in the absence of cerebellar degeneration, which supports the idea that increased kinase activity of PKCγ inhibits Purkinje cell dendritic growth and links it to SCA pathogenesis. On the other hand, we also have created additional SCA14 related mutant PKCγ transgenic mice. One mouse line is carrying the missense mutation G118D (in the C1 regulatory domain) and the second line a deletion of amino acids 260-280 in the C2 domain. The G118D mutation is a SCA14 mutation in human (van de Warrenburg et al., 2003) and this mutation increased the intrinsic kinase activity of PKCγ (Verbeek et al., 2005). The 260-280 deletion has no direct relation to SCA14 so far, but the same deletion in PKCα was shown to have an increased kinase activity (Rotenberg et al., 1998). Interestingly, Purkinje cells from either of these two transgenic mouse lines develop normal dendritic trees in cerebellar slice cultures indicating that there is no biologically relevant increase of PKC activity in Purkinje cells. In order to address the effects of SCA14 related mutations more systematically, we generated expression vectors for several PKCγ mutations and transfected them to Purkinje cells in dissociated cerebellar cultures

(Material and Methods). This in vitro assay confirmed that C1 domain mutations (including G118D mutation) and the 260-280 deletion didn't affect dendritic development. In contrast, an additional kinase domain mutation found in SCA14 patients mediated again a severe inhibition of dendritic development in Purkinje cells. This would be in agreement with the finding of Adachi et al. that in CHO cells the C1 domain mutants failed to regulate $Ca^{2+}$ influx while kinase domain mutants showed an increased inhibition of $Ca^{2+}$ entry into the cells (2008). These findings suggest that there may be diverse mechanisms leading to pathogenesis in SCA14. While for mutations in the kinase domain Purkinje cell dysfunction is likely to be linked to increased PKC activity, this seems not to be the case in C1 domain mutations which rather show a functional deficiency of PKC. The common aspect of the two mechanisms may be that both interfere with the regulated function of the PKCγ – IP3R pathway, the dysfunction of which is tightly linked to the development of the ataxic phenotype (Schorge et al., 2010). This is further discussed in the following paragraph.

### 5.3.3. Car8, IP3R and PKCγ

In this study we found that Car8 and IP3R1 are both upregulated in mutant PKCγ transgenic mice. Interestingly, Car8, IP3R1 and PKCγ proteins are all known to be strongly and specifically expressed in Purkinje cells. The common function among them is that they are involved in calcium influx and regulate calcium homeostasis in Purkinje cells. Disruption of intracellular calcium homeostasis in Purkinje cells is thought to be a key mechanism in the pathogenesis of SCA and at the same time known to control Purkinje cell dendritic development. The dendritic tree size reduction in cerebellar Purkinje cells in slice cultures can be achieved by chronic activation of mGluR1 (Sirzen-Zelenskaya et al., 2006). This reduction of Purkinje cell dendritic development after chronic activation of mGluR1 could be partially rescued by inhibition of T-type and P/Q-type calcium channels (Gugger et al., 2012), indicating that $Ca^{2+}$ influx through T-type and P/Q-type channels is important for mediating dendritic growth inhibition. Inhibition of the plasma membrane $Ca^{2+}$-ATPase2 (PMCA2) activity by carboxyeosin also resulted in an inhibition of Purkinje cell dendritic growth (Sherkhane and Kapfhammer, 2013). Interestingly, it is known that

PMCA2 co-immunoprecipitates with mGluR1, Homer 3 and IP3R1, which indicates that $Ca^{2+}$ pump PMCA2, mGluR1, Homer 3 and the IP3R1 are forming a complex and regulate each other (Kurnellas et al., 2007). Little is still known about the further downstream signaling events eventually interfering with Purkinje cell dendritic development.

Another mutation affecting the $Ca^{2+}$ homeostasis in Purkinje cells is found in *Moonwalker* (*Mwk*) mice which have a gain of function point mutation in the TRPC3 channel. *Mwk* mice develop cerebellar ataxia (Becker et al., 2009) and also have abnormal dendritic arborization during cerebellar development (Sekerkova et al., 2013). Interestingly, TRPC3 knockout mice showed a normal dendritic development (Gugger et al., 2012), highlighting the importance of the increased $Ca^{2+}$ entry in the *Mwk* mutation. Adachi et al. showed that PKCγ with a C1 domain mutation (G128D) failed to inhibit $Ca^{2+}$ entry through the TRPC3 channel. Dulneva et al. showed that CaMKIV is hyper-phosphorylated in the *Mwk* cerebellum and might be one candidate for the downstream regulation of dendritic outgrowth (2015). One of the downstream targets of CaMKIV is RORα which is a key factor for Purkinje cells development at an early stage (Dulneva et al., 2015 and Boukhtouche et al., 2006). In this thesis I also aimed at identifying downstream targets of PKCγ and by a gene array approach and we identified Car8 and IP3R1 as potential candidates for PKCγ downstream signaling. We could confirm that Car8 is involved in Purkinje cell dendritic development but in our experiments Car8 knock down couldn't rescue the PKCγ mediated in inhibition of dendritic growth. Car8 is thus unlikely to be a direct downstream target of PKCγ; alternatively there could be several parallel signaling pathways related to dendritic growth and Car8 might only be part of one of them. The exact function of Car8 function is still rather unclear but its importance is evident from the strong ataxic phenotype found in mice deficient for Car8 (Jiao et al., 2005) and humans (Türkmen et al., 2009). There is evidence that Car8 is modulating IP3R1 function (Hirota et al., 2003) and that the ataxic phenotype could be in part explained by a loss of the precise regulation of IP3R1 activity and that this could also contribute to the abnormal dendritic development of Purkinje cells. We also identified IP3R1 as a candidate for downstream signaling of PKCγ. IP3R1 is the dominant IP3 receptor in Purkinje cells and may be also one of the key proteins in the pathogenesis of SCAs

(Schorge et al., 2010; Tada et al., 2016). Purkinje cells from IP3R1 knock-out (IP3R1KO) mice have a normal or only slightly changed morphology (Hisatsune et al., 2006; Matsumoto and Kato, 2001). On the other hand, these mice are ataxic (Matsumoto et al.,1996). In humans two SCA subtypes are associated with the IP3R1 gene: SCA15/16 is caused by deletions or missense mutations in the IP3R1 gene (Ganesamoorthy et al., 2009; Novak et al., 2010; van de Leemput et al., 2007) and SCA29 is caused by missense mutations in IP3R1 (Sasaki et al., 2015). In both diseases there is a dominant inheritance and it is not entirely clear whether the disease is brought about by a pure loss of function of the IP3R1 (Iwaki et al., 2008). It is possible that the different missense mutation may cause IP3R1 dysfunction in several ways, and the signalling pathway downstream of the mutant IP3R1 could be changed in several ways. IP3R1 is also known to be an upstream protein of PKCγ, therefore there might be some feedback mechanism in the IP3R1- PKCγ signaling cascade in Purkinje cells. Once calcium homeostasis is destroyed, these proteins can be either up- or down-regulated and become causative for abnormal dendritic development and ataxia. Further work will be needed to reveal the exact molecular interactions responsible for the expression of the dendritic phenotype and the development of ataxia.

# *References*

Abeliovich A, Chen C., Goda Y, Silva AJ, Stevens CF, Tonegawa S. (1993). Modified hippocampal long-term potentiation in PKC gamma-mutant mice. *Cell*, 1253-1262.

Adachi N, Kobayashi T, Takahashi H, Kawasaki T, Shirai Y, Ueyama T, Matsuda T, Seki T, Sakai N, Saito N. (2008). Enzymological analysis of mutant protein kinase Cgamma causing spinocerebellar ataxia type 14 and dysfunction in Ca2+ homeostasis. *J Biol Chem*, 19854-19863.

Adcock KH, MetzgerF, Kapfhammer JP. (2004). Purkinje cell dendritic tree development in the absence of excitatory neurotransmission and of brain-derived neurotrophic factor in organotypic slice cultures. *Neuroscience, 127*(1), 137-145.

Andersen B B, Korbo L., Pakkenberg B. (1992). A quantitative study of the human cerebellum with unbiased stereological techniques. *J. Comp. Neuro*, 549–560.

Andrews CV, Hunter D, Engle EC. (2007). Duane Syndrome. *GeneReviews*, 1993-2014.

Armengol JA, Sotelo C. (1991). Early dendritic development of Purkinje cells in the rat cerebellum. A light and electron microscopic study using axonal tracing in 'in vitro' slices. *Brain Res Dev Brain Res*, 95-114.

Aromolaran KA, Benzow K, Cribbs LL, Koob MD, Piedras-Rentería ES. (2010). T-type current modulation by the actin-binding protein Kelch-like 1. *Am J Physiol Cell Physiol*, C1353-1362.

Asai H, Hirano M, Shimada K, Kiriyama T, Furiya Y, Ikeda M, Iwamoto T, Mori T, Nishinaka K, Konishi N, Udaka F, Ueno S. (2009). Protein kinase C gamma, a protein causative for dominant ataxia, negatively regulates nuclear import of recessive-ataxia-related aprataxin. *Hum Mol Genet*, 3533–3543.

Aspatwar A, Tolvanen M, Parkkila S. (2013). An update on carbonic anhydrase-related proteins VIII, X and XI. *J Enzyme Inhib Med Chem*, 1129-1142.

Baader SL, Sanlioglu S, Berrebi AS, Parker-Thornburg J, Oberdick J. (1998). Ectopic overexpression of engrailed-2 in cerebellar Purkinje cells causes restricted cell loss and retarded external germinal layer development at lobule junctions. *J Neurosci*, 1763-1773.

Bai SW, Herrera.-Abreu M, Rohn JL, Racine V, Tajadura V, Suryavanshi N, Bechtel S, Wiemann S, Baum B, Ridley AJ. (2011). Identification and characterization of a set of conserved and new regulators of cytoskeletal organization, cell morphology and migration. *BMC Biol*, 9:54.

Banerjee S, Hasan G. (2005) The InsP3 receptor: its role in neuronal physiology and neurodegeneration. *Bioessays,* 1035-47.

Baptista CA, Hatten M, Blazeski R, Mason CA. (1994). Mason Cell-Cell Interactions Influence Survival and Differentiation of Purified Purkinje Cells In Vitro. *Neuron*, 243-260.

Bastian AJ. (2011). Moving, sensing and learning with cerebellar damag. *Curr. Opin. Neurobiol*, 596–601.

Becker EB, Oliver P, Glitsch MD, Banks GT, Achilli F, Hardy A, Nolan PM, Fisher EM, Davies KE. (2009). A point mutation in TRPC3 causes abnormal Purkinje cell development and cerebellar ataxia in moonwalker mice. *Proc Natl Acad Sci U S A*, 6706-6711.

Becker KP, Hannun Y. (2003). cPKC-dependent sequestration of membrane-recycling components in a subset of recycling endosomes. *J Biol Chem*, 52747-52754.

Bittova L, Stahelin R, Cho W. (2001). Roles of ionic residues of the C1 domain in protein kinase C-alpha activation and the origin of phosphatidylserine specificity. *J Biol Chem*, 4218-4226.

Bornancin F, Parker PJ. (1996) Phosphorylation of threonine 638 critically controls the dephosphorylation and inactivation of protein kinase Calpha. *Curr Biol.* 1114-23.

Boukhtouche F, Doulazmi M, Frederic F, Dusart I, Brugg B, Mariani J. (2006). RORalpha, a pivotal nuclear receptor for Purkinje neuron survival and differentiation: from development to ageing. *Cerebellum, 5*(2), 97-104. doi:10.1080/14734220600750184

Bowers BJ, Wehner J. (2001). Ethanol consumption and behavioral impulsivity are increased in protein kinase Cgamma null mutant mice. *J Neurosci*, RC180.

Brandon NJ, Uren JM, Kittler JT, Wang H, Olsen R, Parker PJ, Moss SJ. (1999). Subunit-specific association of protein kinase C and the receptor for activated C kinase with GABA type A receptors. *J Neurosci.* 9228-34.

Brkanac Z, Bylenok L, Fernandez M. (2002). A new dominant spinocerebellar ataxia linked to chromosome 19q13.4-qter. *Arch Neurol* 1291–1295.

Brunel N, Hakim V, Isope P, Nadal JP, Barbour B. (2004). Optimal information storage and the distribution of synaptic weights: perceptron versus Purkinje cell. *Neuron*, 745-757.

Buerli, T, Pellegrino, C, Baer K, Lardi-Studler B, Chudotvorova I, Fritschy JM Fuhrer, C. (2007). Efficient transfection of DNA or shRNA vectors into neurons using magnetofection. *Nat Protoc, 2*(12), 3090-3101. doi:10.1038/nprot.2007.445

Buttery P, Beg A, Chih B, Broder A, Mason CA, Scheiffele P. (2006). The diacylglycerol-binding protein alpha1-chimaerin regulates dendritic morphology. *Proc Natl Acad Sci U S A*, 1924-1929.

Campbell JM, Gilmore D, Russell D, Growney CA, Favor G, Kennedy AK, Davies RW, Payne AP, Stone TW. (2000). Pharmacological analysis of extracellular dopamine and metabolites in the striatum of conscious as/agu rats, mutants with locomotor disorder. *Neuroscience*, 45-52.

Carlson KM, Andresen J, Orr HT. (2009). Emerging pathogenic pathways in the spinocerebellar ataxias. *Curr Opin Genet Dev 1*, 247–253.

Cazaubon S, Bornancin F, Parker PJ. (1994). Threonine-497 is a critical site for permissive activation of protein kinase C alpha. *Biochem J*, 443-448

Chaumont J, Guyon N, Valera AM, Dugué GP, Popa D, Marcaggi P, Gautheron V, Reibel-Foisset S, Dieudonné S, Stephan A, Barrot M, Cassel JC, Dupont JL, Doussau F, Poulain B, Selimi F, Léna C, Isope P. (2013). Clusters of cerebellar Purkinje cells control their afferent climbing fiber discharge. *Proc Natl Acad Sci U S A*, 16223-16228.

Chen C, Kano M, Abeliovich A, Chen L, Bao S, Kim JJ, Hashimoto K, Thompson RF, Tonegawa S. (1995). Impaired motor coordination correlates with persistent multiple climbing fiber innervation in PKC gamma mutant mice. *Cell*, 1233–1242.

Chen DH, Cimino P, Ranum LP, Zoghbi HY, Yabe I, Schut L, Margolis RL, Lipe HP, Feleke A, Matsushita M, Wolff J, Morgan C, Lau D, Fernandez M, Sasaki H, Raskind WH, Bird TD. (2005). The clinical and genetic spectrum of spinocerebellar ataxia 14. *Neurology*, 1258-1260.

Chen DH, Raskind W, Bird TD. (2012). Spinocerebellar ataxia type 14. *Handb Clin Neurol*, 555-559.

Chen WL, Lin J, Huang HJ, Wang SM, Su MT, Lee-Chen GJ, Chen CM, Hsieh-Li HM. (2008). SCA8 mRNA expression suggests an antisense regulation of KLHL1 and correlates to SCA8 pathology. *Brain Res*, 176-184.

Colon-Gonzalez F, Kazanietz M. (2006). C1 domains exposed: from diacylglycerol binding to protein-protein interactions. *Biochim Biophys Acta*, 827–837.

Craig NJ, Duran AM, Hawker KL, Shiels P, Glencorse TA, Campbell JM, Bennett NK, Canham M, Donald D, Gardiner M, Gilmore DP, MacDonald RJ, Maitland K, McCallion AS, Russell D, Payne AP, Sutcliffe RG, Davies RW. (2001). A candidate gene for human neurodegenerative disorders: a rat PKC gamma mutation causes a Parkinsonian syndrome. *Nat Neurosci*, 1061-1062.

D'Angelo E, Casali S. (2012). Seeking a unified framework for cerebellar function and dysfunction: from circuit operations to cognition. *Front. Neural Circuits*, 6:116.

Doran G, Davies K, Talbot K. (2008). Activation of mutant protein kinase Cgamma leads to aberrant sequestration and impairment of its cellular function. *Biochem Biophys Res Commun*, 447–453.

Duenas AM, Gooold R, Giunti P. (2006). Molecular pathogenesis of spinocerebellar ataxias. *Brain*, 1357–1370.

Dulneva A, Lee S., Oliver PL , Di Gleria K, Kessler BM, Davies KE, Becker EB. (2015). The mutant Moonwalker TRPC3 channel links calcium signaling to lipid metabolism in the developing cerebellum. *Hum Mol Genet, 24*(14), 4114-4125. doi:10.1093/hmg/ddv150

Dupont JL, Fourcaudot E, Beekenkamp H, Poulain B, Bossu JL. (2006). Synaptic organization of the mouse cerebellar cortex in organotypic slice cultures. *Cerebellum*, 243-256.

Dusart I, Airaksinen M, Sotelo C. (1997). Purkinje cell survival and axonal regeneration are age dependent: an in vitro study. *J Neurosci*, 3710-3726.

Dutil EM, Keranen L, DePaoli-Roach AA, Newton AC. (1994). In vivo regulation of protein kinase C by trans-phosphorylation followed by autophosphorylation. *J Biol Chem*, 29359-29362.

Fry MJ, Gebhardt A, Parker PJ, Foulkes JG. (1985). Phosphatidylinositol turnover and transformation of cells by Abelson murine leukaemia virus. *EMBO J, 4*(12), 3173-3178.

Furuya S, Ono K, Hirabayashi Y. (1995). Sphingolipid biosynthesis is necessary for dendrite growth and survival of cerebellar Purkinje cells in culture. *J Neurochem*, 1551-1561.

Gähwiler BH, Capogna M, Debanne D, McKinney RA, Thompson SM. (1997). Organotypic slice cultures: a technique has come of age. *Trends Neurosci*, 471-477.

Ganesamoorthy D, Bruno DL, Schoumans J, Storey E, Delatycki MB, Zhu D, Slater HR. (2009). Development of a multiplex ligation-dependent probe amplification assay for diagnosis and estimation of the frequency of spinocerebellar ataxia type 15. *Clin Chem, 55*(7), 1415-1418. doi:10.1373/clinchem.2009.124958

Gao T, Newton A. (2002). The turn motif is a phosphorylation switch that regulates the binding of Hsp70 to protein kinase C. *J Biol Chem*, 31585-31592.

Gimenez-Cassina A, Lim F, Diaz-Nido J. (2007). Gene transfer into Purkinje cells using herpesviral amplicon vectors in cerebellar cultures. *Neurochem Int*, 181-188.

Giorgione JR, Lin J, McCammon JA, Newton AC. (2006). Increased membrane affinity of the C1 domain of protein kinase C delta compensates for the lack of involvement of its C2 domain in membrane recruitment. *J Biol Chem*, 1660–1669.

Goudreault M, D. Ambrosio L, Kean MJ, Mullin MJ, Larsen BG, Sanchez A, Chaudhry S, Chen GI, Sicheri F, Nesvizhskii AI, Aebersold R, Raught B, Gingras AC. (2009). A PP2A phosphatase high density interaction network identifies a novel striatin-interacting phosphatase and kinase complex linked to the cerebral cavernous malformation 3 (CCM3) protein. *Mol Cell Proteomics*, 157-171.

Gugger OS, Hartmann J, Birnbaumer L, Kapfhammer JP. (2012). P/Q-type and T-type calcium channels, but not type 3 transient receptor potential cation channels, are involved in inhibition of dendritic growth after chronic metabotropic glutamate receptor type 1 and protein kinase C. *Eur J Neurosci*, 20-33.

Gundlfinger A., Kapfhammer JP, Kruse F, Leitges M, Metzger F. (2003). Different regulation of Purkinje cell dendritic development in cerebellar slice cultures by protein kinase Calpha and -beta. *J Neurobiol, 57*(1), 95-109. doi:10.1002/neu.10259

Haag N, Schwintzer L, Ahuja R, Koch N, Grimm J, Heuer H, Qualmann B, Kessels MM. (2012). The actin nucleator Cobl is crucial for Purkinje cell development and works in close conjunction with the F-actin binding protein Abp1. *J Neurosci*, 17842-17856.

Hansra G, Garcia-Paramio P, Prevostel C, Whelan RD, Bornancin F, Parker PJ. (1999). Multisite dephosphorylation and desensitization of conventional protein kinase C isotypes. *Biochem J*, 337-344.

Harris RA, McQuilkin S, Paylor R, Abeliovich A, Tonegawa S, Wehner JM. (1995). Mutant mice lacking the gamma isoform of protein kinase C show decreased behavioral actions of ethanol and altered function of gamma-aminobutyrate type A receptors. *Proc Natl Acad Sci U S A*, 3658-3662.

Hayes WP, Yangco N, Chin H, Mill JF, Pu LP, Taira M, Dawid IB, Gallo V. (2001). Expression and regulation of the LIM-class homeobox gene rlim-1 in neuronal progenitors of the rat cerebellum. *J Neurosci Res*, 237-251.

He Y, Zu T, Benzow KA, Orr HT, Clark HB, Koob MD. (2006). Targeted deletion of a single Sca8 ataxia locus allele in mice causes abnormal gait, progressive loss of motor coordination, and Purkinje cell dendritic deficits. *J Neurosci*, 9975-9982.

Hémart N, Daniel H, Jaillard D, Crépel F. (1995). Receptors and second messengers involved in long-term depression in rat cerebellar slices in vitro: a reappraisal. *Eur J Neurosci*, 45-53.

Hernandez AI, Blace N, Crary JF, Serrano PA, Leitges M, Libien JM, Weinstein G, Tcherapanov A, Sacktor TC. (2003). Protein kinase M zeta synthesis from a brain mRNA encoding an independent protein kinase C zeta catalytic domain. Implications for the molecular mechanism of memory. *J Biol Chem*, 40305-40316.

Hirasawa M, Xu X, Trask RB, Maddatu TP, Johnson BA, Naggert JK, Nishina PM, Ikeda A. (2007). Carbonic anhydrase related protein 8 mutation results in aberrant synaptic morphology and excitatory synaptic function in the cerebellum. *Mol Cell Neurosci*, 161-170.

Hirono M, Sugiyama T, Kishimoto Y, Sakai I, Miyazawa T, Kishio M, Yoshioka T. (2001). Phospholipase Cbeta4 and protein kinase Calpha and/or protein kinase Cbetal are involved in the induction of long term depression in cerebellar Purkinje cells. *J Biol Chem, 276*(48), 45236-45242. doi:10.1074/jbc.M105413200

Hirota J, Ando H, Hamada K, Mikoshiba K. (2003). Carbonic anhydrase-related protein is a novel binding protein for inositol 1,4,5-trisphosphate receptor type 1. *Biochem J*, 435-441.

Hisatsune C, Kuroda Y, Akagi T, Torashima T, Hirai H, Hashikawa T, Mikoshiba K. (2006). Inositol 1,4,5-trisphosphate receptor type 1 in granule cells, not in Purkinje cells, regulates the dendritic morphology of Purkinje cells through brain-derived neurotrophic factor production. *J Neurosci, 26*(42), 10916-10924. doi:10.1523/JNEUROSCI.3269-06.2006

Hodge CW, Mehmert K, Kelley SP, McMahon T, Haywood A, Olive MF, Wang D, Sanchez-Perez AM, Messing RO. (1999). Supersensitivity to allosteric GABA(A) receptor modulators and alcohol in mice lacking PKCepsilon. *Nat Neurosci*, 997-1002.

Höftberger R, Sabater L, Velasco F, Ciordia R, Dalmau J, Graus F. (2014). Carbonic anhydrase-related protein VIII antibodies and paraneoplastic cerebellar degeneration. . *Neuropathol Appl Neurobiol*, 650-653.

Huang H, Nagaraja R, Garside ML, Akemann W, Knöpfel T, Empson RM. (2010). Contribution of plasma membrane Ca ATPase to cerebellar synapse function. *World J Biol Chem*, 95-102.

Hughes C, Galea-Lauri J, Farzaneh F, Darling D. (2001). Streptavidin paramagnetic particles provide a choice of three affinity-based capture and magnetic concentration strategies for retroviral vectors. *Mol Ther, 3*(4), 623-630. doi:10.1006/mthe.2001.0268

Inoue M, Kishimoto A, Takai Y, Nishizuka Y. (1977). Studies on a cyclic nucleotide-independent protein kinase and its proenzyme in mammalian tissues. II. Proenzyme and its activation by calcium-dependent protease from rat brain. *J Biol Chem*, 7610-7616.

Irie K, Nakahara A, Nakagawa Y, Ohigashi H, Shindo M, Fukuda H, Konishi H, Kikkawa U, Kashiwagi K, Saito N. (2002). Establishment of a binding assay for protein kinase C isozymes using synthetic C1 peptides and development of new medicinal leads with protein kinase C isozyme and C1 domain selectivity. *Pharmacol Ther*, 271-281.

Ito M, Yamaguchi K, Nagao S, Yamazaki T. (2014) Long-term depression as a model of cerebellar plasticity. *Prog Brain Res,* 1-30. doi: 10.1016/B978-0-444-63356-9.00001-7.

Iwaki A, Kawano Y, Miura S, Shibata H, Matsuse D, Li W, Fukumaki Y. (2008). Heterozygous deletion of ITPR1, but not SUMF1, in spinocerebellar ataxia type 16. *J Med Genet, 45*(1), 32-35. doi:10.1136/jmg.2007.053942

Jenkins SI, Pickard M, Granger N, Chari DM. (2011). Magnetic nanoparticle-mediated gene transfer to oligodendrocyte precursor cell transplant populations is enhanced by magnetofection strategies. *ACS Nano*, 6527-6538.

Jezierska J, Goedhart J, Kampinga HH, Reits EA, Verbeek DS. (2014). SCA14 mutation V138E leads to partly unfolded PKCγ associated with an exposed C-terminus, altered kinetics, phosphorylation and enhanced insolubilization. *J Neurochem*, 741-751.

Ji J, Hassler M, Shimobayashi E, Paka N, Streit R, Kapfhammer JP. (2014). Increased protein kinase C gamma activity induces Purkinje cell pathology in a mouse model of spinocerebellar ataxia 14. *Neurobiol Dis*, 1-11.

Jiao Y, Yan J, Zhao Y, Donahue LR, Beamer WG, Li X, Roe BA, Ledoux MS, Gu W. (2005). Carbonic anhydrase-related protein VIII deficiency is associated with a distinctive lifelong gait disorder in waddles mice. *Genetics*, 1239-1246.

John A, Brylka H, Wiegreffe C, Simon R, Liu P, Jüttner R, Crenshaw EB 3rd, Luyten FP, Jenkins NA, Copeland NG, Birchmeier C, Britsch S. (2012). Bcl11a is required for neuronal morphogenesis and sensory circuit formation in dorsal spinal cord development. *Development*, 1831-1841.

Johnson JE, Giorgione J, Newton AC. (2000). The C1 and C2 domains of protein kinase C are independent membrane targeting modules, with specifi city for phosphatidylserine conferred by the C1 domain. *Biochemistry* 11360–11369.

Kano M, Hashimoto K, Chen C, Abeliovich A, Aiba A, Kurihara H, Watanabe M, Inoue Y, Tonegawa S. (1995). Impaired synapse elimination during cerebellar development in PKC gamma mutant mice. *Cell* 1223–1231.

Kano M, Hashimoto K, Kurihara H, Watanabe M, Inoue Y, Aiba A, Tonegawa S. (1997) Persistent multiple climbing fiber innervation of cerebellar Purkinje cells in mice lacking mGluR1. *Neuron* 71-9.

Kano M, Hashimoto K, Watanabe M, Kurihara H, Offermanns S, Jiang H, Wu Y, Jun K, Shin HS, Inoue Y, Simon MI, Wu D. (1998) Phospholipase cbeta4 is specifically involved in climbing fiber synapse elimination in the developing cerebellum. *Proc Natl Acad Sci U S A.* 15724-9.

Kapfhammer JP. (2004). Cellular and molecular control of dendritic growth and development of cerebellar Purkinje cells. *Prog. Histochem. Cytochem*, 131–182

Kapfhammer JP. (2010). Cerebellar slice cultures, In: Doering LC (ed), Protocols for Neural Cell Culture. *Humana Press*, 285–298..

Kapfhammer JP. (2005). Cerebellar slice cultures. In P. Poindron, P. Piguet, & E. Förster (Eds.), *New Methods for Culturing Cells from Nervous Tissues* (Vol. 1, pp. 74-81). Basel: Karger.

Kapfhammer JP, Gugger OS. (2012). The analysis of purkinje cell dendritic morphology in organotypic slice cultures. *J Vis Exp*(61). doi:10.3791/3637

Kay Seidel. (2012). Brain pathology of spinocerebellar ataxias. *Acta Neuropathol*, 1–21.

Kaya N, Aldhalaan H, Younes B, Colak D, Shuaib T, Mohaileb F, Sugair A, Nester M, Yamani S, Bakheet A, Hashmi N, Sayed M, Meyer B, Jungbluth H, Owain M. (2011). Phenotypical spectrum of cerebellar ataxia associated with a novel mutation in the CA8 gene, encoding carbonic anhydrase (CA) VIII. *Am J Med Genet B Neuropsychiatr Genet*, 826-834.

Kazanietz MG, Bustelo X, Barbacid M, Kolch W, Mischak H, Wong G, Pettit GR, Bruns JD, Blumberg PM. (1994). Analysis of binding to mutated form of protein

kinase C zeta and the vav and c-raf proto-oncogene products. *J Biol Chem*, 11590–11594.

Kennelly PJ, Krebs E. (1991). Consensus sequences as substrate specificity determinants for protein kinases and protein phosphatases. *J Biol Chem*, 15555-15558.

Khasar SG, Lin Y, Martin A, Dadgar J, McMahon T, Wang D, Hundle B, Aley KO, Isenberg W, McCarter G, Green PG, Hodge CW, Levine JD, Messing RO. (1999). A novel nociceptor signaling pathway revealed in protein kinase C epsilon mutant mice. *Neuron*, 253-260.

Kim JJ, Thompson RF. (1997). Cerebellar circuits and synaptic mechanisms involved in classical eyeblink conditioning. *Trends Neurosci, 20*(4), 177-181.

Kirsch L, Liscovitch N, Chechik G. (2012). Localizing genes to cerebellar layers by classifying ISH images. *PLoS Comput Biol, 8*(12), e1002790. doi:10.1371/journal.pcbi.1002790

Kirwan AF, Bibby A, Mvilongo T, Riedel H, Burke T, Millis SZ, Parissenti AM. (2003). Inhibition of protein kinase C catalytic activity by additional regions within the human protein kinase Calpha-regulatory domain lying outside of the pseudosubstrate sequence. *Biochem J.*, 571-581.

Kitamura K. (2012). Dendritic calcium signaling in cerebellar Purkinje cell. *Neural Networks*.

Kofler K, Erdel M, Utermann G, Baier G. (2002). Molecular genetics and structural genomics of the human protein kinase C gene module. *Genome Biol*, RESEARCH0014.

Krishek BJ, Xie X, Blackstone C, Huganir RL, Moss SJ, Smart TG. (1994). Regulation of GABAA receptor function by protein kinase C phosphorylation. *Neuron*, 1081-1095.

Krotz F. (2003). Magnetofection--a highly efficient tool for antisense oligonucleotide delivery in vitro and in vivo. *Mol Ther*, 700-710.

Kuhar JR, Bedini A, Melief EJ, Chiu YC, Striegel HN, Chavkin C. (2015). Mu opioid receptor stimulation activates c-Jun N-terminal kinase 2 by distinct arrestin-dependent and independent mechanisms. *Cell Signal*, 1799-806

Kumar S, Sieghart W, Morrow AL. (2002) Association of protein kinase C with GABA(A) receptors containing alpha1 and alpha4 subunits in the cerebral cortex: selective effects of chronic ethanol consumption. *J Neurochem.* 110-7.

Kumar S, Suryanarayanan A, Boyd KN, Comerford CE, Lai MA, Ren Q, Morrow AL. (2010) Ethanol reduces GABAA alpha1 subunit receptor surface expression by a protein kinase Cgamma-dependent mechanism in cultured cerebral cortical neurons. *Mol Pharmacol.* 793-803

Kurnellas MP, Lee AK, Szczepanowski, K, Elkabes S. (2007). Role of plasma membrane calcium ATPase isoform 2 in neuronal function in the cerebellum and spinal cord. *Ann N Y Acad Sci, 1099*, 287-291. doi:10.1196/annals.1387.025

Lamont MG, Weber J. (2015). Mice deficient in carbonic anhydrase type 8 exhibit motor dysfunctions and abnormal calcium dynamics in the somatic region of cerebellar granule cells. *Behav Brain Res*, 11-16.

Lee HW, Smith L, Pettit GR, Bingham Smith J. (1996). Dephosphorylation of activated protein kinase C contributes to downregulation by bryostatin. *Am J Physiol*, C304-311.

Lefort JM, Rochefort C, Rondi-Reig L; Group of L.R.R. is member of Bio-Psy Labex and ENP Foundation. (2015) Cerebellar contribution to spatial navigation: new insights into potential mechanisms. *Cerebellum*, 59-62

Leitges M, Kovac J, Plomann M, Linden DJ. (2004). A unique PDZ ligand in PKCalpha confers induction of cerebellar long-term synaptic depression. *Neuron, 44*(4), 585-594. doi:10.1016/j.neuron.2004.10.024

Leontieva OV, Black J. (2004). Identification of two distinct pathways of protein kinase Calpha down-regulation in intestinal epithelial cells. *J Biol Chem*, 5788-5801.

Lim HH, Michael G, Smith P, Lim L, Hall C. (1992). Developmental regulation and neuronal expression of the mRNA of rat n-chimaerin, a p21rac GAP:cDNA sequence. *Biochem J*, 415-422.

Lin D, Shanks D, Prakash O, Takemoto DJ. (2007). Protein kinase C gamma mutations in the C1B domain cause caspase-3-linked apoptosis in lens epithelial cells through gap junctions. *Exp Eye Res*, 113–122.

Lin D, Takamoto D. (2007). Protection from ataxia-linked apoptosis by gap junction inhibitors. *Biochem Biophys Res Commun*, 982–987.

Lin YF, Browning M, Dudek EM, Macdonald RL. (1994). Protein kinase C enhances recombinant bovine alpha 1 beta 1 gamma 2L GABAA receptor whole-cell currents expressed in L929 fibroblasts. *Neuron*, 1421-1431.

Linden DJ, Connor JA. (1995). Long-term synaptic depression. *Annu Rev Neurosci, 18*, 319-357. doi:10.1146/annurev.ne.18.030195.001535

Linden DJ, Dickinson MH, Smeyne M, Connor JA. (1991). A long-term depression of AMPA currents in cultured cerebellar Purkinje neurons. *Neuron, 7*(1), 81-89.

Liu WS, Heckman C. (1998). The sevenfold way of PKC regulation. *Cell Signal* 529–542.

Malmberg AB, Chen C, Tonegawa S, Basbaum AI. (1997). Preserved acute pain and reduced neuropathic pain in mice lacking PKCgamma. *Science*, 279-283.

Martin H, Rostas J, Patel Y, Aitken A. (1994). Subcellular localisation of 14-3-3 isoforms in rat brain using specific antibodies. *J Neurochem*, 2259-2265.

Martin WJ, Liu H, Wang H, Malmberg AB, Basbaum AI. (1999). Inflammation-induced up-regulation of protein kinase Cgamma immunoreactivity in rat spinal cord correlates with enhanced nociceptive processing. *Neuroscience*, 1267-1274.

Matilla-Duenas A, Corral-Juan M, Volpini V, Sanchez I. (2012). The spinocerebellar ataxias: clinical aspects and molecular genetics. *Adv Exp Med Biol, 724*, 351-374. doi:10.1007/978-1-4614-0653-2_27

Matsuda K, Miura E, Miyazaki T, Kakegawa W, Emi K, Narumi S, Fukazawa Y, Ito-Ishida A, Kondo T, Shigemoto R, Watanabe M, Yuzaki M. (2010). Cbln1 is a ligand for an orphan glutamate receptor delta2, a bidirectional synapse organizer. *Science*, 363-368.

Matsumoto M, Kato K. (2001). Altered calcium dynamics in cultured cerebellar cells from IP3R1-deficient mice. *Neuroreport, 12*(16), 3471-3474.

Matsumoto M, Nakagawa, Inoue T, Nagata E, Tanaka K, Takano H, Minowa O, Kuno J, Sakakibara S, Yamada M, Yoneshima H, Miyawaki A, Fukuuchi Y, Furuichi T, Okano H, Mikoshiba K, Noda T. (1996). Ataxia and epileptic seizures in mice lacking type 1 inositol 1,4,5-trisphosphate receptor. *Nature*, 168-171.

Mellor H, Parker P. (1998). The extended protein kinase C superfamily. *Biochem J*, 281–292.

Metzger F, Kapfhammer JP. (2000). Protein kinase C activity modulates dendritic differentiation of rat Purkinje cells in cerebellar slice cultures. *Eur J Neurosci, 12*(6), 1993-2005.

Metzger F, Kapfhammer JP. (2003). Protein kinase C: its role in activity-dependent Purkinje cell dendritic development and plasticity. *Cerebellum*, 206-214.

Meuillet E. (2011). Novel inhibitors of AKT: assessment of a different approach targeting the pleckstrin homology domain. *Curr Med Chem*, 2727-2742.

Moreira MC, Barbot C, Tachi N, Kozuka N, Uchida E, Gibson T, Mendonça P, Costa M, Barros J, Yanagisawa T, Watanabe M, Ikeda Y, Aoki M, Nagata T, Coutinho P, Sequeiros J, Koenig M. (2001). The gene mutated in ataxia-ocular apraxia 1 encodes the new HIT/Zn-finger protein aprataxin. *Nat Genet*, 189–193.

Mori M, Kose A, Tsujino T, Tanaka C. (1990). Immunocytochemical localization of protein kinase C subspecies in the rat spinal cord: light and electron microscopic study. *J Comp Neurol*, 167-177.

Morrison ME, Mason C (1998). Granule neuron regulation of Purkinje cell development: striking a balance between neurotrophin and glutamate signaling. *J Neurosci*, 3563-3573.

Moscat J, Diaz-Meco M, Wooten MW. (2009). Of the atypical PKCs, Par-4 and p62: recent understandings of the biology and pathology of a PB1-dominated complex. *Cell Death Differ*, 1426–1437.

Narita M, Makimura M, Feng Y, Hoskins B, Ho IK. (1994). Influence of chronic morphine treatment on protein kinase C activity: comparison with butorphanol and implication for opioid tolerance. *Brain Res*, 175-179.

Narita M, Mizoguchi H, Narita M, Nagase H, Suzuki T, Tseng LF. (2001). Involvement of spinal protein kinase Cgamma in the attenuation of opioid mu-receptor-mediated G-protein activation after chronic intrathecal administration of [D-Ala2,N-MePhe4,Gly-Ol(5)]enkephalin. *J Neurosci*, 3715-20.

Newton AC. (1995). Protein kinase C: structure, function, and regulation. *J Biol Chem*, 28495–28498.

Newton AC. (1997). Regulation of protein kinase C. *Curr Opin Cell Biol*, 161-167.

Newton AC. (2010). Protein kinase C: poised to signal. *Am J Physiol Endocrinol Metab, 298*(3), E395-402. doi:10.1152/ajpendo.00477.2009

Nishizuka Y. (1995). Protein kinase C and lipid signaling for sustained cellular responses. *FASEB J*, 484-496.

Novak MJ, Sweeney MG, Li A, Treacy C, Chandrashekar HS, Giunti P, Tabrizi SJ. (2010). An ITPR1 gene deletion causes spinocerebellar ataxia 15/16: a genetic, clinical and radiological description. *Mov Disord, 25*(13), 2176-2182. doi:10.1002/mds.23223

O'Brien JA, Lummis SC. (2006). Biolistic transfection of neuronal cultures using a hand-held gene gun. *Nat Protoc, 1*(2), 977-981. doi:10.1038/nprot.2006.145

Ohtani Y, Miyata M, Hashimoto K, Tabata T, Kishimoto Y, Fukaya M, Aiba A. (2014). The synaptic targeting of mGluR1 by its carboxyl-terminal domain is crucial for cerebellar function. *J Neurosci, 34*(7), 2702-2712. doi:10.1523/JNEUROSCI.3542-13.2014

Okubo Y, Kakizawa S, Hirose K, Iino M. (2001). Visualization of IP(3) dynamics reveals a novel AMPA receptor-triggered IP(3) production pathway mediated by voltage-dependent Ca(2+) influx in Purkinje cells. *Neuron*, 113-122.

Osborne NN, Barnett. N., Morris NJ, Huang FL. (1992). The occurrence of three isoenzymes of protein kinase C (alpha, beta and gamma) in retinas of different species. *Brain Res*, 161-166.

Pandolfo M, van de Warrenburg BP. (2005). Spinocerebellar ataxia type 14: opening a new door in dominant ataxia research? . *Neurology* 1113-1114.

Paulson HL. (2009). The Spinocerebellar Ataxias. *J Neuroophthalmol*, 227-237.

Plank C, Scherer F, Schillinger U, Bergemann C, Anton M. (2003). Magnetofection: enhancing and targeting gene delivery with superparamagnetic nanoparticles and magnetic fields. *J Liposome Res, 13*(1), 29-32. doi:10.1081/LPR-120017486

Plank C, Zelphati O, Mykhaylyk O. (2011). Magnetically enhanced nucleic acid delivery. Ten years of magnetofection-progress and prospects. *Adv Drug Deliv Rev, 63*(14-15), 1300-1331. doi:10.1016/j.addr.2011.08.002

Polgár E, Fowler J, McGill MM, Todd AJ. (1999). The types of neuron which contain protein kinase C gamma in rat spinal cord. *Brain Res*, 71-80.

Prevostel C, Alice V, Joubert D, Parker PJ. (2000). Protein kinase C(alpha) actively downregulates through caveolae-dependent traffic to an endosomal compartment. *J Cell Sci.*, 2575-2584.

Pu Y, Peach M, Garfi eld SH, Wincovitch S, Marquez VE, Blumberg PM. (2006). Effects on ligand interaction and membrane translocation of the positively charged arginine residues situated along the C1 domain binding cleft in the atypical protein kinase C isoisoforms. *J Biol Chem*, 33773–33788.

Quittau-Prevostel C, Delaunay N, Collazos A, Vallentin A, Joubert D. (2004). Targeting of PKCalpha and epsilon in the pituitary: a highly regulated mechanism involving a GD(E)E motif of the V3 region. *J Cell Sci*, 63–72.

Reeber SL, Otis TS, Sillitoe RV. (2013). New roles for the cerebellum in health and disease. *Syst. Neurosci.*

Rippey C, Walsh T, Gulsuner S, Brodsky M, Nord AS, Gasperini M, Pierce S, Spurrell C, Coe BP, Krumm N, Lee MK, Sebat J, McClellan JM, King MC. (2013). Formation of chimeric genes by copy-number variation as a mutational mechanism in schizophrenia. *Am J Hum Genet*, 697-710.

Rossi F, Strata P (1995). Reciprocal trophic interactions in the adult climbing fibre-Purkinje cell system. *Prog Neurobiol*, 341-369.

Rotenberg SA, Z. J., Hansen H, Li XD, Sun XG, Michels CA, Riedel H. (1998). Deletion analysis of protein kinase Calpha reveals a novel regulatory segment. *J Biochem.*, 756-763.

Rozengurt, E. (2011). Protein kinase D signaling: multiple biological functions in health and disease. *Physiology (Bethesda), 26*(1), 23-33. doi:10.1152/physiol.00037.2010

Saito N, Kikkawa U, Nishizuka Y, Tanaka C. (1988). Distribution of protein kinase C-like immunoreactive neurons in rat brain. *J Neurosci*, 369–382.

Saito N, Shirai Y. (2002). Protein kinase C gamma (PKC gamma): function of neuron specific isotype. *J Biochem, 132*(5), 683-687.

Sakai N, Saito N, Seki T. (2011) Molecular pathophysiology of neurodegenerative disease caused by γPKC mutations. *World J Biol Psychiatry.* 95-8. doi: 10.3109/15622975.2011.598688.

Sapet C, Laurent N, de Chevigny A, Le Gourrierec L, Bertosio E, Zelphati O, Béclin C. (2011). High transfection efficiency of neural stem cells with magnetofection. *Biotechniques*, 187-189.

Sarna JR, Hawkes R. (2003). Patterned Purkinje cell death in the cerebellum. *Prog Neurobiol*, 473-507.

Sasaki M, Ohba C, Iai M, Hirabayashi S, Osaka H, Hiraide T, Matsumoto N. (2015). Sporadic infantile-onset spinocerebellar ataxia caused by missense mutations of the inositol 1,4,5-triphosphate receptor type 1 gene. *J Neurol, 262*(5), 1278-1284. doi:10.1007/s00415-015-7705-8

Schaefer M, Albrecht N, Hofmann T, Gudermann T, Schultz G. (2001). Diffusion-limited translocation mechanism of protein kinase C isotypes. *FASEB J*, 1634-1636.

Schmahmann JD. (2010). The role of the cerebellum in cognition and emotion: personal reflections since 1982 on the dysmetria of thought hypothesis, and its historical evolution from theory to therapy. *Neuropsychol. Rev*, 236–260.

Scho¨ls L, Bauer P, Schmidt T, Schulte T, Riess O. (2004). Autosomal dominant cerebellar ataxias: clinical features, genetics, and pathogenesis. *Lancet Neurol*, 291–304.

Schorge S, van de Leemput J, Singleton A, Houlden H, Hardy J. (2010). Human ataxias: a genetic dissection of inositol triphosphate receptor (ITPR1)-dependent signaling. *Trends Neurosci*, 211–219.

Schrenk K, Kapfhammer JP, Metzger F. (2002). Altered dendritic development of cerebellar Purkinje cells in slice cultures from protein kinase Cgamma-deficient mice. *Neuroscience*, 675-689.

Sekerkova G, Kim JA, Nigro MJ, Becker EB, Hartmann J, Birnbaumer L, Martina M. (2013). Early onset of ataxia in moonwalker mice is accompanied by complete ablation of type II unipolar brush cells and Purkinje cell dysfunction. *J Neurosci, 33*(50), 19689-19694. doi:10.1523/JNEUROSCI.2294-13.2013

Seki T, Adachi N, Ono Y, Mochizuki H, Hiramoto K, Amano T, Matsubayashi H, Matsumoto M, Kawakami H, Saito N, Sakai N. (2005). Mutant protein kinase Cgamma found in spinocerebellar ataxia type 14 is susceptible to aggregation and causes cell death. *J Biol Chem*, 29096–29106.

Seki T, Shimahara T, Yamamoto K, Abe N, Amano T, Adachi N, Takahashi H, Kashiwagi K, Saito N, Sakai N. (2009). Mutant gammaPKC found in spinocerebellar ataxia type 14 induces aggregate-independent maldevelopment of dendrites in primary cultured Purkinje cells. *Neurobiol Dis*, 260–273.

Seki T, Takahashi H, Adachi N, Abe N, Shimahara T, Saito N, Sakai N. (2007). Aggregate formation of mutant protein kinase C gamma found in spinocerebellar ataxia type 14 impairs ubiquitin-proteasome system and induces endoplasmic reticulum stress. *Eur J Neurosci*, 3126-3140.

Serinagaoglu Y, Zhang R, Zhang Y, Zhang L, Hartt G, Young AP, Oberdick J. (2007) A promoter element with enhancer properties, and the orphan nuclear receptor RORalpha, are required for Purkinje cell-specific expression of a Gi/o modulator. *Mol Cell Neurosci,* 324-42.

Shahraki A, Stone TW. (2002). Long-term potentiation and adenosine sensitivity are unchanged in the AS/AGU protein kinase Cgamma-deficient rat. *Neurosci Lett*, 165-168.

Sherkhane P, Kapfhammer JP. (2013). The plasma membrane Ca2+-ATPase2 (PMCA2) is involved in the regulation of Purkinje cell dendritic growth in cerebellar organotypic slice cultures. *Neural Plast, 2013*, 321685. doi:10.1155/2013/321685

Shirafuji T, Ueyama T, Yoshino K, Takahashi H, Adachi N, Ago Y, Koda K, Nashida T, Hiramatsu N, Matsuda T, Toda T, Sakai N, Saito N. (2014) The role of Pak-interacting exchange factor-β phosphorylation at serines 340 and 583 by PKCγ in dopamine release. *J Neurosci.* 9268-80.

Shuvaev AN, Horiuchi H, Seki T, Goenawan H, Irie T, Iizuka A, Sakai N, Hirai H. (2011). Mutant PKCγ in spinocerebellar ataxia type 14 disrupts synapse elimination and long-term depression in Purkinje cells in vivo. *J Neurosci*, 14324–14334.

Sirzen-Zelenskaya A, Zeyse J, Kapfhammer JP. (2006). Activation of class I metabotropic glutamate receptors limits dendritic growth of Purkinje cells in organotypic slice cultures. *Eur J Neurosci.* 2978-86.

Sjöblom B, Elleby B, Wallgren K, Jonsson BH, Lindskog S. (1996). Two point mutations convert a catalytically inactive carbonic anhydrase-related protein (CARP) to an active enzyme. *FEBS Lett,* 322-325.

Slater SJ, Milano SK, Stagliano BA, Gergich KJ, Curry JP, Taddeo FJ, Stubbs CD. (2000). Interaction of protein kinase C with fi lamentous actin: isozyme specifi city resulting from divergent phorbol ester and calcium dependencies. *Biochemistry,* 271–280.

Smith-Hicks C, Xiao B, Deng R, Ji Y, Zhao X, Shepherd JD, Posern G, Kuhl D, Huganir RL, Ginty DD, Worley PF, Linden DJ. (2010). SRF binding to SRE 6.9 in the Arc promoter is essential for LTD in cultured Purkinje cells. *Nat Neurosci,* 1082-1089.

Soong BW, Paulson HL. (2007). Spinocerebellar ataxias. *Curr Opin Neurol,* 438–446.

Sotelo C, Dusart I. (2009). Intrinsic versus extrinsic determinants during the development of Purkinje cell dendrites. *Neuroscience,* 589-600.

Steinberg SF (2008). Structural basis of protein kinase C isoform function. *Physiol Rev,* 1341-1378.

Stevanin G, Hahn V, Lohmann E, Bouslam N, Gouttard M, Soumphonphakdy C, Welter ML, Ollagnon-Roman E, Lemainque A, Ruberg M, Brice A, Durr A. (2004) Mutation in the catalytic domain of protein kinase C gamma and extension of the phenotype associated with spinocerebellar ataxia type 14. *Arch Neurol,* 1242-8.

Stoppini L, Buchs PA, Muller D. (1991). A simple method for organotypic cultures of nervous tissue. *J Neurosci Methods,* 173-182.

Tabata T, Sawada S, Araki K, Bono Y, Furuya S, Kano M. (2000). A reliable method for culture of dissociated mouse cerebellar cells enriched for Purkinje neurons. *J Neurosci Methods,* 45-53.

Tada M, Nishizawa M, Onodera O. (2016). Roles of inositol 1,4,5-trisphosphate receptors in spinocerebellar ataxias. *Neurochem Int,* doi:10.1016/j.neuint.2016.01.007

Takahashi H, Adachi N, Shirafuji T, Danno S, Ueyama T, Vendruscolo M, Shuvaev AN, Sugimoto T, Seki T, Hamada D, Irie K, Hirai H, Sakai N, Saito N.(2015). Identification and characterization of PKCγ, a kinase associated with SCA14, as an amyloidogenic protein. *Hum Mol Genet, 525-39*

Takanaga H, Mukai. H., Shimakawa M, Konishi H, Kikkawa U, Koizumi T, Ono Y. (1995). Functional characterization of the promoter region of the mouse protein kinase C gamma gene. *FEBS Lett,* 276-278.

Tanaka M. (2009). Dendrite formation of cerebellar Purkinje cells. *Neurochem Res, 34*(12), 2078-2088. doi:10.1007/s11064-009-0073-y

Tanaka M, Yanagawa. Y., Obata K, Marunouchi T. (2006). Dendritic morphogenesis of cerebellar Purkinje cells through extension and retraction revealed by long-term tracking of living cells in vitro *Neuroscience*, 663-674.

Timmann D, Drepper J, Frings M, Maschke M, Richter S, Gerwig M, Kolb FP. (2010). The human cerebellum contributes to motor, emotional and cognitive associative learning. A review. *Cortex, 46*(7), 845-857. doi:10.1016/j.cortex.2009.06.009

Tomomura M, Rice D, Morgan JI, Yuzaki M. (2001). Purification of Purkinje cells by fluorescence-activated cell sorting from transgenic mice that express green fluorescent protein. *Eur J Neurosci*, 57-63.

Türkmen S, Guo G, Garshasbi M, Hoffmann K, Alshalah AJ, Mischung C, Kuss A, Humphrey N, Mundlos S, Robinson PN. (2009). CA8 mutations cause a novel syndrome characterized by ataxia and mild mental retardation with predisposition to quadrupedal gait. *PLoS Genet*, pgen.1000487.

Ubl A, Berg D, Holzmann C, Krüger R, Berger K, Arzberger T, Bornemann A, Riess O. (2002). 14-3-3 protein is a component of Lewy bodies in Parkinson's disease-mutation analysis and association studies of 14-3-3 eta. *Brain Res Mol Brain Res*, 33-39.

Uemura T, Lee S, Yasumura M, Takeuchi T, Yoshida T, Ra M, Taguchi R, Sakimura K, Mishina M. (2010). Trans-synaptic interaction of GluRdelta2 and Neurexin through Cbln1 mediates synapse formation in the cerebellum. *Cell*, 1068-1079.

van de Leemput J, Chandran J, Knight MA, Holtzclaw LA, Scholz S, Cookson MR, Singleton AB. (2007). Deletion at ITPR1 underlies ataxia in mice and spinocerebellar ataxia 15 in humans. *PLoS Genet, 3*(6), e108. doi:10.1371/journal.pgen.0030108

van de Warrenburg BP, Verbeek DS, Piersma SJ, Hennekam FA, Pearson PL, Knoers NV, Sinke RJ. (2003). Identification of a novel SCA14 mutation in a Dutch autosomal dominant cerebellar ataxia family. *Neurology, 61*(12), 1760-1765.

Verbeek DS, Goedhart J, Bruinsma L, Sinke RJ, Reits EA. (2008). PKC gamma mutations in spinocerebellar ataxia type 14 affect C1 domain accessibility and kinase activity leading to aberrant MAPK signaling. *J Cell Sci, 121*(Pt 14), 2339-2349. doi:10.1242/jcs.027698

Verbeek DS, Knight MA, Harmison GG, Fischbeck KH, Howell BW. (2005). Protein kinase C gamma mutations in spinocerebellar ataxia 14 increase kinase activity and alter membrane targeting. *Brain*, 436–442.

Vermassen E, Parys J, Mauger JP. (2004). Subcellular distribution of the inositol 1,4,5-trisphosphate receptors: functional relevance and molecular determinants. *Biol Cell*, 3-17.

Vlak MH, Sinke R, Rabelink GM, Kremer BP, van de Warrenburg BP. (2006). Novel PRKCG/SCA14 mutation in a Dutch spinocerebellar ataxia family expanding the phenotype. *Mov Disord,* 1025–1028.

Wagner W, McCroskery S,  Hammer JA. (2011). An efficient method for the long-term and specific expression of exogenous cDNAs in cultured Purkinje neurons. *J Neurosci Methods*, 95-105.

Wang VY, Zoghbi, HY.  (2001). Genetic regulation of cerebellar development. *Nat Rev Neurosc*, 484-491.

Wellmann H, Kaltschmidt B, Kaltschmidt C. (1999). Optimized protocol for biolistic transfection of brain slices and dissociated cultured neurons with a hand-held gene gun. *J Neurosci Methods, 92*(1-2), 55-64.

Wei-Yu Huang, Shih-Ping Dai, Yan-Ching Chang, Wei-Hsin Sun. (2015). Acidosis Mediates the Switching of Gs-PKA and Gi-PKCε Dependence in Prolonged Hyperalgesia Induced by Inflammation. *PLoS One*, e0125022.

Wetsel WC, Khan WA, Merchenthaler I, Rivera H, Halpern AE, Phung HM, Hannun YA. (1992). Tissue and cellular distribution of the extended family of protein kinase C isoenzymes. *J Cell Biol, 117*(1), 121-133.

White JJ, Sillitoe RV. (2013). Development of the cerebellum: from gene expression patterns to circuit maps. *Wiley Interdiscip Rev Dev Biol*, 149-164.

Xiao DM, Pak JH, Wang X, Sato T, Huang FL, Chen HC, Huang KP. (2000). Phosphorylation of HMG-I by protein kinase C attenuates its binding affinity to the promoter regions of protein kinase C gamma and neurogranin/RC3 genes. *J Neurochem*. 392-9.

Yabe I. (2003). Spinocerebellar ataxia type 14 caused by a mutation in protein kinase C gamma. *Arch Neurol*, 1749–1751.

Yamamoto K, Seki T, Adachi N, Takahashi T, Tanaka S, Hide I, Saito N, Sakai N. (2010). Mutant protein kinase C gamma that causes spinocerebellar ataxia type 14 (SCA14) is selectively degraded by autophagy. *Genes Cells*, 425–438.

Yamashita I, Sasaki H, Yabe I. (2000). A novel locus for dominant cerebellar ataxia (SCA14) maps to a 10.2-cM interval flanked by D19S206 and D19S605 on chromosome 19q13.4- qter. *Ann Neurol*, 156–163.

Zeng L, Webster SV, Newton PM. (2012). The biology of protein kinase C. *Adv Exp Med Biol, 740*, 639-661. doi:10.1007/978-94-007-2888-2_28

Zhang X, Baader SL, Bian F, Müller W, Oberdick J. (2001). High level Purkinje cell specific expression of green fluorescent protein in transgenic mice. *Histochem Cell Biol.*, 455-464.

Zhang Y, Snider A, Willard L, Takemoto DJ, Lin D. (2009). Loss of Purkinje cells in the PKCgamma H101Y transgenic mouse. *Biochem Biophys Res Commun*, 524–528.

Zhao Y, Kwan KM, Mailloux CM, Lee WK, Grinberg A, Wurst W, Behringer RR, Westphal H. (2007). LIM-homeodomain proteins Lhx1 and Lhx5, and their

cofactor Ldb1, control Purkinje cell differentiation in the developing cerebellum. *Proc Natl Acad Sci U S A*, 13182-13186.

Zhuang GZ, Keeler B, Grant J, Bianchi L, Fu ES, Zhang YP, Erasso DM, Cui JG, Wiltshire T, Li Q, Hao S, Sarantopoulos KD, Candiotti K, Wishnek SM, Smith SB, Maixner W, Diatchenko L, Martin ER, Levitt RC. (2015). Carbonic anhydrase-8 regulates inflammatory pain by inhibiting the ITPR1-cytosolic free calcium pathway. *PLoS One*, e0118273

Zu T, Duvick LA, Kaytor MD, Berlinger MS, Zoghbi HY, Clark HB, Orr HT. (2004). Recovery from polyglutamine-induced neurodegeneration in conditional SCA1 transgenic mice. *J Neurosci, 24*(40), 8853-8861.

# *Acknowledgements*

# *Curriculum Vitae*

## Etsuko Shimobayashi (PhD candidate)

Address: Gellertstrasse 86, 4052 Basel, Switzerland

Phone: +41 76 399 97 33

E-mail: etsuko.shimobayashi@unibas.ch

Date of Birth: 23.09.1981

Citizenship: Japan

Gender: Female

Marital Status: Married

## Education & Training

| 2012-2016 | **PhD degree in Life Science,** University of Basel, Department of Biomedicine, Institute of Anatomy<br>• Studies on Mechanisms of dendritic growth inhibition of Cerebellar Purkinje Cells in PKC gamma Transgenic mice | Basel, Switzerland |
|---|---|---|
| 2004-2006 | **Master's degree in Life Science,** Grade A<br>Kyoto University, Department of Lifescience<br>• Studies on a molecular regulation of Ypk1, a downstream target of TOR signaling in Saccharomyces cerevisiae | Kyoto, Japan |
| 2000-2004 | **Bachelor's degree in Pharmacy,**<br>Kyoto University, Department of Pharma | Kyoto, Japan |

## Work Experience

| 2006-2012 | **Dainippon Sumitomo Pharmaceutical Company**<br>Associate Researcher<br>in pharmacology department in Japan<br>• Search for orphan GPCR in vitro and in vivo, which could treat autoimmune disease such as rheumatoid arthritis<br>• Creative and Analyse of antibody drug candidates which were being developed to treat autoimmune diseases such as Inflammatory bowel disease | Osaka, Japan |
|---|---|---|

## General Skills

- Supervision of students & technicians

- Scientific writing

- Managing small scientific projects

- General IT skills –Word, Excel, PowerPoint, Illustrator, Graph Pad Prism

Cell &Molecular Biology:

- Establish the antibody producing hybridoma

- Immune cells culture and T cell differentiation

- Handling of bacteria and yeast

- Organotypic slice cultures of cerebellum

- Dissociated primary culture of cerebellar cells

- Animal techniques, including dissection of brain and body from mice & rats, intracardiac perfusion, drug injection, blood and urine collection, animal husbandry

- Making animal disease models of autoimmune diseases

- Immunostaining & Microscopy fluorescence and analysis

- Molecular Biology including Cloning (PCR, transformation), RNA extraction, Real time PCR and ELISA,

- Western Blotting, Immunoprecipitation, kinase assay, Flow cytometory and cell sorting

- HPLC and TLC

*Further activities and training*

- **Lab Animal Experiments Licence (CH):** LTK Module 1 (University of Zürich, 2012)

- **The pharmacist license in Japan** (Japan, 2004)

- **Teaching Assistants, 2004-2006** Co-teaching undergraduate level courses in Immunology. Sharing responsibility for lectures, laboratory exercises, assignments, and grades.

- **Antelope 2015 (Antelope Novartis) mentee:** mentoring program between University of Basel and Novartis. Mentor: Karin Blumer (PR manager in Novartis)

## Languages

Japanese:         Mother tongue

English:          Fluent in speaking and writing

German:           Basic skills

## Publications

- Shimobayashi Etsuko; Wagner Wolfgang; Kapfhammer Josef P (2015) Carbonic Anhydrase 8 Expression in Purkinje Cells Is Controlled by PKCγ Activity and Regulates Purkinje Cell Dendritic Growth. *Molecular Neurobiology*

- Yamane-Sando Yukari; Shimobayashi Etsuko; Shimobayashi Mitsugu; Kozutsumi Yasunori; Oka Shogo; Takematsu Hiromu (2014) Fpk1/2 kinases regulate cellular sphingoid long-chain base (LCB) abundance and alter cellular resistance to LCB elevation or depletion. *MicrobiologyOpen*

- Jingmin Ji; Melanie L Hassler; Etsuko Shimobayashi; Nagendher Paka; Raphael Streit; Josef P. Kapfhammer (2014) Increased protein kinase C gamma activity induces Purkinje cell pathology in a mouse model of spinocerebellar ataxia 14. *Neurobiology of Disease*

## Conference presentations

June 2013          Neurex Annual Meeting, poster presentation

February 2014      LS2 Annual Meeting 2014 Lausanne, poster presentation

July 2014          FENS forum Milan, poster presentation

September 2014     76th Annual Meeting of the SSAHE, poster presentation

January 2015       SSN Annual Meeting, poster presentation

January 2016       SSN Annual Meeting, poster presentation

July 2016          FENS forum Copenhagen, poster presentation